

# **CCS2022-2024 WP1: The Jammerbugt structure**

Seismic data and interpretation to mature  
potential geological storage of CO<sub>2</sub>

Michael B.W. Fyhn, Anders Mathiesen, Egon Nørmark,  
Finn Mørk, Florian Smit, Henrik Vosgerau, Shahjahan Laghari,  
Thomas Funck, Tomi Jusri & Ulrik Gregersen

# **CCS2022-2024 WP1: The Jammerbugt structure**

Seismic data and interpretation to mature  
potential geological storage of CO<sub>2</sub>

Michael B.W. Fyhn, Anders Mathiesen, Egon Nørmark, Finn Mørk,  
Florian Smit, Henrik Vosgerau, Shahjahan Laghari, Thomas Funck,  
Tomi Jusri & Ulrik Gregersen

## Preface

A new Danish Climate Act was decided by the Danish Government and a large majority of the Danish Parliament on June 26<sup>th</sup>, 2020. It includes the aim of reducing the Danish greenhouse gas emissions with 70 % by 2030 compared to the level of emissions in 1990. The first part of a new Danish CCS-Strategy of June 30<sup>th</sup>, 2021 includes a decision to continue the initial investigations of sites for potential geological storage of CO<sub>2</sub> in Denmark. GEUS has therefore from 2022 commenced seismic acquisition and investigations of potential sites for geological storage of CO<sub>2</sub> in Denmark.

The structures decided for maturation by the authorities, are some of the largest structures onshore Zealand, Jutland and Lolland and in the eastern North Sea (Fig. 1.1). The onshore structures include the Havnsø, Gassum, Thorning, and Rødby structures, and in addition the small Stenlille structure as a demonstration/pilot site. The offshore structures include the Inez, Lisa and Jammerbugt structures. A GEUS Report is produced for each of the structures to mature the structure as part of the CCS2022–2024 project towards potential geological storage of CO<sub>2</sub>.

The intention with the project reporting for each structure is to provide a knowledge-based maturation with improved database and solid basic descriptions to improve the understanding of the formation, composition, and geometry of the structure. It includes a description overview and mapping of the reservoir and seal formations, the largest faults, the lowermost closure (spill-point) and structural top point of the reservoir, estimations of the overall closure area and gross-rock volume. In addition, the database will be updated, where needed with rescanning of some of the old seismic data, and acquisition of new seismic data in a grid over the structures, except for the Inez and Lisa structures, which have sufficient seismic data for this initial maturation.

The reports will provide an updated overview of the database, geology, and seismic interpretation for all with interests in the structures and will become public available. Each reporting is a first step toward geological maturation and site characterization of the structures. A full technical evaluation of the structures to cover all aspects related to CO<sub>2</sub> storage including risk assessment is recommended for the further process.

# Contents

<b>Preface</b>	<b>2</b>
<b>Dansk sammendrag</b>	<b>4</b>
Datagrundlag.....	4
Tolkning .....	5
<b>1. Summary</b>	<b>8</b>
<b>2. Introduction</b>	<b>13</b>
<b>3. Geological setting</b>	<b>14</b>
<b>4. Database</b>	<b>17</b>
4.1 Seismic data.....	17
4.1.1 Processing.....	19
4.1.2 Reprocessing .....	21
4.2 Well data .....	27
<b>5. Methods</b>	<b>28</b>
5.1 Seismic interpretation and well-ties .....	28
5.2 Seismic time to depth conversion .....	29
5.3 Investigation of reservoir and seal .....	36
5.4 Storage capacity modelling.....	36
<b>6. Results</b>	<b>39</b>
6.1 Local Stratigraphy.....	39
6.2 Structure and tectonic development .....	51
<b>7. Geology and parameters of the Jammerbugt structure storage complexes</b>	<b>59</b>
7.1 Reservoirs – Summary of geology and parameters.....	59
7.1.1 The primary reservoir: The Gassum Formation.....	60
7.1.2 Secondary reservoir 2: Haldager Sand Formation.....	61
7.1.3 Secondary reservoir 2 upside: Flyvbjerg Formation.....	62
7.2 Seals – Summary of geology and parameters.....	62
7.2.1 The primary seal (for the Gassum Fm): The Fjerritslev Fm .....	62
7.2.2 Seals of the secondary reservoir/seal pairs: The Børglum and Frederikshavn fms sealing the Haldager Sand Fm .....	66
<b>8. Discussion of storage and potential risks</b>	<b>67</b>
8.1 Volumetrics and Storage Capacity .....	67
8.2 Volumetric input parameters .....	69
8.2.1 Gross rock volume.....	69
8.2.2 Net-to-Gross ratio and porosity .....	70
8.2.3 CO <sub>2</sub> density.....	70
8.2.4 Storage efficiency .....	71
8.2.5 l.....	71
8.3 Storage capacity results .....	72
8.1 Potential risks .....	75
<b>9. Conclusions</b>	<b>76</b>
<b>10. Recommendations for further work</b>	<b>78</b>
<b>11. References</b>	<b>79</b>

## Dansk sammendrag

Jammerbugt strukturen var indtil indsamlingen af nye seismiske data i dette studie en af de mindst kendte strukturer i Skagerrak (Fig. 1.1). Det var således meget usikkert om strukturen karakteriseredes af lukkede dybdekonturer, som i skrivende stund anses som en indledende forudsætning for CO<sub>2</sub> lagring. Indsamling og tolkning af nye seismiske data belyser her Jammerbugt strukturens geologi og tilblivelse, potentiale som CO<sub>2</sub> lager og usikkerheder som bør belyses i fremtidige studier.

## Datagrundlag

Området omkring Jammerbugt strukturen var indtil foråret 2023 dækket af meget få 2D reflektionsseismiske linjer af stærkt varierende kvalitet indsamlet i forbindelse med tidligere olie-gas efterforskning. Godt 1400 km nye seismiske linjer blev indsamlet i foråret 2023 over strukturen og dens flanker og med korrelation til den nærliggende J-1 boring beliggende ved Lisa strukturen (Fig. 1.2). Dataindsamlingen og den efterfølgende processering blev foretaget for GEUS af Bundesanstalt für Geowissenschaften und Rohstoffe (BGR) i Tyskland i samarbejde med Aarhus Universitet. Der blev anvendt en 2100 m lang streamer med 336 kanaler (6.25 m interval). En række af linjerne indsamledes indledningsvis vha. en akustisk kilde bestående af to GI luftkanoner med et samlet volumen på 2,4 liter og betjent ved ca. 135 bar med en skudpunkt interval på 6 sekunder. Sidenhen udskiftedes kilden til en kilde med et samlet volumen på 5,8 liter betjent og et skudpunkts interval på mellem 10 og 12 sekunder. Med skibets hastighed på 4,5 knob gav de to forskellige set-ups en nominal fold på henholdsvis 76 og 38/45. Enkelte af de først indsamlede linjer blev genindsamlet med det nye set-up, men der er kun begrænset kvalitetsforskel mellem de to forskellige set-ups. Indsamlingen begrænsedes til vanddybder større end ti meter, og den inderste del af Jammerbugt lukningen er ikke dækket af de nyeste data (Fig. 1.3). Vintage seismiske data onshore har i stedet bidraget i griddingen af nøgleflader ind mod land. Data er blevet reprocesseret af RealTime Seismic for at forbedre data yderligere.

Idet Jammerbugt strukturen ikke er boret, er der korreleret til nærliggende boringer både på land og offshore for at bistå til forståelsen af de geologiske lag i og omkring strukturen (Fig. 1.2). De fleste boringer stopper i det øverste Trias eller derover, mens Felicia-1a også gennemborer et dybere interval og dermed bidrager med information om den dybere geologi. Samlet set er den seismiske dækning af den vestlige to-tredjedel af strukturen god mens dette ikke er tilfældet for den østlige tredjedel. Datakvaliteten af 2023-surveyet var forholdsvis lav efter første proceseringsfase, påvirket af meget kraftige multipler og et lavt signal/støj-forhold. Kvaliteten forbedredes markant efter reprocessering og er nu moderat sammenlignet med state-of-the-art. Det seismiske net er dog tæt og sammen med boringerne er data fuldt tilstrækkelige til at give en overordnet forståelse af Jammerbugt strukturens størrelse, grundlæggende geologiske forhold og kritiske elementer som bør undersøges yderligere.

## Tolkning

Jammerbugt strukturen er en forkastet 3-vejs lukning afgrænset af en forkastning mod nordvest og nordøst (Fig. 1.3) og beliggende i Fjerritslevtruget, som er en del af Sorgenfrei-Tornquist Zonen. Forkastninger afgrænser og forsætter strukturen på reservoir- og sejl niveau og dannedes som følge af både dyb tektonik med strukturer rodfæstet i grundfjeldet og som følge af udskridninger langs decollementer af både Zechstein og Triassisk salt. Den nordvestlige afgrænsende forkastning dannedes som følge af dybe forsætninger med en rod i grundfjeldet, forkastningerne mod nordøst dannedes som antitetiske forkastninger til en forkastningszone nord for strukturen (Fig. 1.4). Bevægelserne i denne nordlige forkastningszone er rodfæstet i grundfjeldet men de associerede deformationer i den Mesozoiske lagfølge kompliceres af udskridninger i Zechstein niveauet og den nordøstlige lukning af Jammerbugt strukturen må således tilskrives en kombination af sub-Zechstein forkastningsforsæt og udskridning af den Mesozoiske lagpakke i et decollement af duktile Zechstein evaporitter. Den sydvestlige flanke afgrænses af den forholdsvis stejle laghældning hældende mod sydvest, som er skabt af indsynkning langs Fjerritslev Forkastningszonen. Mindre forkastninger nedforsætter desuden den sydvestlige flanke og såler ud i den Midt til Øvre Triassiske Oddesund Formation i et evaporitførende interval og forsætter både reservoir og sejl niveau. De afgrænsende forkastninger fortsætter højt op i stratigrafien og nogle endda til nær havbunden.

Jammerbugt strukturens vestligste spids er underlagt af en mindre saltpude bestående af mobiliseret Oddesund Formation salt. Puden har dog ikke afgørende effekt på selve lukningens geometri, men bidrager til at øge lukningens relief. Strukturel lukning findes på både top-Gassum Formation og Haldager Sand Formation niveau.

Det nye seismiske survey har muliggjort en tektonostratigrafisk analyse af det Triassiske interval. Analysen indikerer en tredeling af Triasset. Den nedre del udgøres af en kilometer-tykk enhed af forholdsvis ensartet tykkelse som tilhører Skagerrak Formation gennemboret i Felicia-1a brønden. Skagerrak Fm dannedes som en post-rift enhed og den ofte fremhævede tolkning af Skagerrak Fm aflejret som alluviale vifter langs det Fennoskandiske skjold bør genovervejes. Over Skagerrak Fm hviler Oddesund Fm, som kendetegnes af en stærkt varierende tykkelse kontrolleret af nedforkastning mod Fjerritslev Truget over Fjerritslev Forkastningszonen. Oddesund Fm dannedes som en syn-rift enhed i sen Mellem Trias til Sen Trias tid. Oddesund Fm draperes af en få hundrede meter tyk enhed kendetegnet af en forholdsvis ensartet tykkelse i Fjerritslev Truget. Enheden svarer til Jyllands Gruppen bestående af Vinding Fm overlejret af Gassum Fm. Tykkelsen af Gassum Fm kan således være forholdsvis ensartet i den nærliggende del af Fjerritslev Truget, hvorfor dens tykkelse over Jammerbugt strukturen er estimeret til at være i omegnen af 200 m efter sammenligning med Felicia-1a, J-1 og Vedsted-1 brøndene. Der er desuden god chance for at der internt i den nedre del af Fjerritslev Fm findes et yngre sandstensindslag som kan henføres til Gassum Fm der kan bidrage til lagring af CO<sub>2</sub>.

Højere oppe i stratigrafien er en betydelig lukning kortlagt i intervallet svarende til Haldager Sand Fm. Haldager Sand Fm har en tykkelse på mellem 19 m (i J-1) og 75 m (i Vedsted-1). Tykkelsen og reservoirkvaliteten varierer betydeligt i de forskellige brønde. Der er anlagt et forsigtigt skøn over Haldager Sand Fm reservoirkvalitet og tykkelse, idet at Jammerbugt strukturen har en geologisk udviklingshistorie som drager paralleller til Lisa strukturens, hvor Haldager Sand Fm har beskedne reservoir egenskaber. Ud over Haldager Sand Fm findes stedvis et reservoir potentiale i den overliggende Flyvbjerg Fm som har en tykkelse på op til få titalsmeter. Flyvbjerg Fm er kun tolket i onshore brønde langs Jammerbugt og tilstedeværelsen i Jammerbugt strukturen er

usikker. Da Flyvbjerg Fm eventuelt vil ligge i direkte kontakt med Haldager Sand Fm, er Flyvbjerg Fm behandlet som et potentielt upside til et Haldager Sand Fm reservoir. Den samlede Haldager Sand – Flyvbjerg succession udgør derfor formentlig et sekundært reservoir interval i Jammerbugt strukturen.

Den seismiske dybdekonvertering tyder på at toppen af Haldager Sand og Gassum Fm ligger i omkring henholdsvis 1160 m og 1620 m dybde på Jammerbugt strukturen, hvilket er i tråd med eksempelvis tids-dybde forholdet i eksempelvis J-1 boringen. Dybdekonverteringen resulterer desuden i at den ca. 200 ms TWT høje lukning konverteres til omtrentlig 400 meter. Dette er noget højere end hvad man normalt vil forvente. Dette bør undersøges nærmere ved ny dataindsamling, idet det kan føre til en overvurdering af lagringsvolumenet og dermed den statiske lagringskapacitet. Lukningsarealet, kortlagt til 142 og 119 km<sup>2</sup> på top Gassum Fm og Haldager Sand Fm-niveau, er behæftet med betydelig usikkerhed pga. hullet i den seismiske datadækning over den indre, sydøstlige del af strukturen. Det kortlagte toppunkt ligger dog inden for det datadækkede område og lukningen syntes reel. Lagringspotentialet på både Gassum Fm og Haldager Sand Fm-niveau er således behæftet med betydelig usikkerhed først og fremmest afspejlende usikkerhed i lukningsarealet, men også afspejlende usikkerheden i tykkelsen af de to reservoirer. Potentialet syntes væsentligst på Gassum Fm-niveau. Den reservoirholdige Gassum Fm har formentlig et net-to-gross på ca. 50% at dømme ud fra nærliggende brønde vurderet på baggrund af petrofysiske data. Den overlejres af omtrentlig 500 meter Fjerritslev Fm bestående overvejende af tætte mudder- og lersten, som forventes at have gode segl- egenskaber og til at udgøre det primære segl for Gassum Fm. Højere oppe i stratigrafien draperes Haldager Sand og Flyvbjerg formationerne af Børglum Fm som udgør det primære segl over disse reservoirenheder og måler 48–113 m i tykkelse i de nærliggende brønde boret i Fjerritslev Truget.

Mindre forkastninger forsætter både Gassum, Fjerritslev, Haldager, Flyvbjerg, og Børglum formationerne. Der er ikke detekteret igangværende naturlig seismisk aktivitet i Jammerbugt området i form af jordskælv, men da nogle af forkastningerne fortsætter til nær havbunden, bør højopløselige seismiske data dog bruges til at vurdere om Holocæn tektonisk aktivitet har fundet sted i området. Forkastningsforsætning af både reservoir og segl kan have negativ indvirkning på både seglets effektivitet samt Gassum reservoirs sammenhængskraft og dermed den samlede lagringseffektivitet.

Jammerbugt strukturen har et forventet areal, reservoirtykkelse og kvalitet, der gør, at store mængder CO<sub>2</sub> formentlig vil kunne lagres, med det forbehold, at fremtidige undersøgelser kan verificere, at seglene har tilstrækkelig tykkelse, kvalitet og tæthed, også i forhold til forkastninger, til at holde CO<sub>2</sub> fanget i reservoir, og at reservoir i Gassum, Haldager og Flyvbjerg formationerne samlet set er sammenhængende nok til, at CO<sub>2</sub> kan injiceres effektivt.

Lagring i Jammerbugt strukturen kan således formentlig finde sted i to geologiske niveauer (Gassum Fm og Haldager Sand/Flyvbjerg Fm) beliggende i forskellig dybde og adskilt af mellemliggende segl bjergarter. Heraf vurderes det, at de største mængder kan lagres i Gassum Fm, mens lager potentialet i Haldager Sand Fm formentlig er beskedent. Monte Carlo simulering baseret på en 5 til 15% lagringseffektivitetskoefficient sandsynliggør et samlet lagerpotentiale på mellem 129 (P90) og 319 (P10) megaton CO<sub>2</sub> (gennemsnit: ca. 217 megaton). Dette estimat afhænger af faktorer, som formentlig vil ændres når nye data indsamles over strukturen og i takt med, at den regionale stratigrafiske tolkning og dybdekonvertering forbedres. Estimatet er særligt påvirkeligt af den anvendte lagringseffektivitetskoefficient og af det kortlagte lagringsvolumen. Gassum Fm vil jf. dette estimat bidrage med mellem ca. 122 (P90) og 289 (P10) megaton (gennemsnit:

199 megaton CO<sub>2</sub>), og anses således at udgøre det væsentligste reservoir i Jammerbugt strukturen. Vurderingen af lagerpotentialet er behæftet med usikkerhed og vil utvivlsomt ændres med fremtidig dataindsamling og analyse.

Yderligere dataindsamling af bl.a. 2- og 3D seismik på tværs af hele strukturen inklusiv det kystnære område, kortlægning og detailstudier af reservoirer, segl, forkastninger og andre geologiske risici, testboring, vurdering af trykforhold, reservoirsammenhæng, geomekanik og bjergartsstress, påvirkninger af geokemi og mineraler, modelleringer, detailevalueringer af CO<sub>2</sub> lagringskapacitet, tekniske risici bl.a. ifbm. boringer, osv., ligger udover dette projekt, men anbefales udført, f.eks. som led i en yderligere modning og evaluering forud for egentlig lagring.

# 1. Summary

Permanent CO<sub>2</sub> storage in geological subsurface structures is an efficient way for lowering emissions of greenhouse gases to the atmosphere. The Jammerbugt structure, located around 10 km offshore northwestern Jutland may be suited for permanent CO<sub>2</sub> storage depending on the results of future data acquisition and studies (Fig.1.1). Collection of around 1400 km of 2-D seismic data covering most of the structure in a systematic and relatively dense grid has enabled a first analysis of the structure and its storage potential (Fig.1.2). Data were collected using a 2.1 km long Sercel Sentinel SSRD streamer cable with 336 channels and using two GI airgun arrays of 2.4 to 5.8 L, respectively, operated at around 135 bar and fired in intervals of 6, 10 and 12 seconds. This yielded a nominal fold of 76, 45 and 38. Seismic quality of the reprocessed data is moderate, but the dense seismic grid over the study area enables a sufficient first characterization and mapping of the Jammerbugt structure. Seismic acquisition was restricted to water depth greater than 10 meters, and the near-shore part of the structure lacks seismic coverage.

The Jammerbugt structure outlines a three-way closure with two flanks confined by extensional faults and the opposite flanks delineated by the stratigraphic plunge (Figs.1.3; 1.4). Faults formed in response to Triassic–Cretaceous pulses of deep-seated extension. In addition, fault detachment in Zechstein salt caused roll-over folding in the overlying Mesozoic section, which influenced the structural architecture of the Jammerbugt structure giving rise to an anticlinal element in the closure geometry. Apart from the confining faults, the stratigraphy within the Jammerbugt structure – including reservoirs and seals – is offset by faults rooted in Triassic Oddesund Fm salt. Growth of an Oddesund Fm salt pillow under the northwestern part of the structure contributed to the closure relief in overlying section. Similarly, inversion doming associated with Late Cretaceous to Paleogene structural inversion of the Fjerritslev Trough slightly added to the closure relief of the Jammerbugt structure.

The Jammerbugt structure is undrilled, but correlation to wells drilled in the vicinity suggest the presence of two reservoir levels under structural closure: (1) the Gassum Fm and (2) the Haldager Sand Fm. Depth converted seismic mapping places the top of the Gassum Fm at around 1620 m and the Haldager Sand Fm at 1160 m at the crest of Jammerbugt structure. Closure size is mapped to be 119 km<sup>2</sup> and 142 km<sup>2</sup>, respectively and since Gassum Fm is tentatively anticipated to have a thickness of around 200 m, a net-to-gross of 0.5 and an average porosity around 20%, it is considered as the main reservoir with a modelled unrisked mean static CO<sub>2</sub> storage capacity of 199 megatons (MT) but ranging between 122 MT CO<sub>2</sub> (P90) and 289 MT CO<sub>2</sub> (P10). With a much lesser anticipated thickness and net-to-gross, the Haldager Sand Fm is modelled to have a mean static CO<sub>2</sub> storage capacity of 16 MT ranging between 7 MT CO<sub>2</sub> (P90) and 30 MT CO<sub>2</sub> (P10). In total, an unrisked mean storage potential of the 217 MT CO<sub>2</sub> is modelled for both reservoir units with a range between 129 MT CO<sub>2</sub> (P90) and 319 MT CO<sub>2</sub> (P10). The highly variable range mostly reflects the uncertainty in storage efficiency factor, reservoir quality and the prediction of gross reservoir rock volume that relies on the estimated reservoir thickness, closure size and height, all three of which is associated with considerable uncertainty due to the lack of state-of-the-art seismic coverage of the entire structure and intersecting wells.

The two reservoir intervals are overlain by thick mudstone successions. Seismic mapping and comparison to nearby wells suggest the Lower Jurassic Fjerritslev Fm overlying the Gassum Fm to measure a few hundred meters in thickness over the Jammerbugt structure and to be mudstone-dominated. The Fjerritslev Fm forms the primary seal for the Gassum Fm and is predicted

to comply with the seal recommendations for CO<sub>2</sub> storage. The Haldager Sand Fm is anticipated to be overlain by thickly developed Upper Jurassic Børglum Formation claystones that form a sealing unit. Information from nearby wells intersecting the fine-grained unit and seismic mapping suggest a great thickness of the Børglum Fm at the Jammerbugt structure that is also likely to comply with the seal recommendations for CO<sub>2</sub> storage.

A geological risk defined at this stage is associated with faulting of reservoir and seals with some fault continuing to near the seabed. Faults introduce a risk for reservoir leakage and compartmentalisation. The potential risk for leakage along fault planes needs further investigation. Additional seismic acquisition is therefore recommended including seismic acquisition over the presently uncovered nearshore part of the structure. While most wells suggest a great reservoir potential of the Gassum Fm, the vintage interpretation of the Upper Triassic to Lower Jurassic interval in the Fjerritslev-2 well located near Jammerbugt interferes with this image. The section in this well should therefore be reinvestigated if possible.

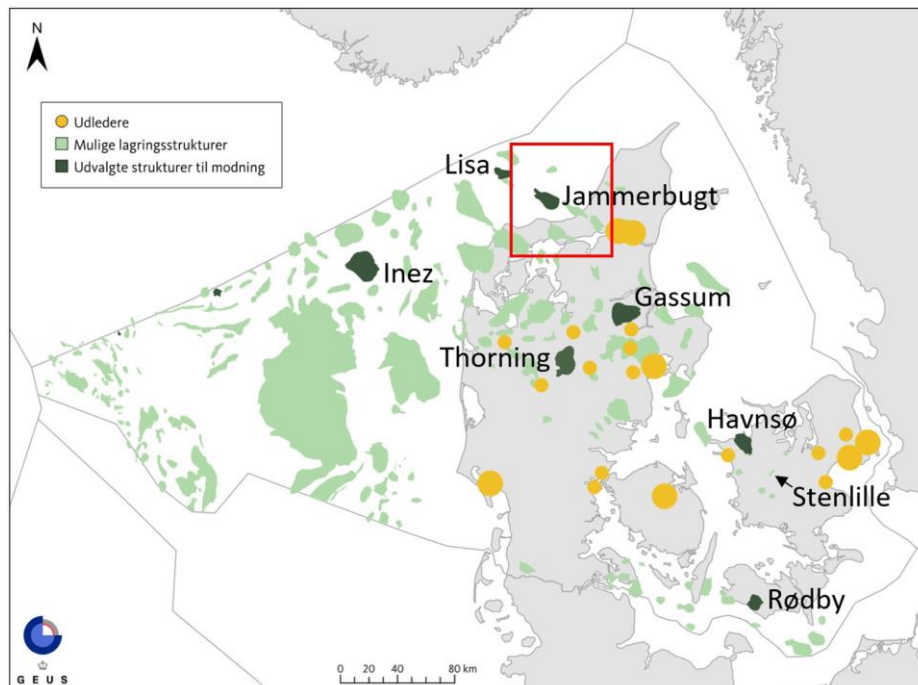


**Figure 1.1.** Map showing Danish subsurface structures potentially suited for geological CO<sub>2</sub> storage. Named structures are being matured in feasibility studies by GEUS. The Jammerbugt structure is the focus of the current study. Yellow circles denote major CO<sub>2</sub> point sources. Modified from Hjelm et al. (2022). The study area is outlined by a red box.

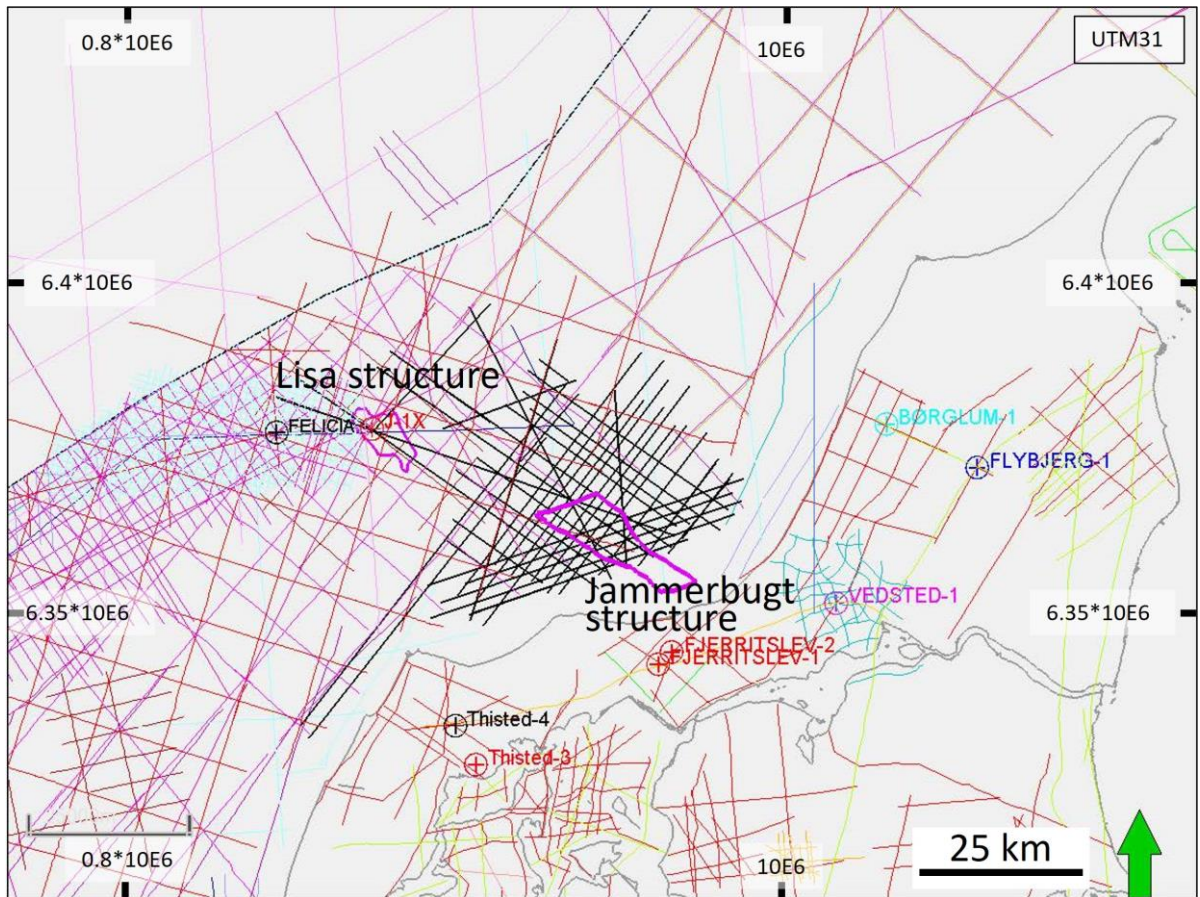


**Figure 1.2.** Map locating seismic data and wells around the Jammerbugt structure. The structure is outlined by bold pink polygon that denotes the mapped closures at the top of the Gasum Formation. Also indicated is the Lisa structure drilled by the J-1 well. Bold black lines denote the new Jammerbugt seismic survey (GEUS2023-JAMMERBUGT, Funck et al. 2023). Map projected in UTM31.

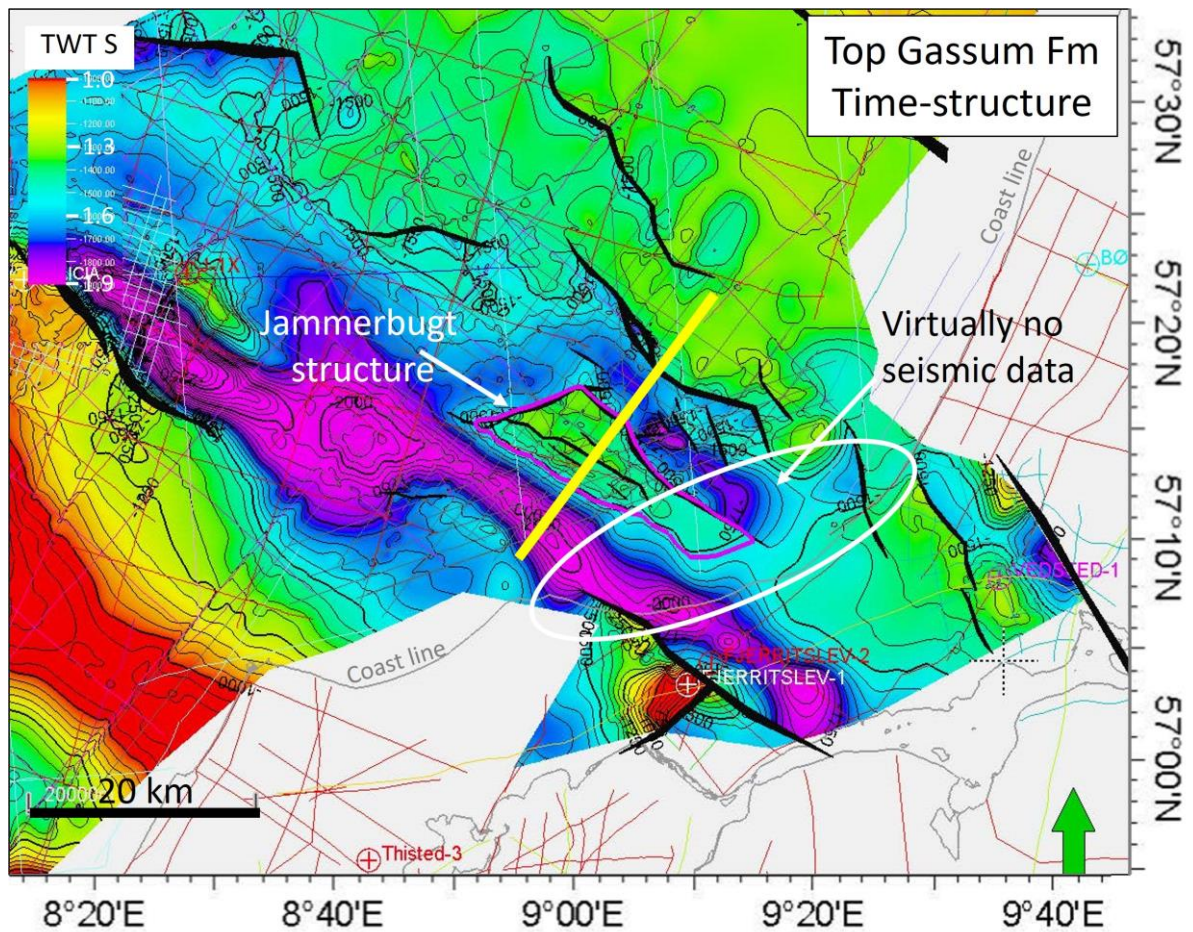


**Figure 1.3.** Two-way travel time (TWT) depth map to the top Gassum surface showing a well-defined, roughly 0.2 second high three-way closure outlined by the purple curve. Also shown are the position of seismic data and deep wells. Note the gap in seismic coverage over the near-coastal part of the Jammerbugt structure. The location of figure 1.4 is indicated by the yellow line.

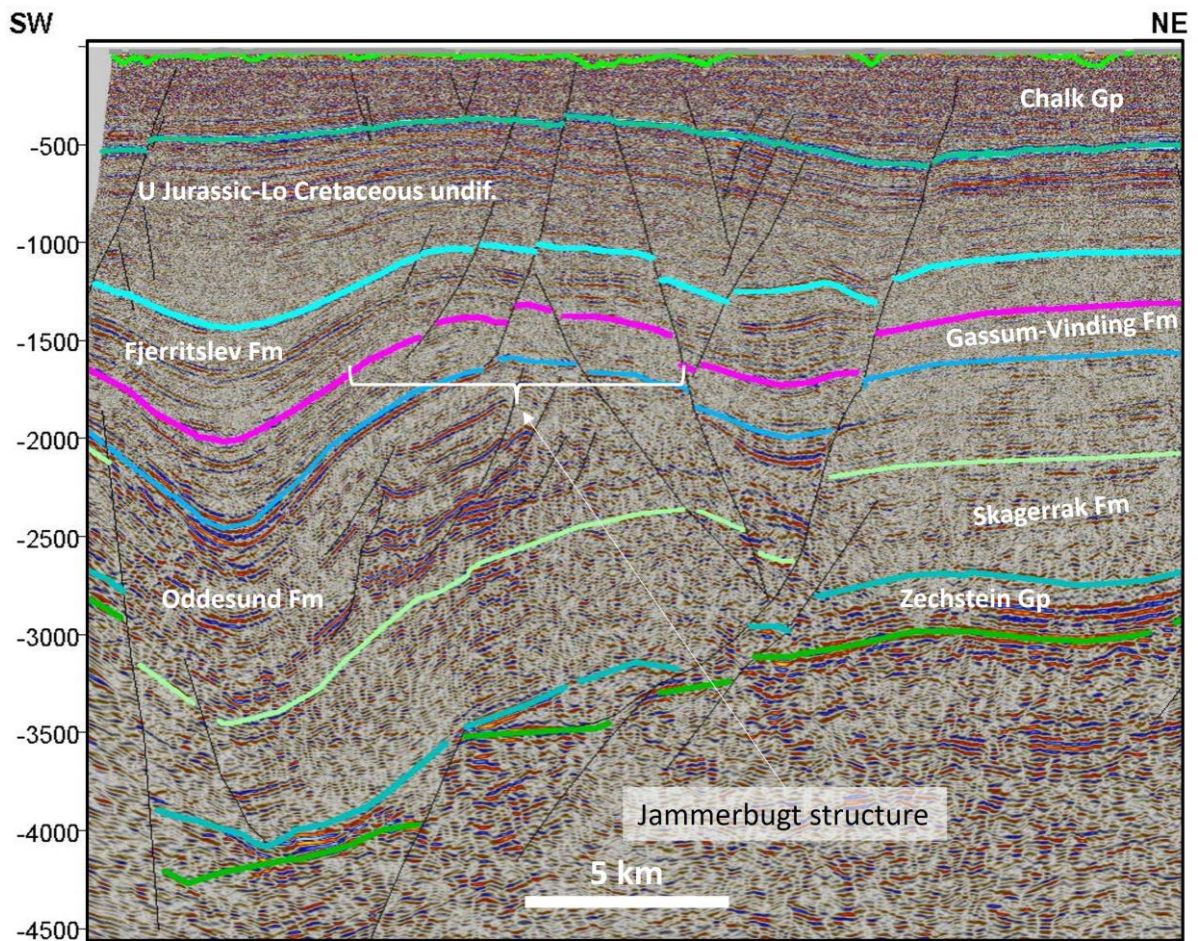


**Figure 1.4.** Seismic section across the Jammerbugt structure illustrating the seismic stratigraphic and structural geometry. Depth indicated in TWT milliseconds. Location shown in Figure 1.3.

## 2. Introduction

Sedimentary aquifers are well suited for permanent CO<sub>2</sub> storage, and carbon capture and storage (CCS) is an important instrument for considerably lowering atmospheric CO<sub>2</sub> emissions (IPCC 2022). The Danish subsurface is highly suited for CO<sub>2</sub> storage, and screening studies document a large geological storage potential that is widely distributed across the country and adjacent seaways [Fig. 1.1] (Frykman et al. 2009; Hjelm et al. 2022; Mathiesen et al. 2022). The significant Danish storage potential is rooted in the favorable geology that includes excellent and regionally distributed reservoirs, tight seals, large structures and a relatively quiescent tectonic environment. The largest storage potential is contained within saline aquifers (Hjelm et al. 2022). Subsurface aquifers overlain by tight cap rocks (reservoir/seal pairs) of variable age exist underneath most of Denmark, and the greatest number of documented reservoir/seal pairs occurs in the North Sea part of the Norwegian–Danish Basin (Mathiesen et al. 2022). Moreover, this part of the North Sea hosts many large structures, and the offshore area is considered to hold a significant CO<sub>2</sub> storage potential (Mathiesen et al. 2022). The Jammerbugt structure is one of the least known of these structures located in the nearshore, Danish part of Skagerrak in the north-eastern North Sea. In a geological context, the structure is located in the Fjerritslev Trough [also referred to as the Aalborg Graben] (Fig. 2.1) [Christensen & Korstgård 1994]. The Jammerbugt structure is in a very early stage of maturation partly covered by a regular 2-D seismic grid but remains to be drilled. In this study, the Jammerbugt structure and the adjacent area is investigated geologically based on available seismic and well data in order to characterize its tectonic and depositional evolution and to investigate if the structure could be suited as geological CO<sub>2</sub> storage site pending on further maturation.

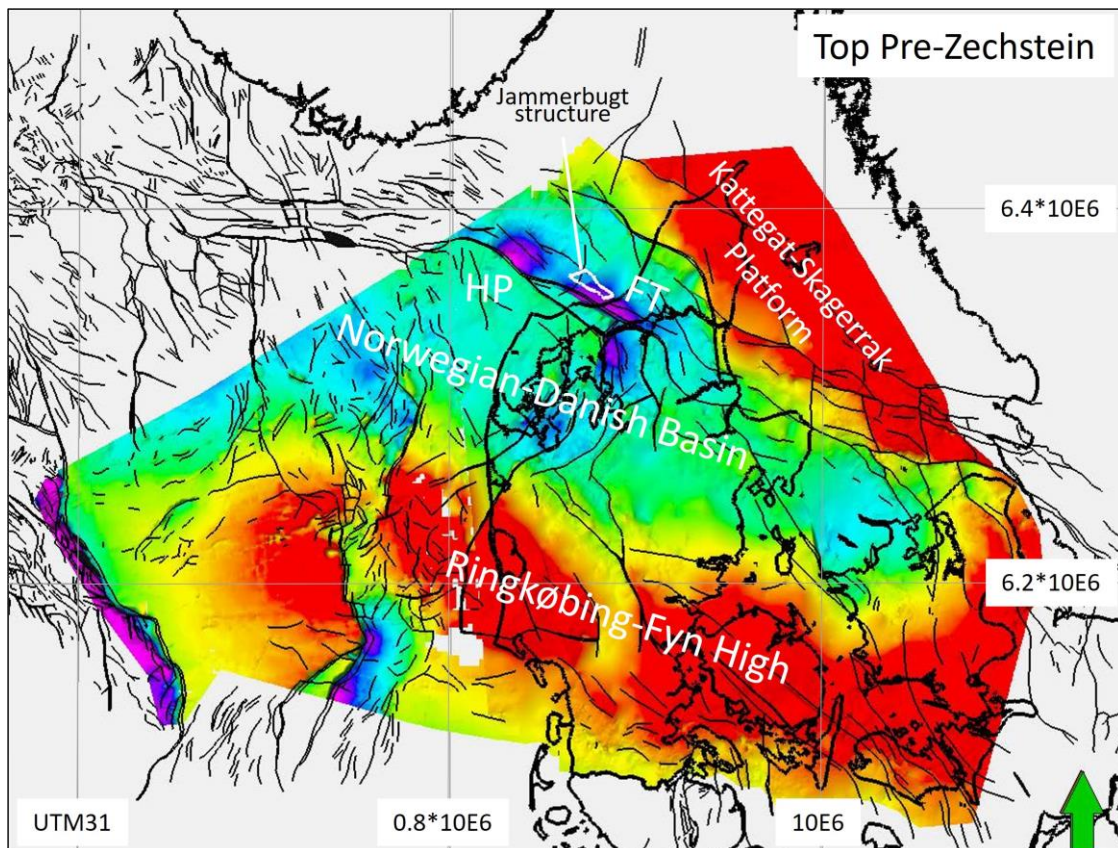


**Figure 2.1.** Regional structural setting shown on a Top pre-Zechstein structure map. Structural highs indicated by yellow to red colours while blue to purple colours outline depressions. HP: Hurup Plateau; FT: Fjerritslev Trough. Map projected in UTM 31.

### 3. Geological setting

The Fjerritslev Trough extends from the Norwegian–Danish shelf and continues onshore Jutland to the southeast (Fig. 2.1). The trough forms part of the Sorgenfrei–Tornquist Zone that physically borders the Norwegian–Danish Basin separating it from the Fennoscandia shield to the northeast (Thybo 2000). The offshore part of the trough is little investigated (Christensen & Korstgård 1994; Liboriussen et al. 1987; Fyhn et al. 2023). It is separated from the Hurup Plateau to the southwest by the Fjerritslev Fault and passes into the Skagerrak–Kattegat Platform that forms a ramp towards the northeast. Towards the northwest, the Fjerritslev Trough grades into the Norwegian Farsund Basin. The Fjerritslev Trough in the Jammerbugt structure area outlines a half-graben confined by the NW–SE-striking Fjerritslev Fault Zone located around twenty km southwest of the structure (Fig. 2.1). The fault zone, as the rest of the Sorgenfrei–Tornquist Zone, has experienced different phases of deformation since the Late Palaeozoic (Mogensen & Korstgård 2003; Fyhn et al. 2023).

The Norwegian–Danish Basin together with the Fjerritslev Trough is filled with Palaeozoic through Cenozoic deposits and is floored by crystalline basement and presumable sedimentary patches of lower Palaeozoic age (Vejbæk 1997). Late Palaeozoic extension laid the ground for the subsequent basin formation and is reflected in thickly developed Devonian(?) to Permian syn-rift deposits and Upper Carboniferous–Permian volcanic rocks filling grabens and half-grabens (Stemmerik et al. 2000). The upper Palaeozoic syn-rift succession is overlain by Zechstein (Upper Permian) evaporites formed after the Palaeozoic rifting in response to episodic marine, restricted connections northward through the proto-northern North Atlantic seaway in a warm arid climate (Glennie et al. 2003). While rifting recommenced during the Early Triassic in much of the North Sea area (McKie 2014), thermal contraction and post-rift subsidence continued in the Norwegian–Danish Basin (Fyhn et al. 2023). So did the dryland climate; and at the same time, the marine influence retreated (McKie & Williams 2009). This paved the way for a fluvial-playa-dominated depositional environment in the Early Triassic associated with deposition of the Bunter Shale-, Bunter Sandstone- and the Skagerrak formations (Fm) in the Norwegian–Danish Basin, the latter of which formed in fluvial-dominated, more proximal settings next to the uplifted Fennoscandia shield [Fig. 3.1] (Bertelsen 1980; Michelsen & Clausen 2002; McKie & Williams 2009). Michelsen and Clausen (2002) restricted the use of the Bunter Shale- and Bunter Sandstone fms to the North German Basin and attributed all of the Lower Triassic and most of the Middle Triassic in the Danish part of the Norwegian-Danish Basin to the Skagerrak Fm. We here follow their recommendation.

In the Middle and Late Triassic, rifting on a regional scale continued, the shores of the Tethys Ocean shifted northwards, and precipitation increased slightly (McKie 2014). Combined, this enhanced playa development often associated with evaporites. The Sorgenfrei–Tornquist Zone was affected by right-lateral transtension during part of the Triassic. In the northern end of the Sorgenfrei–Tornquist Zone - and forming the continuation of the Fjerritslev Trough - the Farsund Basin experienced Triassic extension (Phillips et al. 2018) (Fig. 2.1). Even so – and in contrast to the findings of this study, Liboriussen et al. (1987) and Fyhn et al. (2023a) – Christensen and Korstgård (1994) interpreted the Triassic Fjerritslev Trough as tectonically quiescent. Instead, they interpreted the significant intra-Triassic fault offsets and considerable lateral thickness variations to be associated with mobilization and evacuation of underlying Zechstein salt. Christensen and Korstgård (1994) similarly interpreted the Jurassic to mid-Cretaceous as a tectonically calm period in the Fjerritslev Trough, once again contrasting with the findings of this study and the coeval

rifting and transtension in the neighbouring Farsund Basin and other parts of the Sorgenfrei-Tornquist Zone farther east (Mogensen & Jensen 1994; Phillips et al. 2018).

A restricted connection to the Tethys existed episodically in the Late Triassic (Bertelsen 1980; 1978; McKie & Williams 2009), which developed into a more permanent connection during Rhaetian time. As climate became more humid during the Rhaetian, deltas developed along the northern and north-western fringe of the Norwegian-Danish Basin associated with deposition of the sandy Gassum Fm (Nielsen 2003). The Gassum Fm is up to more than 200 m thick and consists of sandstones and mudstones with a higher compositional maturity than older Triassic strata. While the Gassum Fm signifies a regionally wetter climate and an increase in compositional maturity, it has a significant feldspar content in especially the north-western part of the basin (Olivarius et al. 2022).

Transgression continued during Hettangian–Sinemurian time. The basin became subject to open marine conditions and the shaly Fjerritslev Fm developed (Michelsen et al. 2003). Sand incursion persisted into the Early Jurassic, and sand interludes belonging to the Gassum Fm exist encased in the Fjerritslev Fm in the northeastern part of the basin (Nielsen 2003; Vosgerau et al. 2016). (Bertelsen 1978; Nielsen 2003). Rapid Early Jurassic subsidence resulted in the Fjerritslev Fm being up to more than a kilometre thick in the Fjerritslev Trough.

Middle Jurassic uplift and erosion led to the establishment of the mid-Cimmerian unconformity regionally over the Danish area (Nielsen 2003). Uplift and erosion were largely insignificant over the central Fjerritslev Trough and the event is here recorded as a basinward shift in facies and the development of the sand-prone Haldager Sandstone Fm containing compositionally mature, fluvial to shallow marine sandstones typically with an excellent reservoir potential interbedded with mudstones. The Haldager Sandstone Fm is typically thickest developed within the Sorgenfrei-Tornquist Zone but also here varies greatly in thickness. Renewed subsidence led to flooding over the Danish area during Jurassic times, which led to deposition of Flyvbjerg and Børglum fms mudstones that are typically thickest developed in the Fjerritslev Trough and other depressions within the western Sorgenfrei-Tornquist Zone (Nielsen and Japsen 1991). However, much of the Hurup Plateau presumably remained above sea level and was subject to erosion during most of the rest of the Jurassic and only became flooded in the latest Jurassic or Early Cretaceous (Fyhn et al. 2023).

The Middle Jurassic to Lower Cretaceous is thickly developed within the Fjerritslev Trough and the Børglum Fm is overlain by Frederikshavn Fm silt-, fine-grained sand- and mudstones and Vedsted Fm mudstones that typically has a combined thickness of several hundred meters within the trough (Nielsen and Japsen 1991).

These Middle Jurassic to Lower Cretaceous mostly fine-grained siliciclastic deposits are overlain by the Upper Cretaceous Chalk Group. Chalk in the Fjerritslev Trough varies in thickness. This is mostly due to differential erosion caused by localized inversion of the Fjerritslev Trough and associated doming followed by Neogene regional uplift (Mogensen and Jensen 1994; Japsen et al. 2007). The Jammerbugt area has experienced around 800 meters to one kilometre of uplift and erosion since the Late Cretaceous (Japsen et al. 2007). The chalk therefore sub-crops the seabed in places or is capped by a thin veneer of Pleistocene fluvial and/or glaciogenic deposits and Holocene strata.

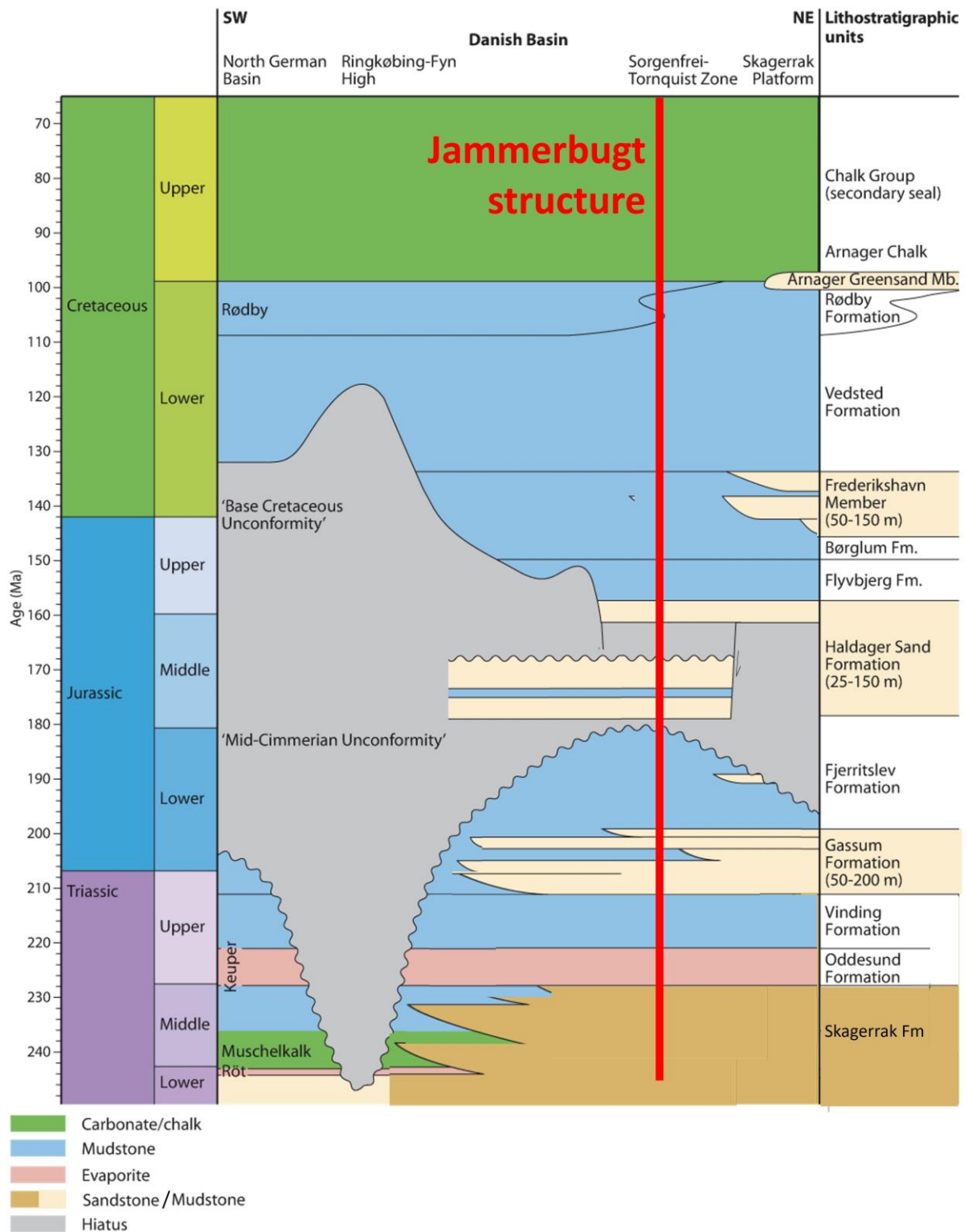


**Figure 3.1.** Simplified Mesozoic stratigraphy of the Danish North Sea area outside Central Graben illustrating the anticipated stratigraphy at the Jammerbugt structure. Modified from Mathiesen et al. (2022) and Nielsen (2003).

## 4. Database

### 4.1 Seismic data

Before 2023, the Jammerbugt structure and the surrounding area had a very limited 2-D seismic coverage of lines ranging from good to poor quality. In April 2023, around 1400 km of 2-D seismic data were collected in the Jammerbugt covering most of the Jammerbugt structure in a dense and systematic grid. The acquisition was carried out using the Faroese research vessel Jákup Sverri. For safe navigation, the survey was limited to areas with a water depth of at least 10 m. In addition, a minimum distance of 10 km had to be kept to the Natura2000 marine protected areas. Apart from covering most of the structure, three ties to the J-1 well were achieved as well as to the existing vintage seismic grid. Acquisition was carried out in collaboration with the Federal Institute for Geosciences and Natural Resources (Bundesanstalt für Geowissenschaften und Rohstoffe, BGR) in Hanover, Germany, and Aarhus University using BGR's 2100-m-long Sercel Sentinel SSRD streamer cable. Acquisition parameters are summarized in Table 4.1.1.

**Table 4.1.1.** Summary of acquisition parameters

Parameter	Setup A	Setup B
GI-gun: volume of generator	45 cubic inches (0.7 L)	250 cubic inches (4.1 L)
GI-gun: volume of injector	105 cubic inches (1.7 L)	105 cubic inches (1.7 L)
Gun operation mode	True GI-mode	Harmonic mode
Number of GI-guns in cluster	2	2
Depth of seismic source	3 m	3 m
Depth of streamer cable	3 m	4 m / 5 m
Pressure of GI-guns	2000 psi (138 bar)	1958 psi (135 bar)
Sample interval	1 ms	1 ms
Record length	5 s	6 s
Shot delay	50 ms	50 ms
Number of channels	336	336
Distance between channels	6.25 m	6.25 m
Shot interval	6 s	10 s / 12 s
Shot spacing	~14 m	~23 m / ~27 m

Thirty-nine seismic lines were collected (JB-1 to JB-39) (Fig. 4.1.1). Two different setups were used for the seismic sources (Table 4.1.1). Setup A used a source with a combined volume of 150 cubic inches (2.4 L) operated at 138 bar and fired every 6 seconds. During the cruise, the configuration was changed to setup B in order to test the effect on data quality of using a larger acoustic source of 355 cubic inches (5.8 L) operated at roughly the same pressure but with longer shot spacings ranging from 10 to 12 seconds. Lines GEUS23\_JB\_01 to 10 were collected using Setup A, while lines GEUS23\_JB\_11 through 39 were collected using setup B (Table 4.1.2). Lines GEUS23\_JB\_01 to 05 were re-shoot or partly re-shoot (GEUS23\_JB\_35 to 39) at the end of the survey to determine the variation in data quality. An inspection of the seismic records shows only minor differences between the two setups. This likely reflects that the higher fold of setup A compensates for the somewhat greater amount of energy sent into the subsurface using setup B. Acquisition details are specified in Funck et al. (2023). Data are available online for download: [GEUS2023-JAMMERBUGT-RE2023 report](#).



**Table 4.1.2.** Summary of recording parameters for individual lines. Lines GEUS23\_JB\_35 through 39 are re-shootings of lines GEUS\_JB\_04, 05, 08, and 09, using the larger GI-gun array.

Line name GEUS23 _JB_*	Record length (s)	Shot inter- val (s)	Source depth (m)	Strea- mer depth (m)	Source (with generator/in- jector volume in cubic in.)	Comments
01	5	6	3	3	2 GI (45/105)	
01A	5	6	3	3	2 GI (45/105)	
02	5	6	3	3	2 GI (45/105)	
03	5	6	3	3	2 GI (45/105)	
04	5	6	3	3	2 GI (45/105)	
05	5	6	3	3	2 GI (45/105)	
06	5	6	3	3	2 GI (45/105)	
07	5	6	3	3	2 GI (45/105)	
08	5	6	3	3	2 GI (45/105)	
09	5	6	3	3	2 GI (45/105)	
10	5	6	3	3	2 GI (45/105)	
11	5	12	3	4	2 GI (250/105)	
12	6	12	3	4	2 GI (250/105)	
13	6	12	3	4	2 GI (250/105)	
14	6	12	3	4	2 GI (250/105)	
15	6	12	3	4	2 GI (250/105)	
16	6	12	3	4	2 GI (250/105)	
17	6	12	3	4	2 GI (250/105)	Streamer at 6 m (SP 2262-2560)
18	6	12	3	4	2 GI (250/105)	
18A	6	12	3	5	2 GI (250/105)	
19	6	12	3	5	2 GI (250/105)	
19A	6	10/12	3	5	2 GI (250/105)	Testing shot interval
20	6	10	3	5	2 GI (250/105)	Streamer at 7 m (SP 3128-3252)
21	6	10	3	5	2 GI (250/105)	
21B	6	10	3	5	2 GI (250/105)	
22	6	10	3	5	2 GI (250/105)	
22A	6	10	3	5	2 GI (250/105)	
23	6	10	3	5	2 GI (250/105)	
24	6	10	3	5	2 GI (250/105)	
25	6	10	3	5	2 GI (250/105)	
26	6	10	3	5	2 GI (250/105)	
27	6	10	3	5	2 GI (250/105)	
28	6	10	3	5	2 GI (250/105)	
29	6	10	3	5	2 GI (250/105)	
29A	6	10	3	5	2 GI (250/105)	Lower pressure (SP 1020-1077)
30	6	10	3	5	2 GI (250/105)	
31	6	10	3	5	2 GI (250/105)	Issues with one gun (SP 1050-1300)
32	6	10	3	5	2 GI (250/105)	Lower Pressure (SP 1022-1107)
33	6	10	3	5	2 GI (250/105)	
34	6	10	3	5	2 GI (250/105)	
35	6	10	3	5	2 GI (250/105)	Re-shoot of line GEUS23_JB_10
36	6	10	3	5	2 GI (250/105)	Re-shoot of line GEUS23_JB_09
37	6	10	3	5	2 GI (250/105)	Re-shoot of line GEUS23_JB_08
38	6	10	3	5	2 GI (250/105)	Re-shoot of line GEUS23_JB_05
39	6	10	3	5	2 GI (250/105)	Re-shoot of line GEUS23_JB_04

### 4.1.1 Processing

The initial processing of the Jammerbugt-2023 survey performed at the University of Aarhus consisted of the following steps:

- Reading SEG-D data
- Definition of geometry. Events are related to files number so that source positions can be imported. Water depth has been entered as well.
- CDP binning have been accomplished using a CDP bin size of 3.125 m.
- Geometry has been loaded into the seismic data
- Low cut filter (in order to get rid of swell noise). Ormsby filter cut off: 8-12 Hz
- Header statics (-50 ms) to compensate for gun delay
- Compensating for spherical divergence and absorption correction
- Spike-Noise burst edit.
- Suppression of bubble pulse by applying low cut filter in a narrow time window around the bubble pulse: Ormsby filter: cut off frequency 20-25 Hz
- High-Cut filter in two time windows: Top window: High cut filter Ormsby filter: 140-170 Hz. Bottom window: High cut filter Ormsby filter: 120-160 Hz
- In second pass: Application of CDP trim statics
- Top mute in order to remove direct and refracted waves
- Normal Move Out (NMO) correction. Velocities from velocity analysis.
- Top mute (second pass)
- FK-filter to suppress linear noise both moving away from the seismic vessel and toward the vessel. FK-filter have been applied in two time windows. The most effective and narrow acceptance FK-filter has been applied in the bottom time window.
- Inverse Normal Move Out correction
- Trace length reduced to 5500 ms
- Output of processed shotgathers
- Velocity analyses
- Normal Move Out correction
- Median filtered water depth read into the seismic headers
- Estimated two-way time for water bottom reflection have been found from median filtered water depth
- Trace length reduction to 5000 ms.
- CDP stacking.
- Output of stack data set.
- Spectral shaping: Reduction of low frequency amplitudes in an attempt to get a flatter amplitude spectrum.
- FX deconvolution.
- SEG-Y output. File names \*\_ver3.
  - I. CDP coordinates transferred to source and receiver positions in SEG-Y headers.
- Trace mix over three traces (weight 1, 2, 1).
- Automatic Gain Control (AGC) window 500 ms blended with AGC window length of 100 ms.
- Trace length reduced to 5000 ms.
- Predictive deconvolution in two time windows. Prediction gap based on Water bottom time.

- Operator length 25 ms. Prewhitening 1 %.
- Bandpass filter in three time windows: High-cut filter:
  - I. Top window: Ormsby filter: 100-120 Hz.
  - II. Center window: Ormsby filter: 80-100 Hz.
  - III. Bottom window: Ormsby filter: 70-90 Hz.
- SEG-Y output. File names \*\_ver3d.
  - CDP coordinates transferred to source and receiver positions in SEG-Y headers.
- Trace mix over three traces (weight 1, 2, 1).
- AGC window 500 ms blended with an AGC with a window length of 100 ms.
- Trace length reduced to 5000 ms.
- AGC 500 ms window length.
- FK Stolt migration. Velocity field: smoothed velocity field from the velocity analysis.
- Applying the three-window bandpass filter as mentioned above.
- SEG-Y output. File names \*\_ver3d\_mig.
  - I. CDP coordinates transferred to source and receiver positions in SEG-Y header.
  - II. Trace mix over three traces (weight 1, 2, 1).
- AGC window 500 ms blended with an AGC with a window length of 100 ms.
- Trace length reduced to 5000 ms.

The top of the chalk forms a hard surface located closely beneath the seabed or even subcropping the seafloor in Jammerbugt. The base of the chalk on the other hand forms a very significant soft surface characterized by a downwards decrease in acoustic impedance. Together with shallow water, this has a tendency of causing very strong multiples and challenges transmittal of adequate acoustic energy into the sub-chalk section. The initial processing steps left many peg-leg and seabed multiples and a low signal-to-noise ratio in the main target interval of this study (Triassic-Jurassic). A reprocessing of the data was therefore commissioned.

#### **4.1.2 Reprocessing**

In October 2023, GEUS hired the geophysical company Realtimeseismic (RTS) to reprocess the 2D seismic data sets from the GEUS2023-JAMMERBUGT survey with the following objectives:

1. Obtaining optimal resolution for identifying key geologic formations and features in the area.
2. Suppressing noise, primarily multiple reflections.
3. Ensuring the optimal tie between the seismic lines.

In general, the reprocessing aimed to improve the migrated stack sections from the original processing and help the current geological interpretation of the Jammerbugt structure. The reprocessing project was officially named GEUS2023-JAMMERBUGT-RE2023 and took around seven weeks, from October 9 until December 15, 2023. The reprocessed seismic data and the reprocessing report are available and can be accessed from GEUS [GEUS2023-JAMMERBUGT-RE2023 report](#) (Realtime Seismic 2023).

**Table 4.1.2.1** Processing sequence implemented in the reprocessing.

<b>No.</b>	<b>Processing component</b>
1	Input analysis
2	Geometry QC
3	Acquisition delay correction
4	Low-cut filter
5	Spherical divergence correction
6	Swell noise attenuation
7	Surface-consistent amplitude correction
8	Receiver motion correction
9	Linear noise attenuation (LNA)
10	Deghosting
11	Designature
12	Surface-related multiple elimination (SRME)
13	Q compensation in phase
14	Residual denoising
15	3D regularisation
16	Migration velocity updating
17	Residual moveout (RMO) correction
18	Prestack time migration (PSTM)
19	High-resolution radon demultiple
20	Q compensation in amplitude
21	Trim statics
22	Spectral shaping
23	Outside mute
24	Dip estimate
25	Structure-oriented denoising (SOD)
26	Post-stack enhancement

RTS initiated the reprocessing through an assessment and reprocessing test on seismic line GEUS23\_JB\_30. Based on the reprocessing test result, which met our expectations, we evaluated, modified, and approved the processing sequence proposed by RTS. The general processing sequence implemented in the reprocessing is given in Table 4.1.2.1. The detailed processing sequence and parameters used in the reprocessing are shown in the reprocessing report (Realtime Seismic 2023).

Processing multichannel, shallow marine seismic data for a deep target is particularly challenging because of noise recorded at the acquisition stage. Understanding the source and the trigger mechanism of the noise and its characteristics on a seismic profile is the key to determining an optimal processing sequence and parameters for noise attenuation. Once the recorded noise is understood, the success of the noise attenuation strongly depends on a proper

selection of the denoising technique, which constitutes the domain in which the noise can be separated from the signal, such as the time domain, frequency-offset (FX) domain, and frequency-wave number (FK) domain. In the following part, the types of noise that mainly affect seismic data acquired from the GEUS2023-JAMMERBUGT survey are described. Understanding them is crucial to assess the relevance of the processing sequence implemented in the reprocessing (Table 4.1.2.1).

A: Multiple reflections

Multiple reflections occur when the seismic waves propagate along the same ray path more than once, producing seismic wave arrivals that repeat themselves on the shot gathers and stack profiles. The first multiple arrival time of the seabed is exactly twice the actual arrival time of the seabed. If the seabed is dipping, the dip of its multiple reflections increases on the stack sections. In general, demultiple techniques fall under two categories (Yilmaz, 2001; Bashir et al., 2022): 1) based on moveout discrimination between the primary and multiple reflections, such as radon transform, and 2) based on a prediction theory, such as surface-related multiple eliminations (SRME) [Verschuur et al., 1992]. Both radon transform and SRME were implemented in the reprocessing.

B: Swell noise

Swell noise is the most dominant type of marine seismic data noise caused by waves and turbulence during seismic data recording. This noise is characterized by its low frequency, which is usually in the range of 0 – 10 Hz, and high amplitude, and it can be recognized by its distinctive linear pattern and streaks on a shot record (Fig. 4.1.2.1). Swell noise can be suppressed using low-cut and FX filters. The reprocessing included both low-cut and FX (swell noise attenuation) filters.

C: Mechanical cable noise (tug and strum)

Mechanical cable noise is often indicated by diagonal crossing streaks dominating a shot record (Fig. 4.1.2.2). This noise is caused by the stretch tensile of both the vessel and tail buoy on the streamer during towing (Dondurur, 2018). If the noise comes from the far offset, it has negative dip and is known as the tug. If the noise comes from the opposite direction, it has a positive dip referred to as strum. This noise can be suppressed using dip-based filters such as structure-oriented denoising (SOD), which was also used in the reprocessing.

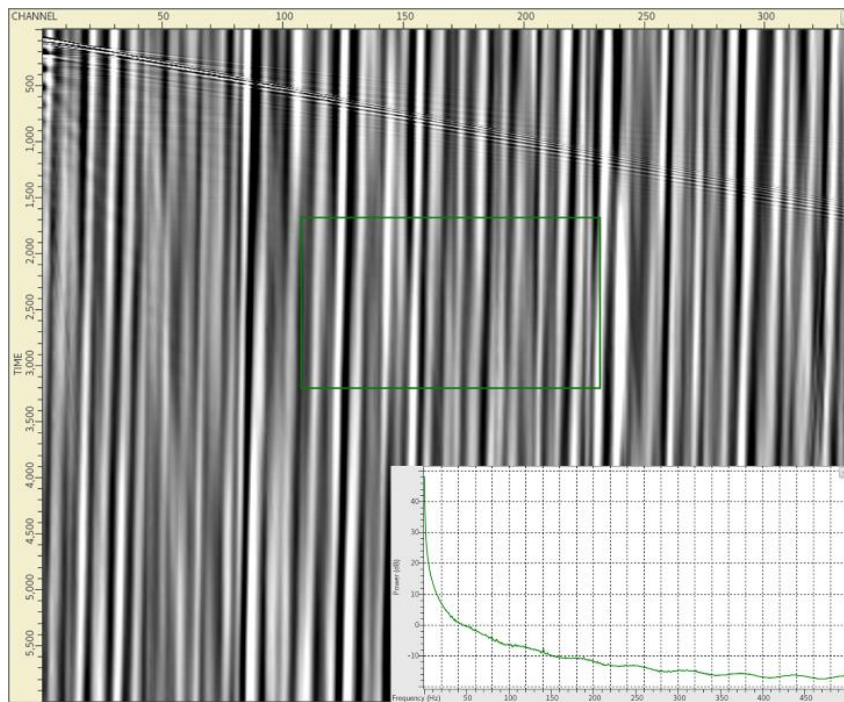


**Figure 4.1.2.1.** Swell noise on a raw shot profile from line GEUS23\_JB\_20. The inset displays the amplitude spectrum from the area highlighted by the green box, showing a high amplitude between 0 and 10 Hz

#### D: Direct waves

Direct waves propagate directly from the source to the receivers, making the first arrivals at each receiver (Fig. 4.1.2.2). The time difference between the primary seabed reflections and the direct waves is maximum at the nearest receiver and decreases with offset (Dondurur, 2018). The direct waves are asymptotic to the seabed reflections at infinite offset. Direct waves never interfere with the seabed reflections; therefore, they are usually not a big issue for processing. Direct waves can be removed by muting all amplitudes before the seabed arrivals (top mute).

#### E: Refracted waves

Refracted waves or head waves travel horizontally along the near-surface sediments before they reach the receivers (Fig. 4.1.2.2). Since they travel with the propagation velocity of the sediments, they always have higher velocity and lower dip than the direct waves on the shot records. Like the direct waves, refracted waves always come at the receivers before the seabed reflections and are usually not problematic for processing. Refracted waves can be removed by using a top mute.

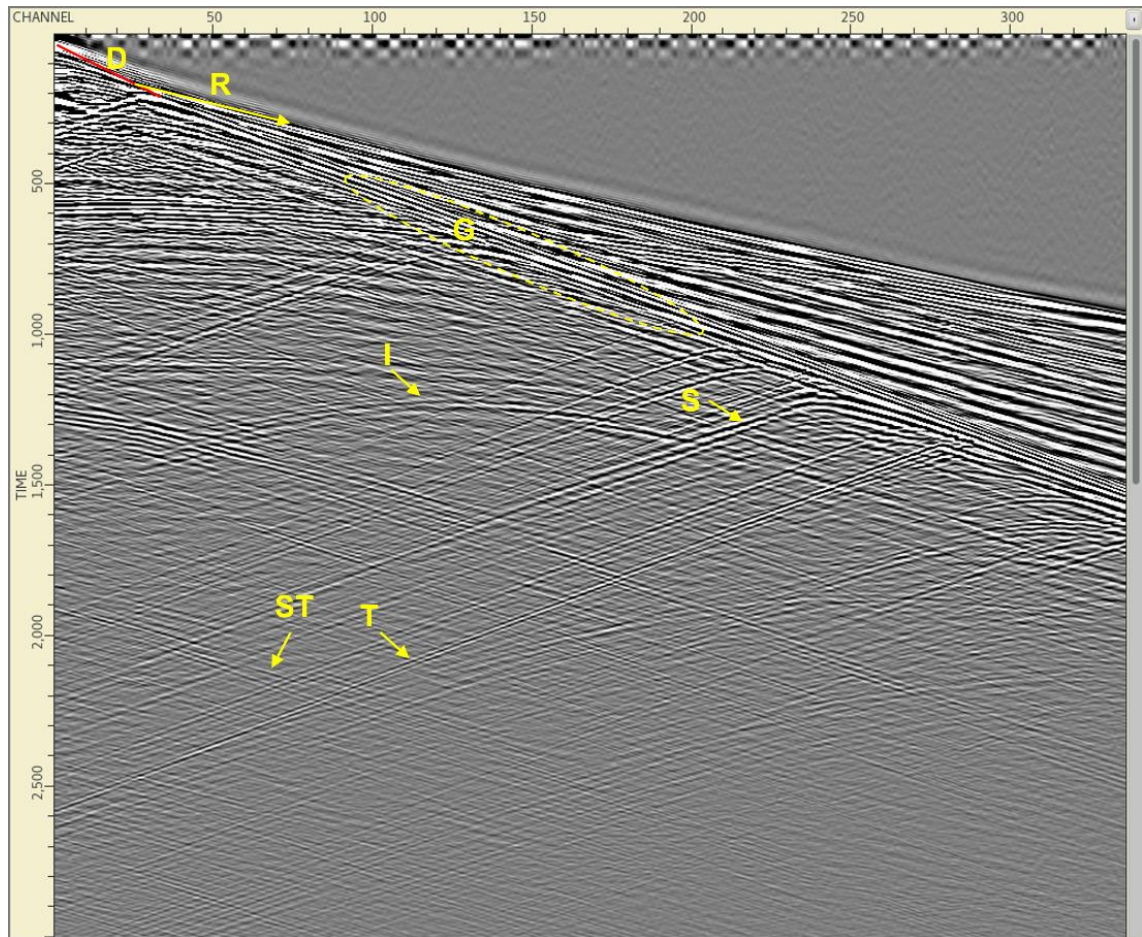


**Figure 4.1.2.1.** A shot record from line GEUS23\_JB\_35 showing some noise, including direct waves (D), refracted waves (R), guided waves (G), seismic interference from another vessel close to the center part of the streamer (I), diffractions (S), strum (ST) and tug (T) with possible interference with the diffractions. Red and yellow lines highlight the different trend angles of the direct and refracted waves. Note that some noise requires additional analysis to be identified with certainty.

F: Diffractions and side-sweeps.

Diffractions are produced by water bottom anomalies, usually represented by seafloor morphology irregularities, or subsurface discontinuities such as faults and act as point scatterers. These irregularities produce diffraction hyperbolas on the shot records (Fig. 4.1.2.2). and stack sections. When the diffractions come from the out-of-plane of a 2D profile, they are also known as side-sweeps. Side-sweeps in the shot gather can be suppressed by using radon transform, which was included in the reprocessing. On a 2D stack profile, in-line diffractions can be entirely removed by a suitable 2D migration algorithm. In contrast, side-sweeps often remain since 2D migration cannot remove the 3D (out-of-plane) effects from the seismic data. Prestack time migration (PSTM) applied in the reprocessing can also be seen as a technique to collapse the diffractions in the seismic data.

G: Guided waves

Guided waves are caused by a strong velocity contrast between the water layer and the substratum (Fig. 4.1.2.2). The velocity contrast causes the waves to be trapped and

travel horizontally within the water layer. Guided waves also make up the early arrivals and include supercritical multiple reflections. Guided waves can be suppressed using radon transform, which was utilized in the reprocessing.

#### H: Seismic interferences

Seismic interferences are noise caused by external seismic sources, such as a seismic source from another vehicle in the surroundings. Noise coming from another marine seismic vehicle has trace-to-trace consistency on the shot records and emerges at regular time intervals following the shooting rate of the noise source. The noise shape and techniques to suppress it depend on the direction of the interference source relative to the recording streamer. If the source position is somewhere close to the centre of the streamer, the noise appears as a hyperbolic moveout (Fig. 4.1.2.2). This noise can be removed by stacking and radon transform, which were accommodated in the reprocessing.

Most of the dominant noise contamination in the seismic data from the GEUS2023-JAMMER-BUGT survey was understood and anticipated before and during the reprocessing so that the reprocessing could be tailored to deal with them. Besides the denoising techniques, the migration technique to correct reflector positions, also dictated the effectiveness of the reprocessing. The reprocessing utilized a PSTM technique to anticipate conflicting dips with different stacking velocities and complex non-hyperbolic moveouts.

The reprocessing results in terms of PSTM stack profiles show significant improvement from the migrated stacks produced by the original processing, especially at zones where multiples are prominent on the profiles from the original processing. As an example, Figure 4.1.2.3 shows the comparison of the original and reprocessing results for line GEUS\_JB\_20.

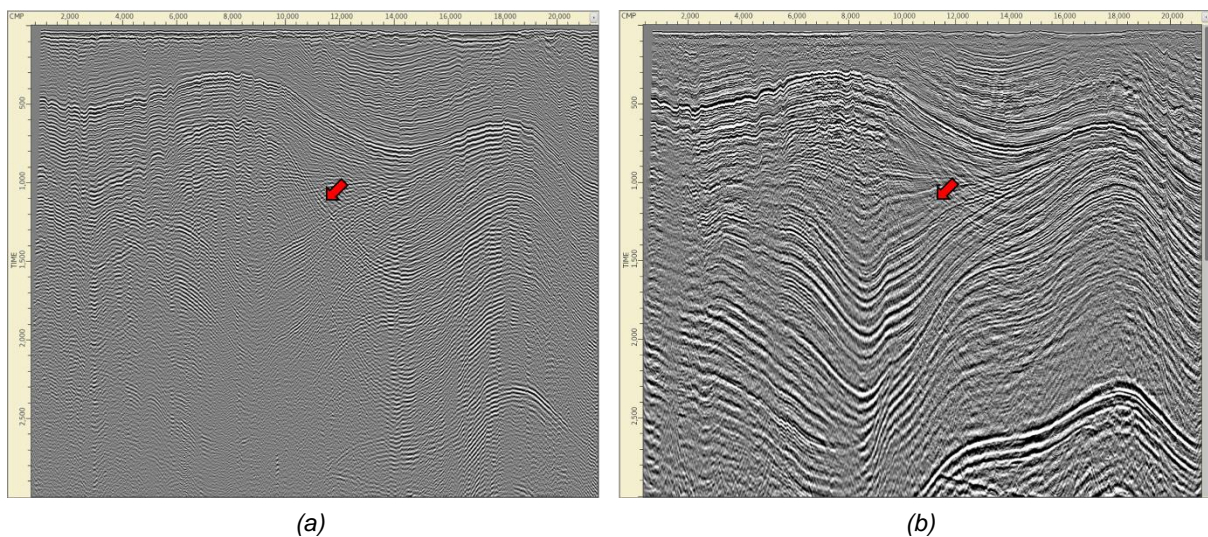


**Figure 4.1.2.3.** Comparison between (a) the original processing and (b) reprocessing results on line GEUS23\_JB\_30. The results were processed with poststack time migration and prestack time migration for the original processing and reprocessing, respectively. No automatic gain control (AGC) was applied. The red arrows highlight the multiple reflections in the original processing, and they were removed in the reprocessing results.

The reprocessing still leaves room for improvement. To some extent, the overall signal-to-noise ratio of the PSTM stacks is often compromised, most likely as the side effect of aggressive denoising techniques. Different denoising techniques and parameters could be tested more thoroughly to justify the most optimal ones that could suppress the noise as good or even better without degrading the overall signal-to-noise ratio. However, this suggestion is often difficult to implement. Marine seismic data quality is prone to the acquisition artefacts (noise). They usually hit the recorded data badly, are persistent, and cannot be avoided, such as bad weather, shallow water depth and irregular seabed morphology. Under project time pressure, such a case often puts the processor in a difficult situation to choose aggressively suppressing the persistent noise with the cost of compromising reflection coherency. Another possible improvement can be achieved by implementing a prestack depth migration (PSDM) technique, including iterative velocity field updates obtained from reflection tomography. While this imaging technique is usually implemented to correct reflector position in the depth domain and in the present strong lateral velocity variations associated with complex overburden structures, the iterative reflection tomography that comes with it might help to reconstruct and enhance the reflection coherency. Thorough tests on denoising techniques and parameters, as well as PSDM, require more time than available within the tight time frame available for the present reprocessing project. Apart from the time limitation, the processing sequence implemented in the reprocessing was arguably the most practical approach to meet both the reprocessing objectives and the project deadline.

## 4.2 Well data

The Jammerbugt structure is untested by deep wells. The nearest offshore deep wells are the J-1 and the Felicia-1a wells drilled in 1969-1970 and 1987-1988, respectively (Fig. 1.2). The wells were drilled in the pursuit for hydrocarbons but was water-bearing. Felicia-1a TD'ed in 5281 m below msl and intersected an Upper Cretaceous to Permian succession flooring in the Rotliegende Group. J-1 TD'ed in 1952 below msl and intersected an Upper Cretaceous to Upper Triassic interval. Available petrophysical logs comprise calliper, gamma ray, sonic, resistivity, neutron porosity and density. In the J-1 well, no conventional cores were cut, but 28 plugs were retrieved from the deeper part of the well from 1380–1950 m b. msl with the main aim of improving stratigraphic control and screen for source rocks. Investigations of mechanical properties, *in situ* stress or rock failure studies on the J-1 well or well material have been made to the knowledge of the authors. Two cores were cut from the Permian section in Felicia-1a.

These two wells have been tied to seismic data and comprise the primary stratigraphic control for evaluating the offshore Jammerbugt structure. In addition, stratigraphic information has been extracted from the Vedsted-1, Fjerritslev-1 and -2 boreholes, the Flyvbjerg-1, Børglum-1 and Thisted 1-4 wells drilled in the nearby onshore area in support of the reservoir, seal and seismic stratigraphic interpretation.

## 5. Methods

### 5.1 Seismic interpretation and well-ties

The Jammerbugt structure is evaluated based on conventional analysis of all available 2-D seismic data over the greater Jammerbugt area (Fig. 1.2). Interpreted seismic horizons and units were tied to wells to build a stratigraphic framework (Fig. 5.1.1). Seismic horizons, seismic successions are interpreted relying on reflector continuity/discontinuity and lapping pattern. The horizons are essentially sequence stratigraphic/chronostratigraphic surfaces but can in this limited area be regarded as near base/top of formations, with horizon names similar to the formations tied from the wells. The seismic interpretation and well-ties with synthetic seismograms are performed on a workstation with Petrel (2023) software.

Eight surfaces were mapped systematically over the area due to their importance for defining reservoir-seal pairs, structural closures, and for determining the geological evolution of the area. These are from oldest to youngest the (1) Top pre-Zechstein, (2) Top Zechstein, (3) Top Skagerrak Fm, (4) Top Oddesund Fm (5) Top Gassum, (6) near-Top Haldager Sandstone, (7) Base Chalk, and (8) Top Chalk. To aid analysis of the tectonic and depositional development in Jammerbugt, approximate chronostratigraphic ages were assigned based on biostratigraphy in the J-1 and Felicia-1a wells and adjacent onshore wells and on regional considerations.

Faults were identified and mapped based on gaps in reflection continuity, lateral thickness changes, and shifts in reflector inclinations. At the same time, salt structures and folds were identified and mapped. The structural evolution was analyzed based on a study of these structures in combination with observations of thickness variations of seismic packages, internal reflector geometries, -lapping and -thickness patterns and their relation to faults and structures. The structural analysis forms the basis for a tectonic analysis integrating structural observations with the chronostratigraphic framework permitted by well correlations. The storage complex including identification of reservoir-seal pairs was investigated and evaluated based on the structural and stratigraphic analysis and based on the available well data.

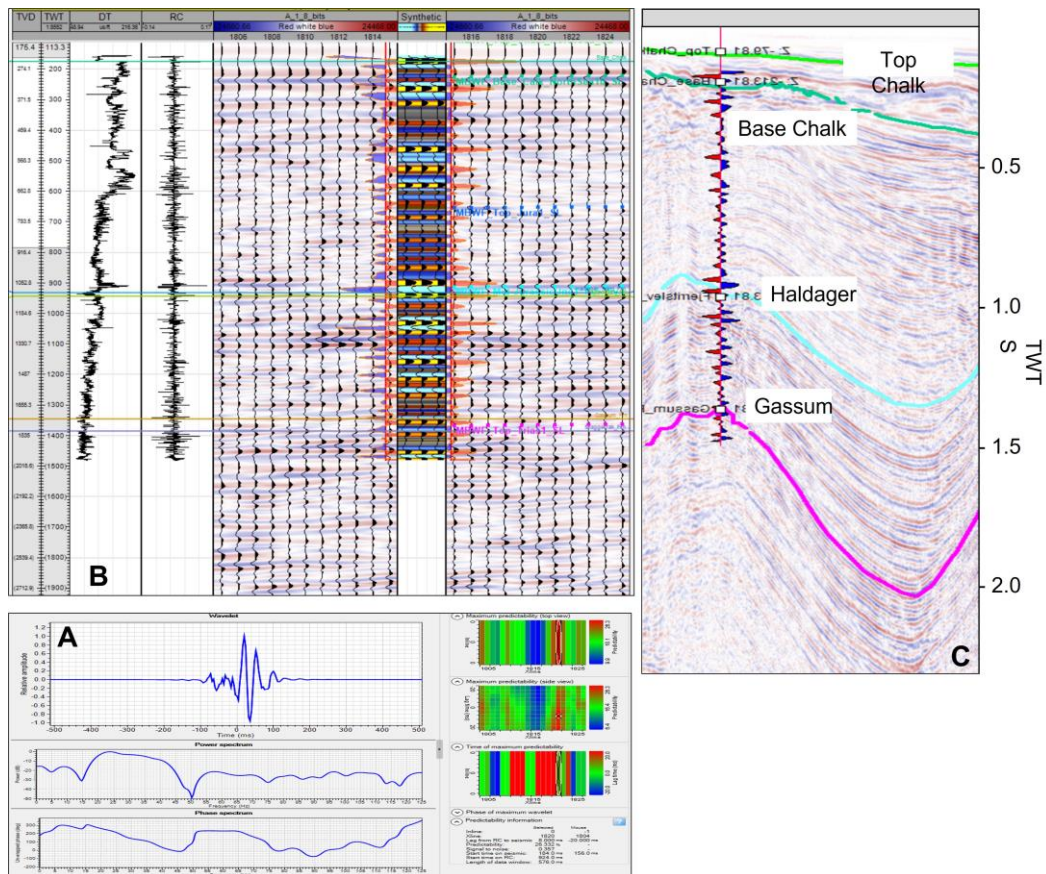


**Figure 5.1.1.** A deterministic wavelet along the J-1 borehole was extracted and used for forward modeling and generation of a synthetic seismogram (A). A window of 11 traces on both sides of the borehole are used to predict the best possible wavelet with maximum correlation. Wavelet convolved with the spike function generated along the borehole using sonic log generates a synthetic seismogram for Inez-1 which overall shows a good fit with the existing seismic intersecting the well (B). The stratigraphy picked in the Inez-1 well fits well with the seismically picked stratigraphic surfaces (C). Correlation with PGS line mc2d-fab2003\_line2004\_t100901f-0006.

## 5.2 Seismic time to depth conversion

A regional velocity model was constructed to convert the interpreted horizons from the time domain to the depth domain. The Jammerbugt structure is not drilled, and in order to provide calibration data for the velocity model, the model area was enlarged to include the Felicia-1a, J-1 in the NW corner of the model and Fjerritslev-2 and Vedsted-1 in the southern part of the model (Fig. 5.2.1), and the model area therefore spans 92.5 km by 51.5 km.

The data available included:

- 1) Regional TWT seismic horizons of the main stratigraphic units and velocity boundaries using the new 2D GEUS2023-RTS-Jammerbugt data and available older regional lines were gridded to 250x250m and well-adjusted to match the TWT markers in the boreholes:
  - a. Top Chalk Group
  - b. Base Chalk Group
  - c. Near Top Haldager Fm
  - d. Top Trias (Top Gassum Fm)

- e. Top Oddesund Fm.
  - f. Top Zechstein
  - g. Top pre-Zechstein
- 2) Well top markers
  - 3) Seismic migration (RMS) velocities from the newly acquired 2D lines (GEUS2023-RTS-Jammerbugt)

In order to account for vertical and lateral variations in average velocities found within the stratigraphic units as seen in the Time-Depth Relations (TDRs) in boreholes and 2D seismic migration velocities, the velocity model was constructed in two steps, followed by depth-conversion of the TWT seismic horizons:

- 1) First, seismic migration velocities from the 2D lines were upscaled into a structural 3D grid (using arithmetic mean), and subsequently extrapolated within each zone using full tension option in Petrel (spline in tension algorithm).
- 2) Second, a multi-layer velocity model was created using the modelled 3D average velocities as velocity input, and 3D horizons and well tops to correct the velocity values to achieve a match between depth-converted horizon and well top.
- 3) Finally, TWT seismic horizons were depth-converted using the created velocity model.

To achieve the velocity model, a workflow was performed within Petrel 2023 by the following steps:

1. Input data and QC of TDR:
  - seismic-well-ties; checking that the TDR of the borehole has geologically reasonable average velocities and fits the seismic data. Only J-1 (full stratigraphy) and Felicia-1A (from 2200-5300 m) had sonic and density logs, in addition to checkshots, allowing a seismic well tie to the 2D lines. For Fjerritslev-2 and Vedsted-1, only GR/SP and resistivity logs were available, impeding a seismic well tie. However, a TDR could be established from checkshot data in well Fjerritslev-2, and with manual well top adjustments fine-tuned. For Vedsted-1 a manual TDR was assigned to match well top and mapped seismic marker.
  - Gridding of the horizons to 250 x 250m and using well-adjustment to make sure the TWT surface fits the corresponding TWT top in the boreholes, using global adjustment.
  - A seismic velocity to point cloud Petrel workflow was used in order to sample the RMS velocity data from the JB1–JB39 lines, using a vertical sampling rate of 20 ms, and horizontal spacing of 3 m.
2. Defining a 3D modelling grid (250x250m) based on the QC-ed TWT horizons using the Petrel structural modelling tool:
  - Model zonation was made according to the following horizons (Fig. 5.1).:
    - MSL (0 ms) (top model)
      - Zone: Quaternary + Cenozoic

- Top Chalk Group
    - Zone: Chalk Group
  - Base Chalk Group
    - Zone: Middle – Upper Jurassic + Lower Cretaceous
  - Near Top Haldager Sand Fm
    - Zone: Fjerritslev Fm.
  - Top Trias (Top Gassum Fm.)
    - Zone: Gassum Fm. + Vinding Fm.
  - Top Oddesund Fm.
    - Zone: Upper part Oddesund Fm. (little evaporites)
    - Zone: Lower part Oddesund Fm. (evaporites), using Intra Oddesund well top
  - Top Zechstein
    - Zone: Zechstein Group (evaporites)
  - Top Pre-Zechstein (base model)
- Buried Pleistocene (sub-glacial?) valleys have cut deeply into the Chalk Group and are filled with undifferentiated unconsolidated young sediments, are included in the model due to the new mapping (Fig. 5.2.2). An extra zone was placed between Top Oddesund Fm. and Top Zechstein Group to account for a zone of Triassic-aged salt. Vertical layering was defined such that layer thickness was on average 20 m, which was a trade-off between getting enough velocity samples and computational time.
3. Property modelling to compute an RMS velocity cube (Fig. 5.2.3)
- Upscaling the RMS velocity point cloud obtained from the 2D seismic RMS migration velocities into the structural grid using arithmetic mean. The property grid then contains RMS velocities where the 2D lines occur.
  - Extrapolation of the 2D RMS (migration) velocity upscaled cells into the entire structural grid using extrapolation with full tension (spline in tension option in Petrel). The minimum curvature option yielded poor results and was not used. It maintains trends and upscale extreme, geologically unrealistic, low or high velocities in areas with limited data coverage. The applied full tension extrapolation tends to flatten values and appears more realistic.
  - Due to local variations in RMS velocities between the different 2D lines, a 10x smoothing was applied to generate a more consistent and smooth 3D property which was used as velocity function.

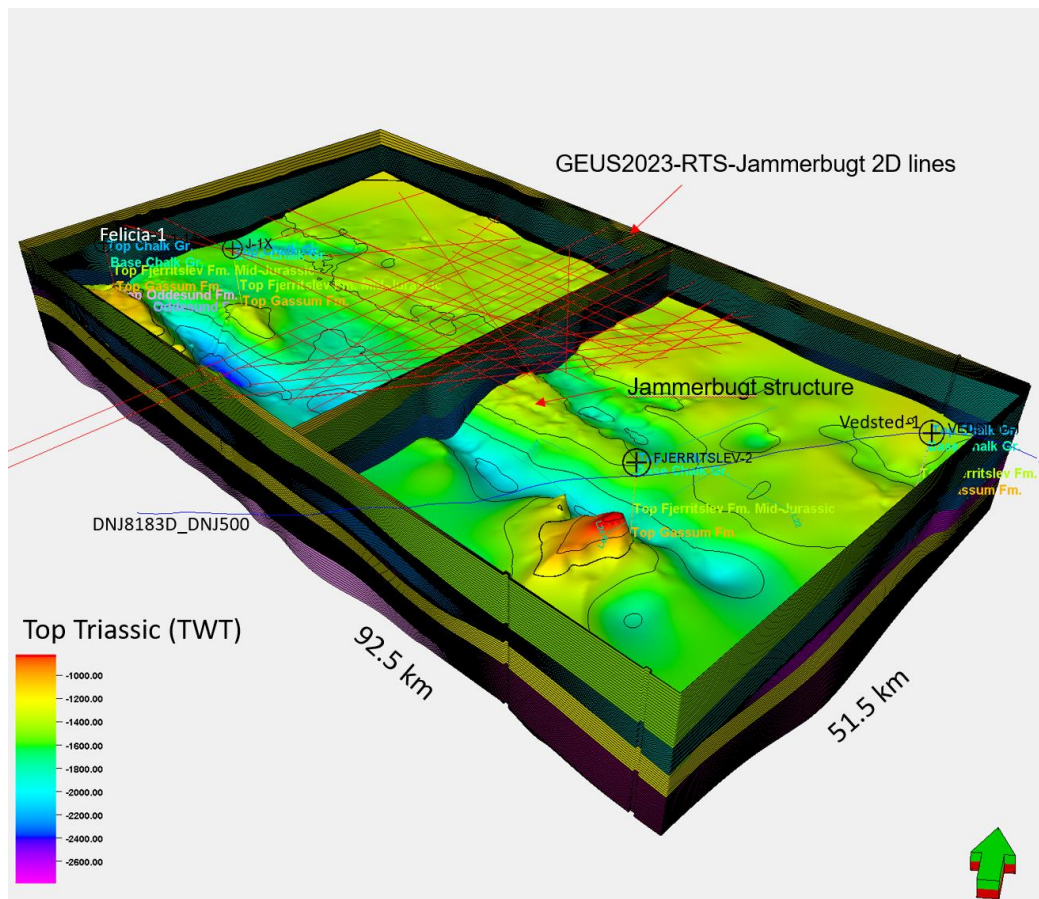


**Figure 5.2.1.** Regional structural framework used for the Jammerbugt structure, in order to obtain some borehole information (TDRs, well tops) for calibration of the velocities. The horizon is the Top Trias (Top Gassum Fm.) TWT structure map.

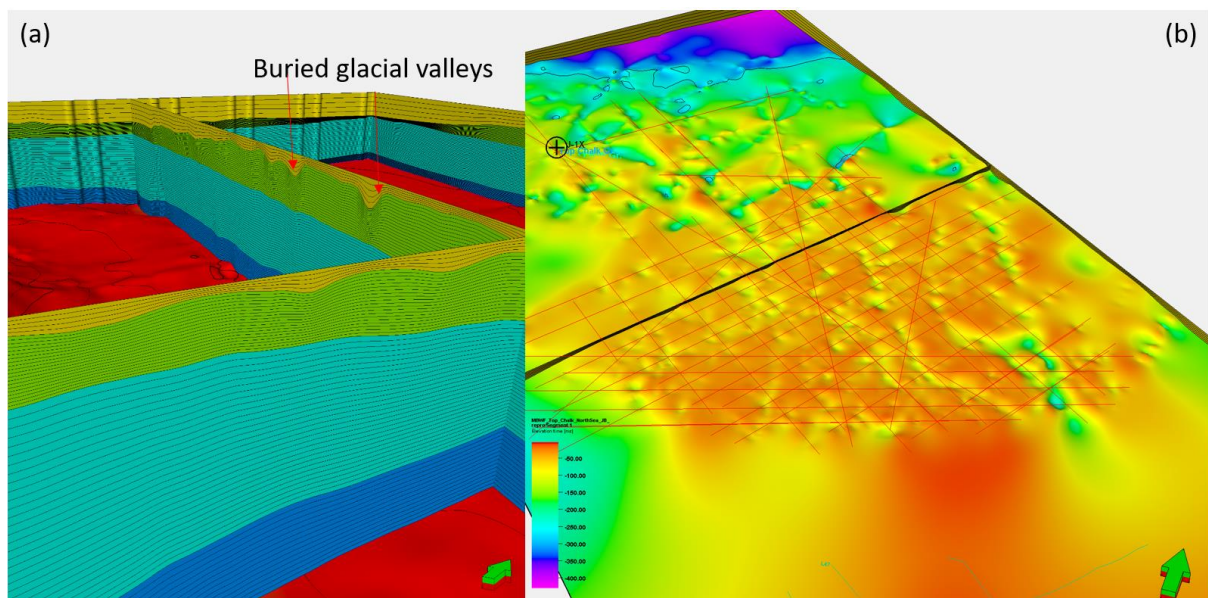


**Figure 5.2.2.** (a) Zoom in of the structural grid showing in yellow the Quaternary + Cenozoic including buried Pleistocene valleys 1-3 km across, 20 – 50 ms deep; Upper Cretaceous Chalk Group (green); Lower Cretaceous (turquoise), Upper Jurassic (blue); Fjerritslev Fm., Gassum Fm. (red). (b) Map view of Top Chalk Group, showing the buried Pleistocene (sub-glacial?) valleys which have cut into the Chalk Group.

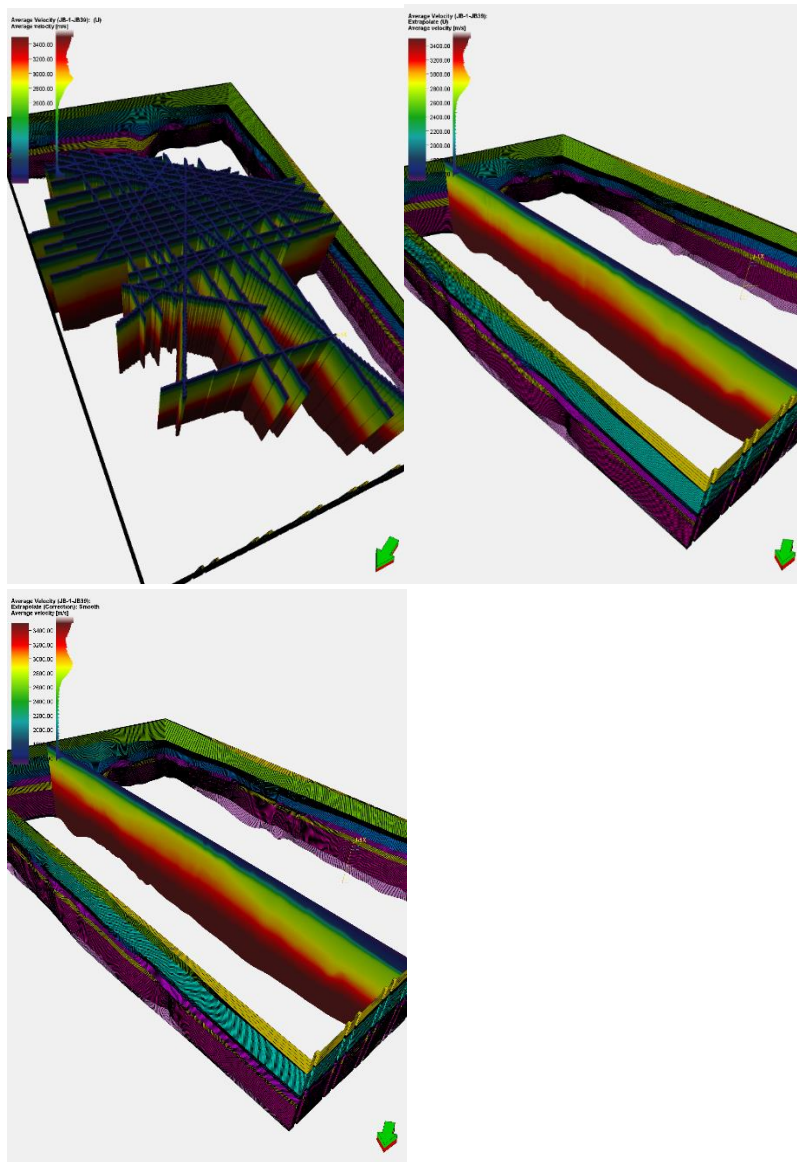


**Figure 5.2.3.** (a) Upscaled 2D seismic RMS (migration) velocities and (b) 3D RMS velocities property from extrapolation of the 2D data. Locally, still some velocity artefacts occur which were minimized through smoothing. (c) 10x smoothing to remove artefacts.

4. Create an “advanced velocity model” using the same 3D seismic horizons (tied in TWT to boreholes from seismic-well-tie Time-Depth Relationship), well tops for calibration, and the 3D average velocity grid from the previous step as velocity model (Fig. 5.2.4). Without applied correction, the average depth residual was in the order of 100 – 500 m, reflecting that the seismic RMS velocities are roughly reflecting the actual interval velocities but that corrections are needed from boreholes. The final velocity model used the well tops (“global correction”) to adjust the velocities in order to minimize the depth residuals between depth-converted horizon and well top (Fig. 5.2.5).
  - Depth-convert the TWT horizons using the constructed velocity model (Fig. 5.2.6).
  - The velocity model is called: V2 Velocity model (JB1-JB39) (Corrected)

To make the velocity model more accurate, the following steps could be undertaken in future studies:

1. Include additional velocity data from older seismic lines. For some lines, stacking velocities may be available in the onshore-to-offshore transition.
2. Perform comprehensive data analysis on the upscaled cells to obtain geostatistical information of the upscaled cells for kriging purposes (variogram ranges, nugget, azimuths for each zone), and use kriging of the upscaled cells. This may provide for each zone a trend in velocities depending on the geology, rather than the full tension extrapolation.
3. Use the volume derived from point 2 and use co-kriging of average velocities from well TDRs and the 3D property grid as 3D trend.

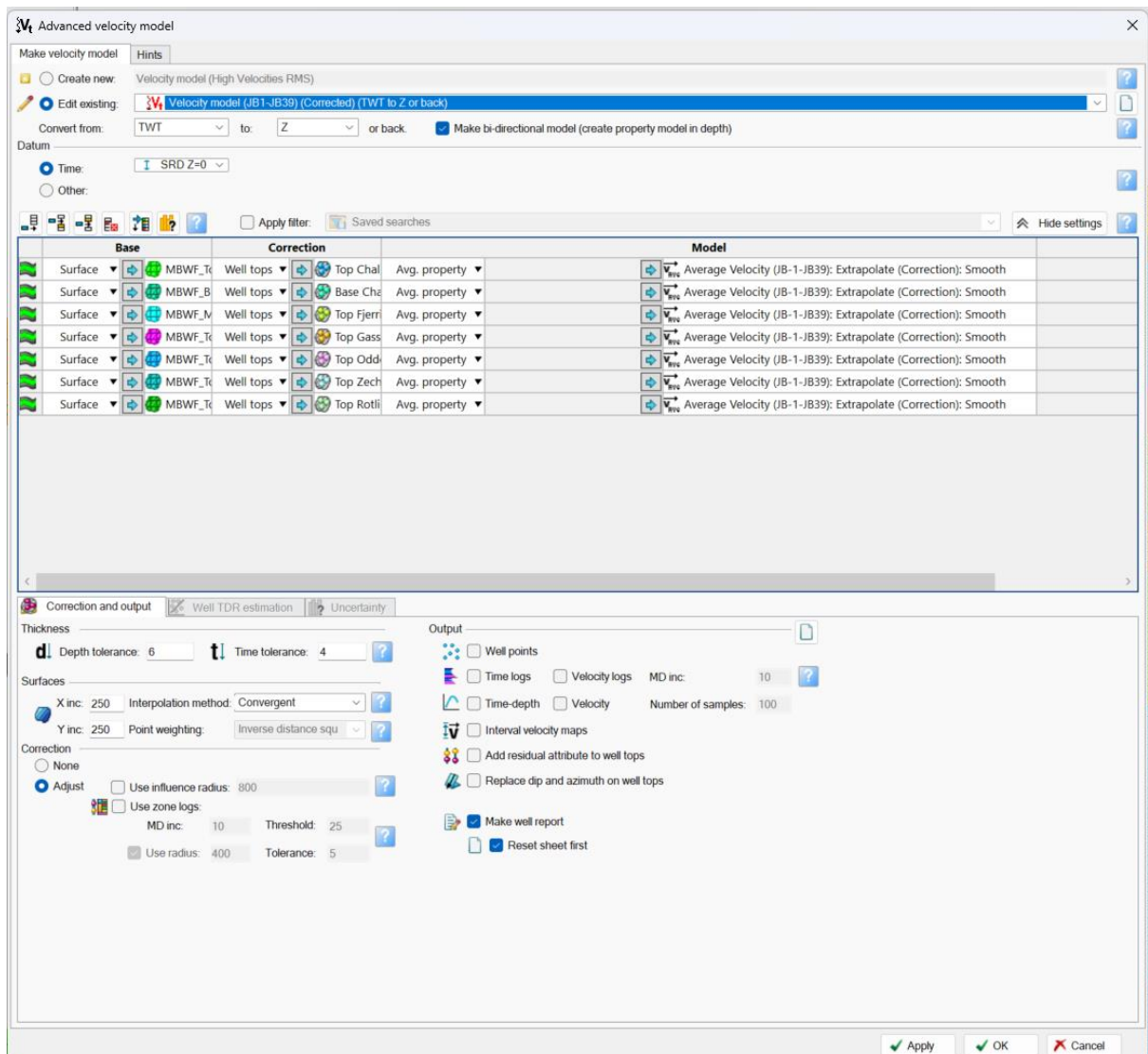


**Figure 5.2.4.** The advanced velocity model setup to depth convert the seismic horizons using the well-tied TWT horizons, well tops for calibration of the velocities, and the 10x smoothed 3D seismic RMS velocity grids.

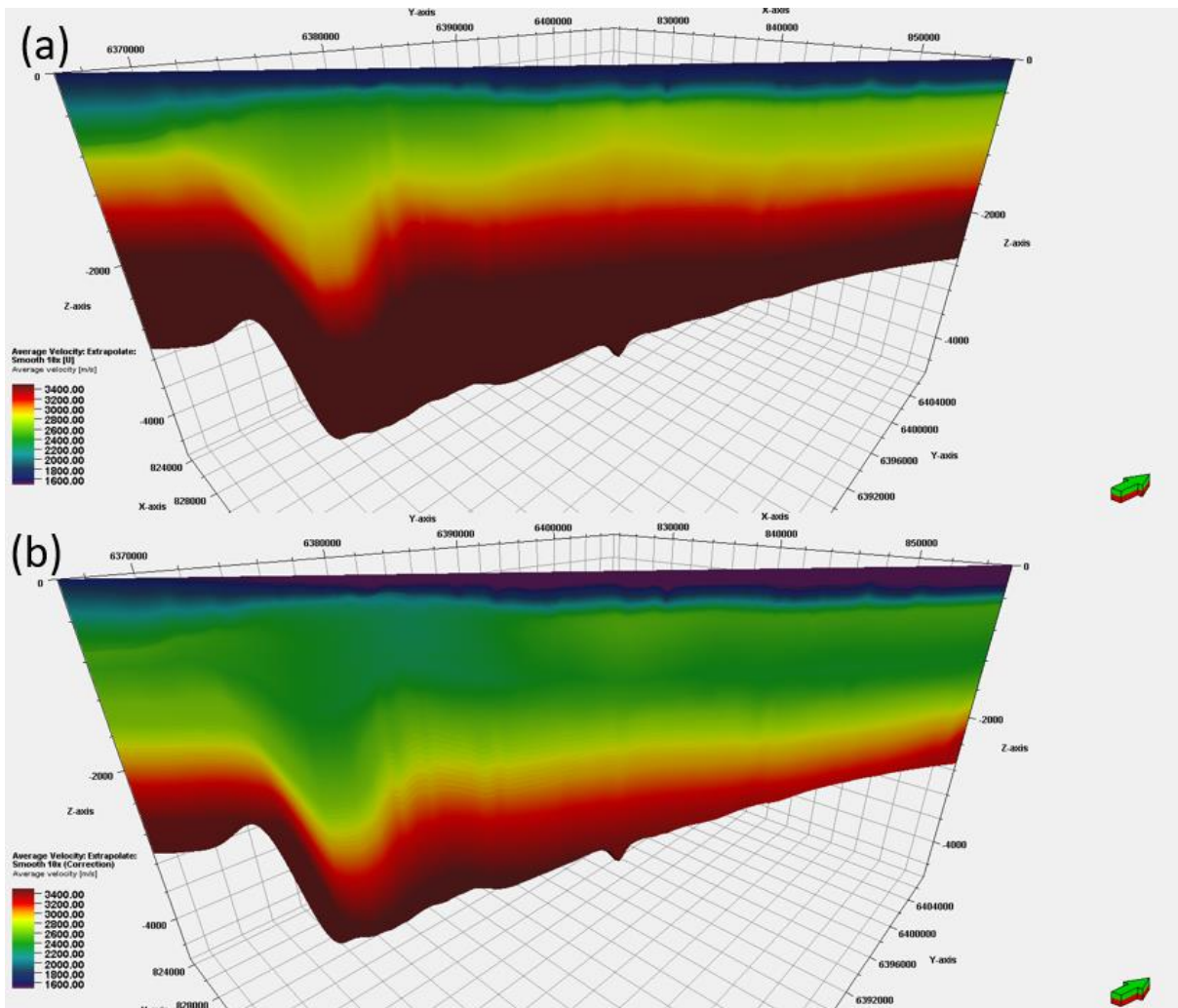


**Figure 5.2.5.** (a) N-S oriented cross section through extrapolated 2D seismic RMS velocities; and (b) Velocities are corrected to let depth-horizons match the borehole depths in J-1, Felicia-1a, Fjerritslev-2, Vedsted-1. Note significantly lower velocities in the upper 2000 m in order to match depths in the boreholes.

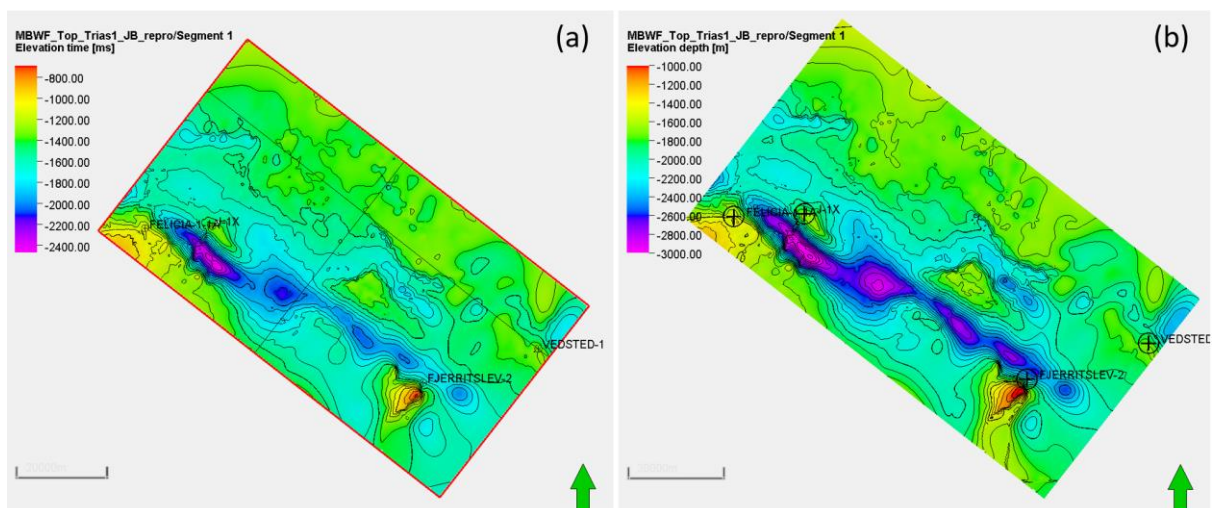


**Figure 5.2.6.** (a) Time structure map of the Top Trias (Top Gassum Fm.), contouring every 100 ms. (b) Depth-converted structure map, with contouring every 100 m.

### 5.3 Investigation of reservoir and seal

The reservoir characteristics presented below and in Chapter 7 are derived mainly from the obtained wireline logs but cross-checked against descriptions of cuttings and sidewall cores. Potential reservoir units were identified on wireline logs by their low formation resistivity, low formation density and a natural radioactivity as seen by low GR log readings and in cuttings containing sand-sized quartz grains. Reservoir parameters were evaluated based on well data with emphasis on data from the J-1, Felicia-1a, Vedsted-1 and Thisted-3 located close to the Jammerbugt structure. A sandstone is defined on the petrophysical data as a rock having < 50% volume of shale, and a reservoir sandstone has estimated effective porosity (PHIE) of > 0.1. The volume of shale is estimated based on a combination of the gamma ray, deep resistivity, density and neutron porosity logs, while the effective porosity is calculated based on the volume of shale along with the density and neutron porosity logs. The permeability is based on an in-house established data relation between porosity and permeability. As there are no cores from relevant reservoir intervals and therefore no conventional core analysis in the offshore part of the Norwegian–Danish Basin, the permeability is based on a best fit relation between measured core porosities to measured permeabilities from onshore Denmark.

Seal grain-sizes were similarly evaluated based on petrophysical logs from wells located near the Jammerbugt structure. Mudstone sections that will act as seal were identified from wireline logs by having high formation resistivity, high formation density and having high natural radioactivity reflected in high GR log readings. In addition, information on the regional composition such as total organic carbon (TOC) content and clay mineralogy of the potential sealing units were included in the seal analysis together with seal quality analysis performed on these units from other Danish wells. Borehole data contributed to the evaluation of seal thickness evaluation in conjunction with seismic mapping.

### 5.4 Storage capacity modelling

To be able to compare the potential CO<sub>2</sub> storage structures, GEUS uses a simple widely accepted equation for saline aquifers (Goodman et.al., 2011). The storage capacity of reservoir units with buoyant trapping is estimated from:

$$SC = GRV * N/G * \phi * \rho_{CO2R} * S_{Eff}$$

where:

- SC** Storage Capacity or Mass of CO<sub>2</sub> (MT).
- GRV** Gross Rock Volume is confined within the upper and lower boundary of the gross reservoir interval (t) and above of the deepest closing contour from where spillage from the trap will occur. To get a representative GRV the lower boundary may be moved to a position closer to the upper boundary so expected the gross reservoir interval in the structure represents the surrounding wells. This will give a more correct estimation of the GRV.
- N/G** Average net to gross reservoir ratio of aquifer across the entire trap (GRV).
- $\phi$**  Average effective reservoir porosity of aquifer within trap (GRV).
- $\rho_{CO2R}$**  Average CO<sub>2</sub> density at reservoir conditions across all of trap.

$S_{Eff}$  Storage efficiency factor relates to the fraction of the available pore volume that will store CO<sub>2</sub> within the trap (GRV). This fraction depends on the size of storage domain, heterogeneity of formation, compartmentalization, permeability, porosity, and compressibility, but is also strongly influenced by different well designs and injection schemes (e.g. Wang *et al.* 2013).

Storage capacity (SC) is related to communication within the reservoir and the degree of pressurization, where pressurization depends on the difference between the fracturing pressure and the relation between pressure and volume increase, and compressibility of the rock and the fluids in the reservoir.

In open aquifers, as used here, a CO<sub>2</sub> storage injection phase is most likely pressure-limited during the entire operation, and the reservoir pressure will stay constant during injection, as the water will be pushed beyond the boundaries. The calculated stored CO<sub>2</sub> will be the amount injected until it reaches the boundaries (e.g. 'lowermost closed contour'). The calculation used here assumes a static approach where the pores in the trap is considered to be 100% connected. However, it does not include dynamic pressure build-up and movement of CO<sub>2</sub> and in-place brine(water) in the saline aquifer, neither in-side nor out-side the trap. Furthermore, it does not regard the solubility of CO<sub>2</sub> in water, where more than 10% can normally be dissolved in the water.

A more precise dynamic simulation of the potential CO<sub>2</sub> storage capacity carried out is typically the next step in the maturation of specific structures integrating operational and regulatory factors in the modelling. However, this is beyond the scope of this study.

The CO<sub>2</sub> storage efficiency factor ( $S_{Eff}$ ) is used in regional-scale assessments of storage capacity in the United States and Europe. The efficiency of CO<sub>2</sub> storage is regarded as a combination of factors, and with values typically ranging from <1% to more than 20%, emphasizing that no single value or set of values apply universally. Regional storage efficiency values are around 1–4 %, while trap specific storage efficiency have values around ~4-18% for clastic sediments (Gorecki *et.al.*, 2009); ~3-10% (US-DOE; Goodman *et.al.*, 2011) and ~5-20% is applied by BGR for traps in their assessment of the German North Sea area.

The storage efficiency factor represents the fraction of the total available, trapped pore volume in the saline aquifer that will be occupied by the injected CO<sub>2</sub> (i.e. the GRV). The efficiency factor has both a space and time dependency. It depends primarily on the relationship between the vertical and horizontal permeability, where a low vertical to horizontal permeability ratio will lateral distribute the CO<sub>2</sub> better over the reservoir than a high ratio. Furthermore, the storage efficiency factor depends on the size of the storage domain, heterogeneity of the formation, compartmentalization, porosity, permeability, pressure, temperature, salinity and compressibility, but also depends on the number of injection wells, design and injection strategy.

Storage efficiency values from 5 to 10% are commonly applied in structures without or with only limited well- and 3D seismic data.

Storage-capacity calculations are biased by imperfect seismic and reservoir data, depth conversion, reservoir thickness estimates, CO<sub>2</sub> density. To address the uncertainties ranges input parameters have been chosen to reflect each parameter uncertainty, and the distribution has been modelled utilizing a simple Monte Carlo simulation in-house tool. To achieve stable and adequate statistical representation of both input distribution and result output, 10.000 trials are calculated for each simulation. This methodology is simplistic and does not incorporate e.g., correlations of

input parameters. However, for the purpose of initial estimation of volumes and CO<sub>2</sub> storage capacities, the methodology is considered relevant and adequate. The method is used for the calculations in Chapter 8.

## 6. Results

### 6.1 Local Stratigraphy

Located in the Fjerritslev Trough, the Jammerbugt structure area contains a more than 4 s TWT thick sedimentary succession resting on the top of the pre-Zechstein (Fig. 6.1.1). Reflectivity below the Zechstein succession suggest the presence of older deposits of unknown thickness. The Zechstein Group is thickly developed over the Hurup Platform but thins to the north into the Fjerritslev Trough located on the down-thrown side of the Fjerritslev Fault (Fig. 6.1.2). Smaller pockets of Zechstein deposits exist in the Jammerbugt area locally with thicknesses up to around 0.3 s TWT. Above the Zechstein, the succession correlating with the Skagerrak Fm and the underlying Bacton Group in the Felicia-1a well is thickly developed. We here follow the recommendation of Michelsen and Clausen (2002) for the Triassic stratigraphic subdivision in the Danish part of the Norwegian-Danish Basin and include the entire section within the Skagerrak Fm. Skagerrak Fm is characterized by low-amplitude, parallel to sub-parallel reflections and ranges between c. 0.8 and 1.2 s TWT in thickness (Fig. 6.1.2). No thickness changes are noted across faults documenting deposition during a tectonically tranquil period without faulting. This contrasts with the overlying succession correlating with the Oddesund Fm in Felicia-1a showing a thickness range between close to 0 and 1.5 s TWT. The Oddesund Fm thickness changes distinctly across the Fjerritslev Fault Zone and faults located in the Fjerritslev Trough and over the Skagerrak Platform (Fig. 6.1.2). In the central offshore part of the Fjerritslev Trough, the supra-Zechstein interval formed over and next to a relay ramp (Fig. 6.1.3). Here, the Oddesund Fm wedges through internal onlap towards the southwest documenting a certain syn-depositional relief between the Hurup Plateau and the Fjerritslev Trough (Fig. 6.1.4). The Oddesund Fm is characterized by strongly reflected strata but in the depocenter of the Fjerritslev Trough also contains intervals and lenses of more subdued reflectivity. In the depocenter, including at the Jammerbugt structure, the formation is internally folded and faulted with deformation soling out in the less reflective intervals. In line with the nature of the Oddesund Fm met in Felicia-1a (6.1.5), this reflection pattern is interpreted as a clastic succession interbedded with widespread, strongly reflected anhydrite interludes. The less reflective lenses in the depocenter presumably consists of halite also met in Felicia-1a prone to deformation and mobilisation.

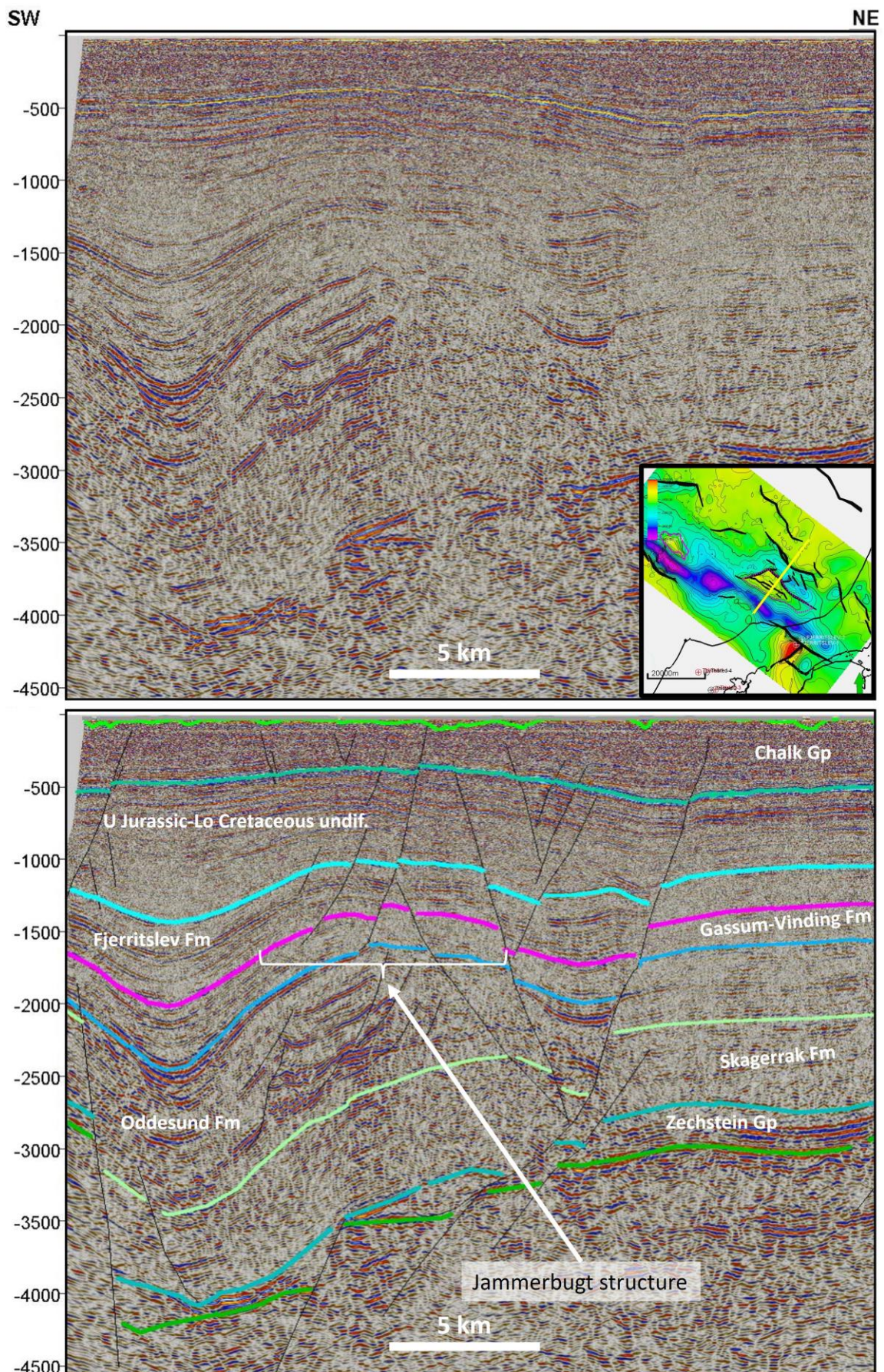


**Figure 6.1.1.** Seismic section crossing the Jammerbugt structure illustrating the interpreted seismic stratigraphy (uninterpreted and interpreted).

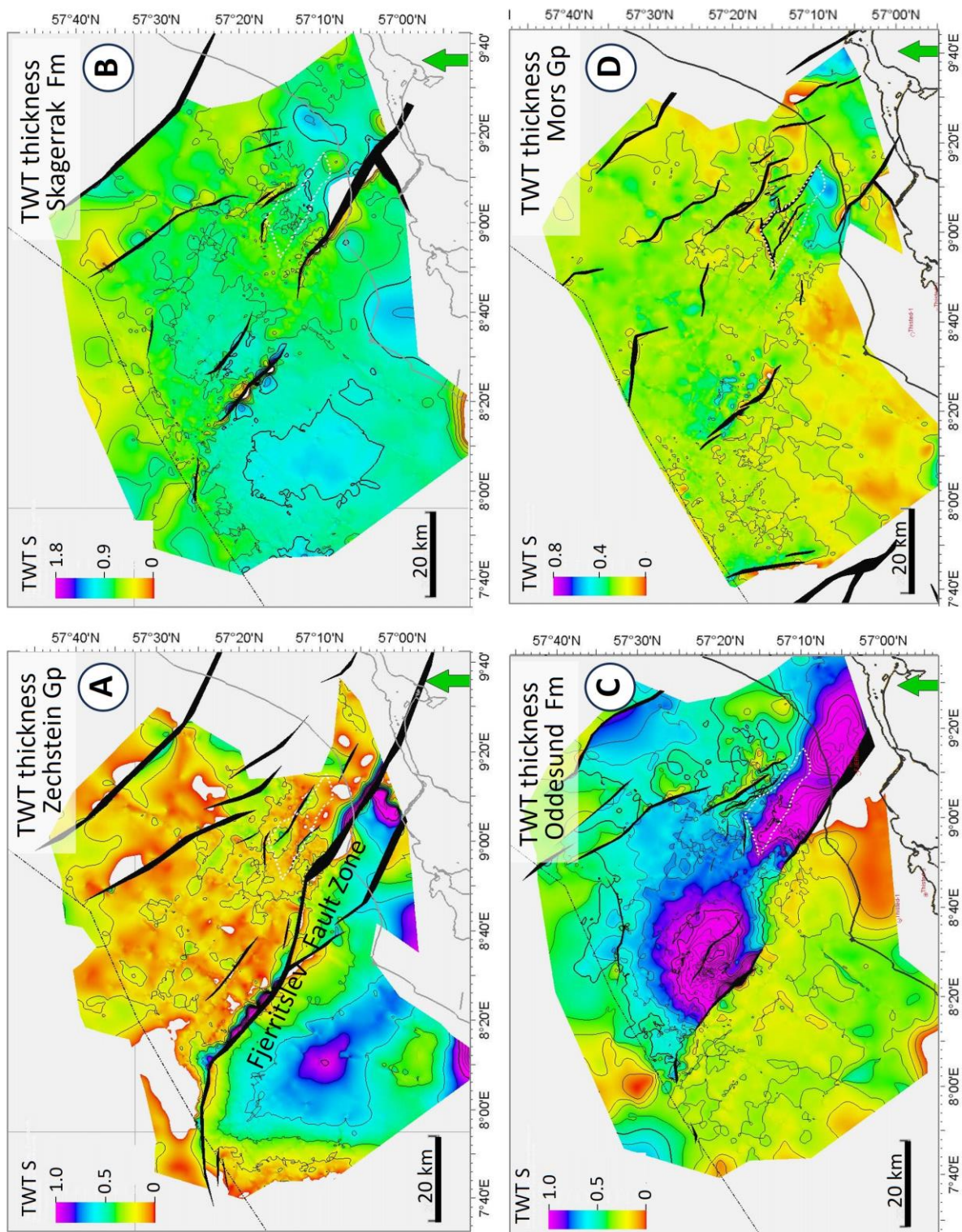


**Figure 6.1.2.** TWT isochore maps of the man stratigraphic intervals in the greater Jammerbugt structure area. **A** Zechstein, note the modest Zechstein thickness in the Fjerritslev Trough and farther north. **B** TWT thickness of the Skagerrak Fm (Lower to Middle Triassic). Thickness variations are subtle relative to other intervals due to virtual absence of syn-depositional tectonism; **C** Oddesund Fm TWT thickness (uppermost Middle and lower Upper Triassic). Significant thickness variations occur due to syn-depositional rifting and down-faulting of the Fjerritslev Trough. **D** TWT thickness of the Mors Gp composed by the Vinding and Gassum Fm. Thickness variations are relatively modest compared to Oddesund Fm reflecting a Late Triassic paucity of rifting.

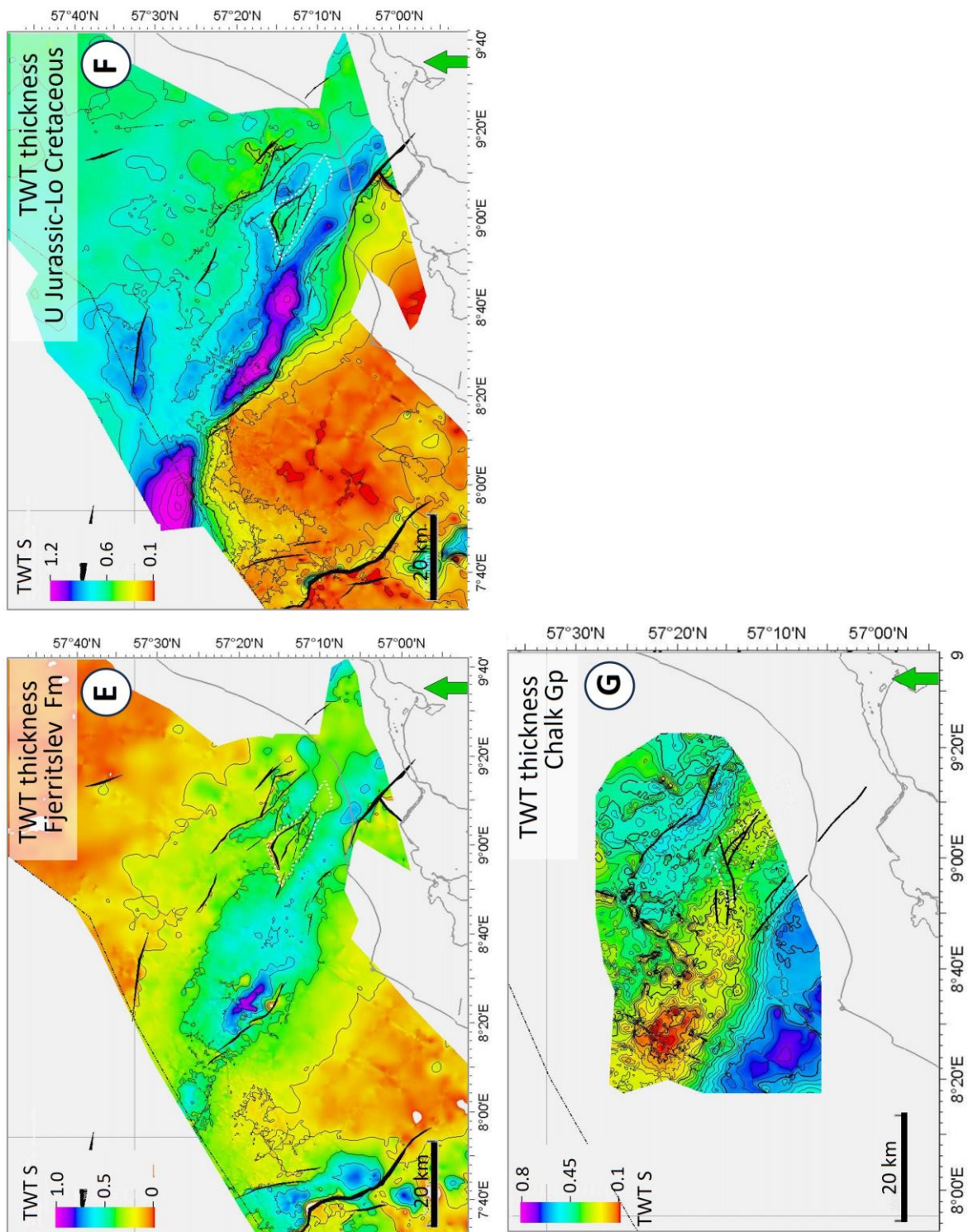


**Figure 6.1.2. Continued.** **E** Fjerritslev Fm (Lower Jurassic) show strong thickness variation reflecting crustal stretching largely buffered from piercing through by ductile deformation of the Zechstein Gp- and Oddesund Fm salt. **F** TWT thickness variations even increase within the Upper Jurassic to mid-Cretaceous, again reflecting crustal stretching largely buffered from piercing through by ductile deformation of Zechstein Gp- and Oddesund Fm salt. In addition, thickness variations occur due to mobilization of Oddesund Fm salt and local salt pillow growth in the Fjerritslev Trough. **G** Thickness variations within the Chalk Gp mostly reflects near-seabed erosion governed by structural inversion of the Fjerritslev Trough but also reflecting depositional thinning across the trough due to syn-depositional initial inversion and doming. Chalk is also distributed outside the mapped area that merely depicts the area with the best top-chalk seismic resolution.

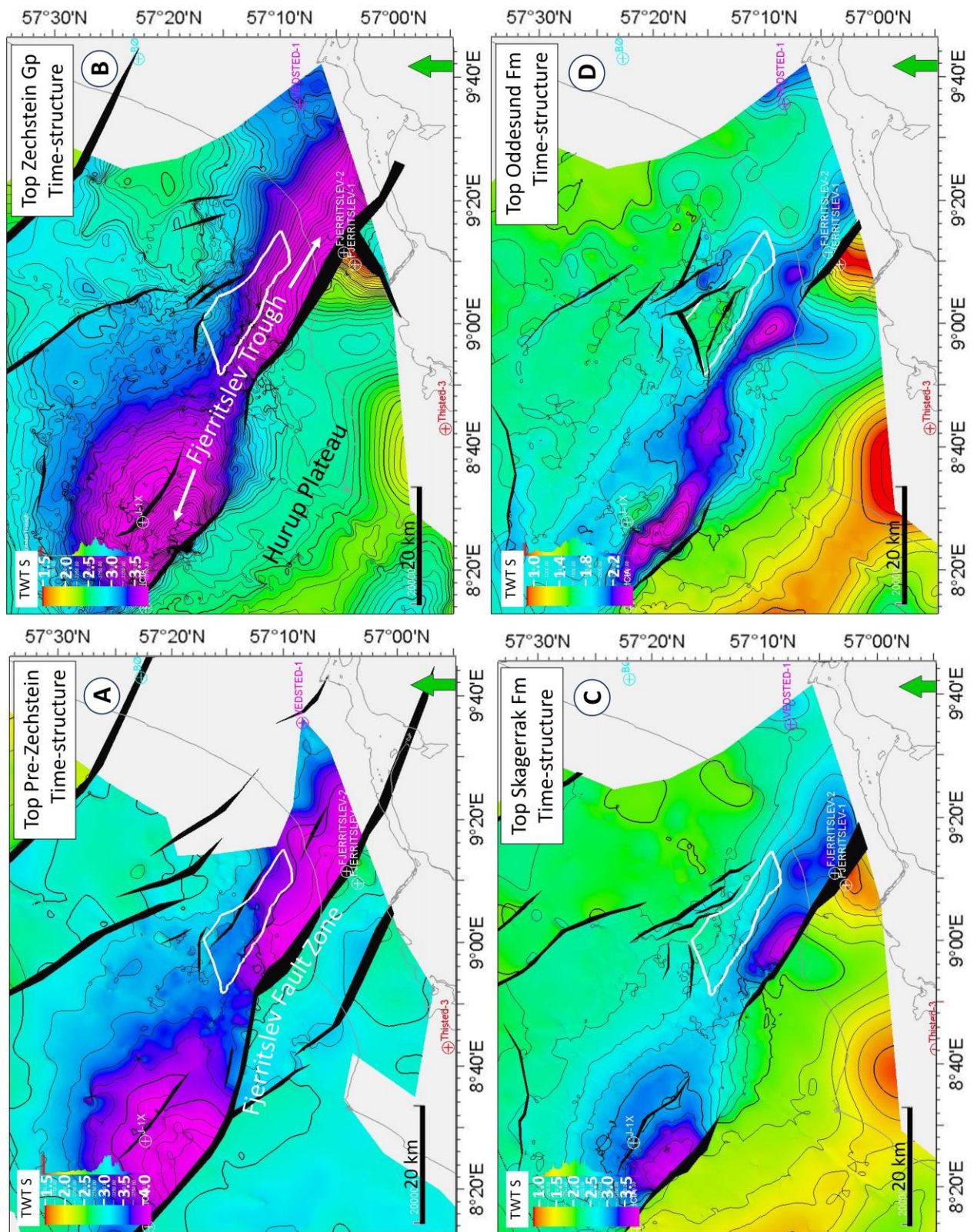


**Figure 6.1.3.** Seismic TWT structure maps. **A** Base Zechstein, 200 ms contouring. The Fjerritslev Fault Zone delineates a continuous fault zone at this level separating the Hurup Plateau from the Fjerritslev Trough. **B** Top Zechstein, 50 ms contouring. Zechstein salt buffers fault break-through in the least offset part of the Fjerritslev Fault Zone; **C** near-Top Skagerrak Fm (intra Middle Triassic); 200 ms contouring. The Skagerrak Fm is deeply downfaulted over part of the Fjerritslev Fault Zone. **D** near top Oddesund Fm (intra Upper Triassic), 100 ms contouring. The top of the Oddesund Fm is less faulted than the Skagerrak Fm;

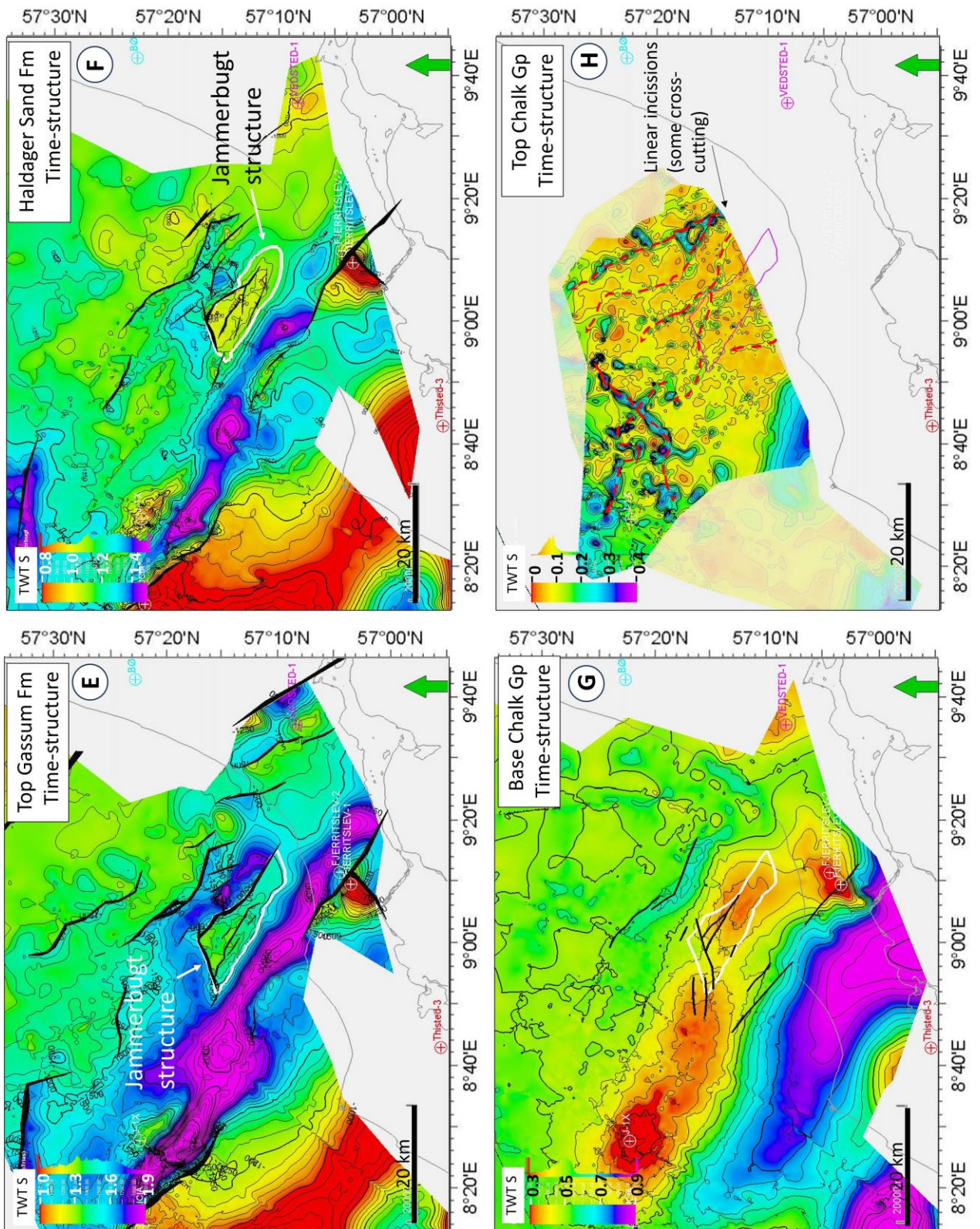


**Figure 6.1.3 Cont.** *E* Top Gassum Fm (Near-top Triassic); 50 ms contouring interval. Structural closure is indicated with bold contour lines at reservoir level.; *F* near top Haldager Sand Fm (Near-top Lower Jurassic); 50 ms contouring interval. Structural closure is indicated with bold contour line at reservoir level.; *G* Base Chalk (intra-mid-Cretaceous), 50 ms contouring interval. Note the elongated high following the length of the Fjerritslev Trough, which represent an inversion anticlinal structure. *H* Top Chalk (intra Paleocene), 25 ms contouring. Please note the elongated depressions in the top Chalk surface interpreted as fluvial incisions. Some of these are cross-cutting suggesting channels of different generations. At least channels located along strike with the general depth contours of the surface likely formed sub-glacially.

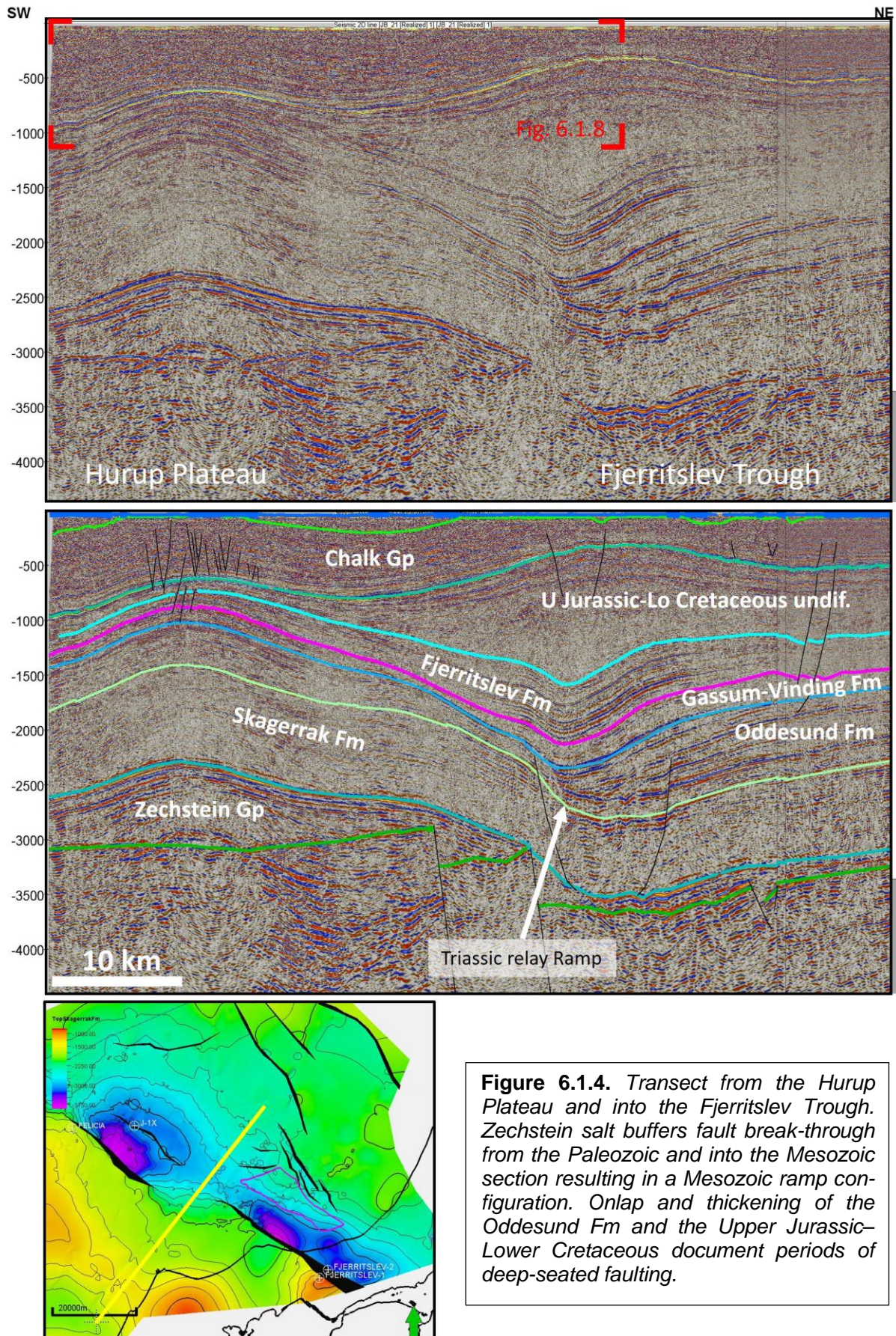


**Figure 6.1.4.** *Transect from the Hurup Plateau and into the Fjerritslev Trough. Zechstein salt buffers fault break-through from the Paleozoic and into the Mesozoic section resulting in a Mesozoic ramp configuration. Onlap and thickening of the Oddesund Fm and the Upper Jurassic–Lower Cretaceous document periods of deep-seated faulting.*

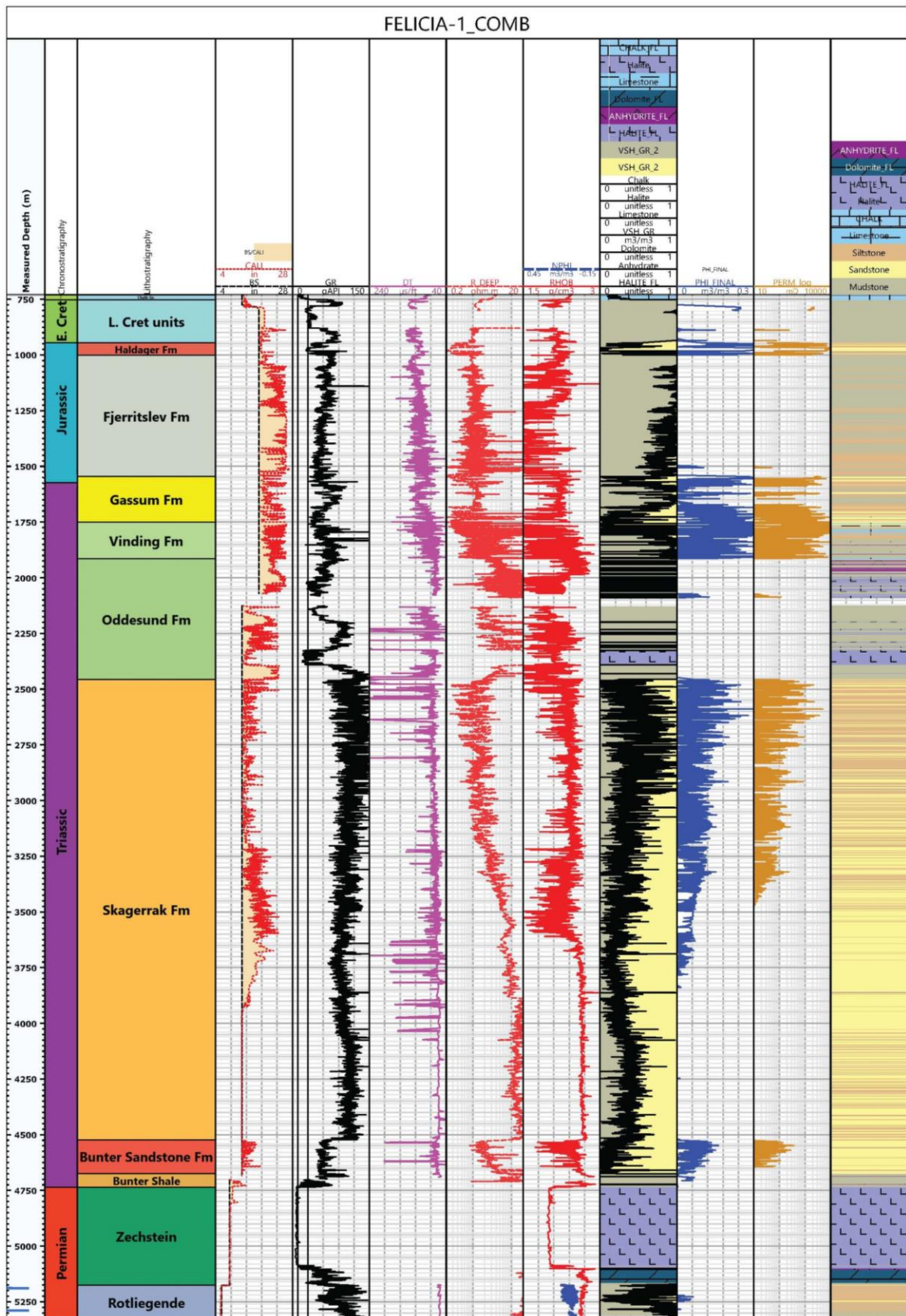


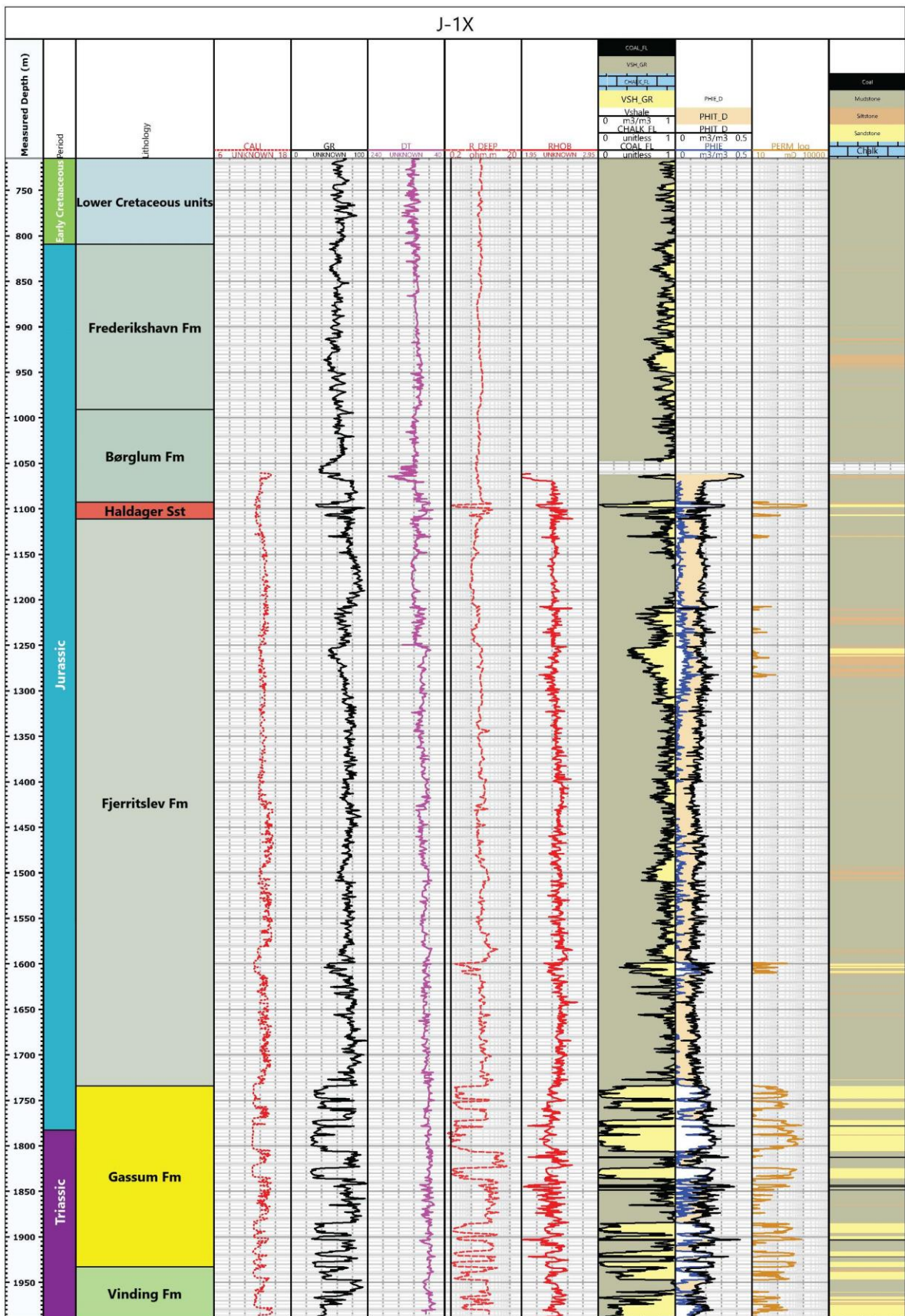
**Figure 6.1.5.** Lithostratigraphy and age of the Felicia-1a well section (two left columns) next to composite wireline logs depicted in the five central panels. Fourth column from the right depicts the calculated shale proportion (Vshale) in the interval next to calculated porosities and permeabilities and interpreted lithology in the far-right panel.

Above the Oddesund Fm occurs a succession typically ranging in thickness between 0.2 and 0.3 s TWT at the Jammerbugt structure and slightly thinner over part of the Hurup Plateau (Fig. 6.1.2), but without or only limited thickness variations across faults. The succession corresponds to the Mors Group consisting of the Vinding and Gassum fms intersected in Felicia-1a. Vinding Fm is mudstone-dominated but with limestone interbeds and only minor sandstone interludes (Fig. 6.1.5). The Vinding Fm is overlain by Rhaetian–Hettangian Gassum Fm that consists of interbedded sandstones, mudstones, claystones and minor limestones as well as traces of coal (Nielsen 2003). The Gassum Fm formed in a transitional marine/shore face-deltaic to non-marine environment (Nielsen 2003). It attains a thickness of 220 m in Felicia-1a and is interpreted to measure 199 m in J-1 (Figs. 6.1.5.; 6.1.6) [Statoil 1988; Fyhn et al. 2023]. In Vedsted-1, the Gassum Fm is parted into two separated by a 120 m thick mudstone-dominated interlude forming the lower part of the Fjerritslev Fm (Fig. 6.1.7). The younger part of the Gassum Fm measures around 50 m in thickness and is sandstone dominated. The lower part consists of interbedded sand and mudstones. The lowermost section in the well was attributed to the Skagerrak Fm (Nielsen and Japsen 1993). However, a recent inspection of a core from this deep part of the well has revealed coal clasts within interbedded sand- (coarse) and mudstones, resembling a coarse variation of the Gassum Fm. These new observations suggest a thickness of the lower part of the Gassum Fm in Vedsted-1 area exceeding 158 m (Fig. 6.1.7). The Fjerritslev-2 well located nearby the Jammerbugt structure also encountered the Gassum Fm (Berthelsen 1978), but a lesser thickness of 96 m was interpreted. The lower part of the well, including the potential Gassum Fm interval, was not logged petrophysically and a reassessment has not been attempted. However, judging from the Fjerritslev-2 completion report (Dapco 1958), the picked Gassum Fm interval seems far more mud-prone compared to all other wells drilled in the region. It is unclear whether this reflects:

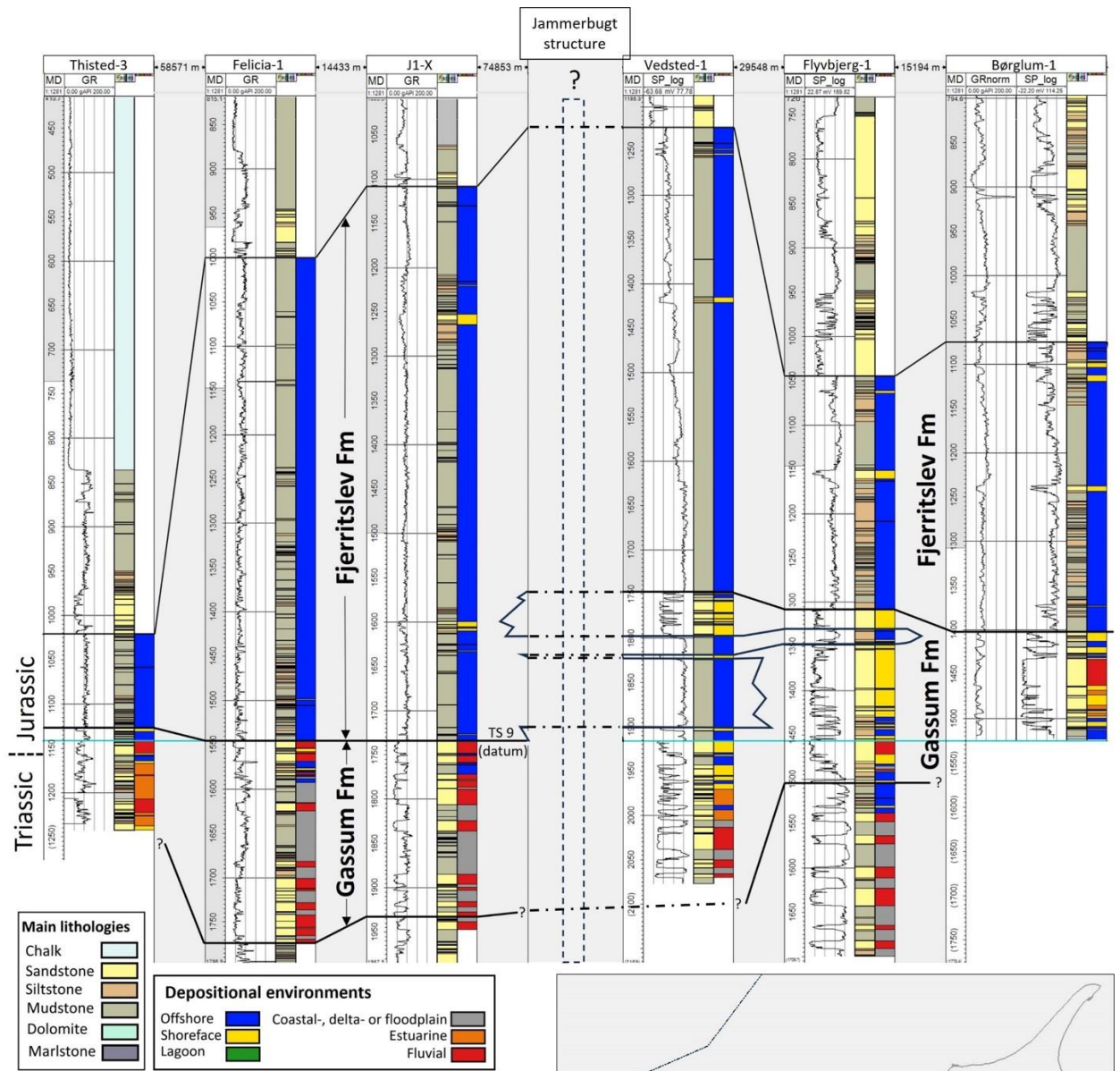
- (1) a real, but unusual and locally restricted muddy Gassum Fm facies,
- (2) an underestimation of the sand content in the intersected interval logged entirely based on cuttings, or rather
- (3) a result of a jump in stratigraphy across a normal fault intersected by the well located less than a kilometer away from the main Fjerritslev Fault Zone.

Therefore, information from the Fjerritslev-2 is treated with utmost caution. It should be noted that Sorgenfrei and Buch (1964) upgraded the sand content in the Lower Jurassic and Rhaetian interval of the well, although the basis for their reevaluation is unspecified.

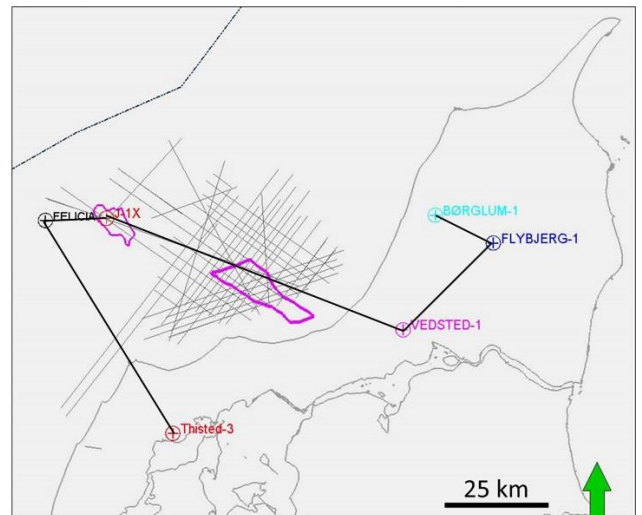
The Gassum Fm is overlain by a well-reflected, Lower to Middle Jurassic succession 0.3–0.4 s TWT thick over the Jammerbugt structure, which correlates with the Fjerritslev Fm in boreholes. The thickness increases to around 0.6 s TWT away from the structure and into the depocenter of the Fjerritslev Trough. The Fjerritslev Fm is claystone-dominated and met in both the J-1 (623 m), Felicia-1a (543 m), Vedsted-1 (674 m) and in the Fjerritslev-1 and 2 (>327 m and 911 m, respectively). The top of the Fjerritslev Fm is outlined by the Mid-Cimmerian unconformity and signs of truncation is seen over especially the Hurup Plateau (Fig. 6.1.8) but also locally north of the Jammerbugt structure.



**Figure 6.1.6.** Lithostratigraphy and age of the J-1 well section (two left columns) next to composite wireline logs depicted in the five central panels. Fourth column from the right depicts the calculated relative lithology next to calculated porosities and permeabilities and interpreted lithology in the far-right panel.



**Figure 6.1.7.** Composite well log panel illustrating the lateral variation of the Gassum and Fjerritslev fms and how this may be used to predict the nature of the lithostratigraphic units at the Jammerbugt structure. Location of wells are shown in insert map.



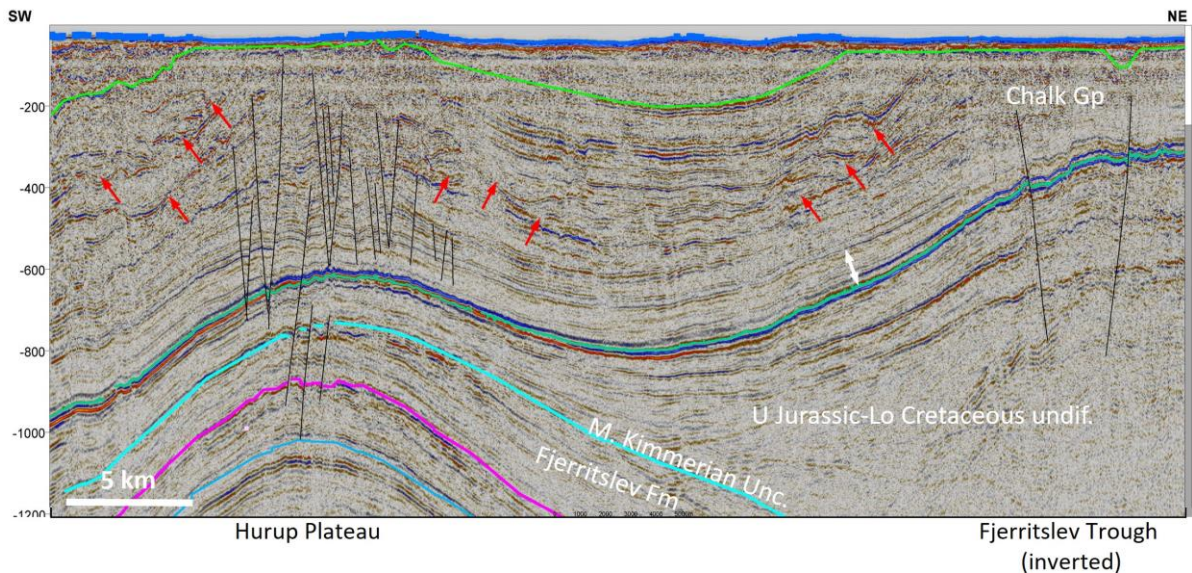


**Figure 6.1.8.** Detail of Fig. 6.1.4 illustrating a transect across the Hurup Plateau and the southwestern flank of the inverted Fjerritslev Trough. White double arrow highlight the wedging lower Chalk Group thinning towards the Fjerritslev Trough inversion anticline documenting the onset of inversion. Red arrows pin point the moat and trough architecture within some of the Chalk Group documenting a system of Late Cretaceous contourites. Please note that the youngest contourites exist southwest of the Hurup Plateau. Depth in TWT milliseconds.

The Middle Jurassic to Lower Cretaceous succession overlying the Mid-Cimmerian unconformity is generally less reflective than the underlying (Fig. 6.1.4). It is floored by the Haldager Sand Fm containing variable amounts of sand. Seismic resolution is inadequate to resolve the presence and thickness of the unit across the Jammerbugt structure, but it measures 57 m in Felicia-1a, only 19 m in J-1, 27 to 34 m in Fjerritslev-1 and 2 and 75 m in Vedsted-1. The overlying low-reflective Upper Jurassic to Lower Cretaceous interval is intersected in J-1 where it consists of an almost 500 m thick, mudstone-dominated succession floored by the Børglum Fm. The seismic reflection pattern at the Jammerbugt structure supports a similar interpretation. The Upper Jurassic succession onlaps the top of the Haldager Sand Fm towards the south and its distribution is mostly limited to the Fjerritslev Trough and the Skagerrak Platform while being absent over much of the Hurup Plateau.

The Upper Jurassic to Lower Cretaceous succession is overlain by the Chalk Group and the transition from siliciclastic-dominated deposits to limestones is accompanied by a strong contrast in acoustic velocity and density resulting in a very strong reflection set. The Chalk Group varies greatly in thickness in the Jammerbugt area (Fig. 6.1.2). The variation is first of all a result of differential erosion towards the base of the Quaternary. Erosion is deepest along the axis of the Fjerritslev Trough but also deep over the crest of the Hurup Plateau.

The Jammerbugt 2023 seismic survey has a high resolution of the Upper Cretaceous and younger stratigraphy. The resolution offers an improved imaging of the internal depositional architecture in the Upper Cretaceous showing that internal variation within the Chalk Group contribute to the overall thickness variation. The lower part of the Chalk Group is characterised by sub-parallel reflectors, but subtle bi-directional wedging towards the axis of the Fjerritslev Trough contributes to the thinning over the Fjerritslev Trough (Fig. 6.1.8) reversing the thickness trend compared with Middle Triassic through Lower Cretaceous units being thickest developed in the trough. In the middle part of the chalk group, a characteristic and complex drift-and-moat architecture exists

south of the Fjerritslev Trough decreasing over the central Hurup Plateau but increasing again along the southern flank of the plateau (Fig. 6.1.8). This pattern records the northwestern extend of Late Cretaceous ocean currents acting along the length of the Sorgenfrei-Tornquist Zone formerly described by Surlyk and Lykke, (2007). The drift and moat architecture along both the northern and southern flanks of the Hurup Plateau indicate a certain Late Cretaceous seabed relief of the plateau influencing ocean currents. A slight diachronic nature in the drift and moat system across the area seems to exist with the older drift and moats being better developed along the southern Fjerritslev Trough flank than coeval ocean current deposits south of the Hurup Plateau. Here, drift and moats with the greatest relief developed slightly higher in the stratigraphy suggesting a southwards shift in Late Cretaceous ocean currents across the region. South of the Hurup Plateau, much of the youngest Chalk Group seems affected by ocean current features, while the uppermost part of the Chalk Group consists of mostly sub-parallel reflectors appearing next to the Fjerritslev Trough.

Siliciclastic Paleogene strata above the chalk is only preserved in a shallow trough north of Hansholm; otherwise, chalk subcrops the seabed or the base of Quaternary strata; this is also the case at the Jammerbugt structure. Quaternary sediments are most thickly developed in the numerous fluvial incisions intersecting Jammerbugt. The incisions are up to a few hundred milliseconds deep and filled by sediments (Fig. 6.1.3H). Some incisions are associated with velocity pull-downs while others are not, suggesting variations in infill lithologies. Moreover, while some incisions are interconnected, other incisions intersect suggesting different generations of incision and channel in-fill. A few incised valleys are buried underneath the seabed over the Jammerbugt structure.

## **6.2 Structure and tectonic development**

### **Sub-regional tectonic development**

The Jammerbugt structure is a faulted three-way closure formed in the Fjerritslev Trough in response to the complicated geological evolution of the trough (Figs. 6.1.1; 6.1.3). The Fjerritslev Trough is a half-graben confined by the Fjerritslev Fault Zone that delineates a continuous fault at top-Pre-Zechstein level (Fig. 6.1.3A). The hangingwall block has been down-thrown with as much as 1.6 s TWT probably corresponding to more than 3 km, but heave varies considerably along the length of the fault and two extreme lows exist; one southwest of the Lisa structure and another southwest of the Jammerbugt structure extending shoreward across part of Jutland. In the areas with the largest fault throw, faults break through the entire Permian through Jurassic succession (Fig. 6.1.3C–F), while in the area with the least fault throw, fault throw is taken up within the Zechstein salt that deforms and fills in fault relief through differential salt motion (Fig. 6.1.4). Here, overlying strata bend to form a ramp-like monocline from the Hurup Platform towards the Fjerritslev Trough. Faulting thus occurred after the Permian despite only breaking through the top of the salt in the areas with the largest fault offset.

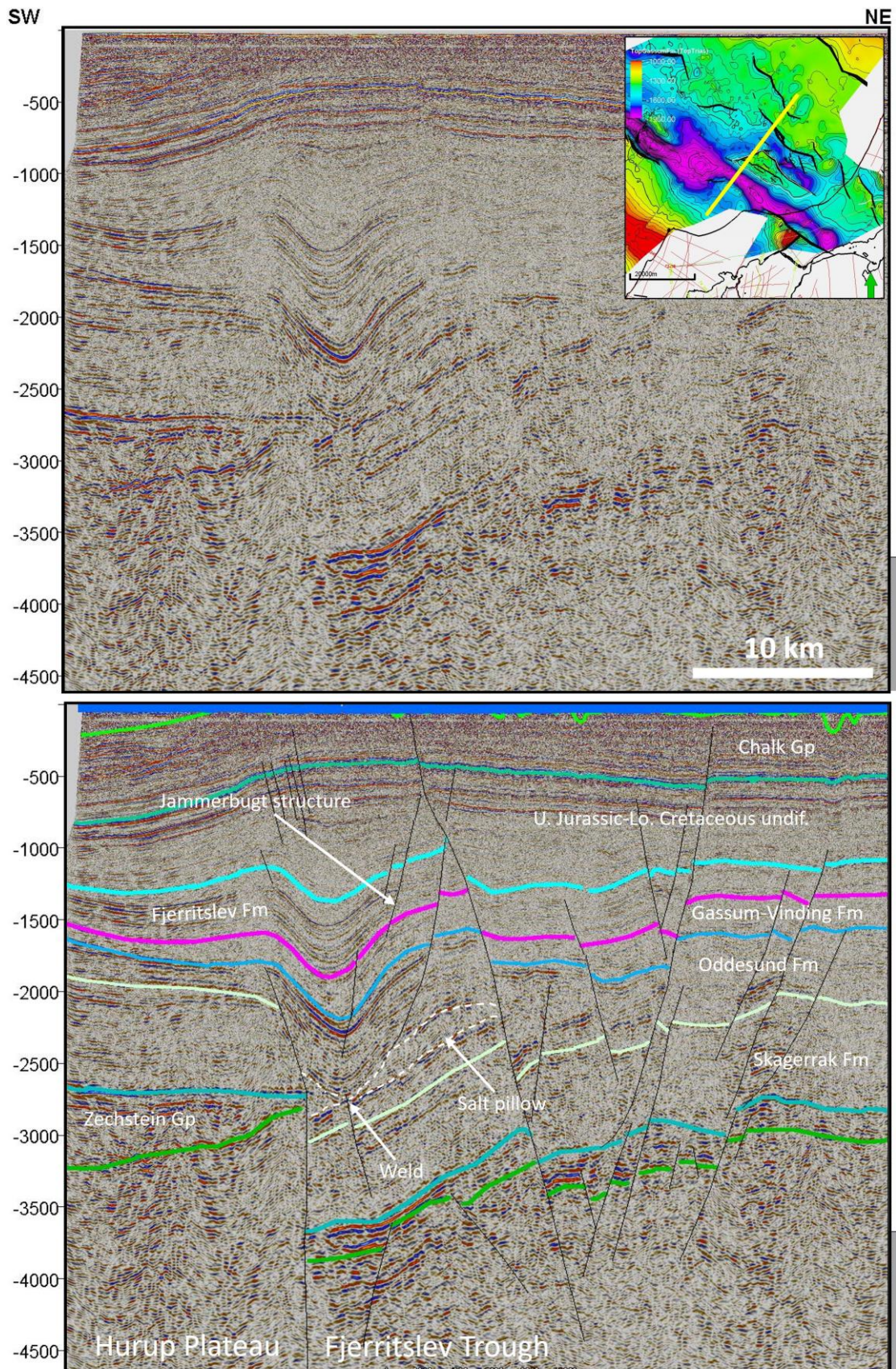


**Figure 6.2.1.** Transect over the northwestern part of the Jammerbugt structure and the ESE-WSW-striking boundary fault intersecting to near the seabed. Note fault-controlled thickening of the Oddesund Fm from the Hurup Plateau to the Fjerritslev Trough, the subtle Oddesund Fm salt pillow underneath the Jammerbugt structure and the associated Fjerritslev Trough salt weld. Depth in TWT milliseconds.

The unaffected thickness of the Skagerrak Fm across the Fjerritslev Fault Zone, and the strong thickness variation of the Oddeund Fm show that rifting only commenced in the latest part of the Middle Triassic (Figs. 6.1.3C & D; 6.2.1). The Oddeund Fm thickness mimics the areas with the greatest downfaulting towards the Fjerritslev Trough and the latest Middle to Late Triassic succession clearly formed as a syn-rift unit associated with the initiation of the Fjerritslev Trough (Figs. 6.1.2C; 6.2.1). Locally, Oddeund Fm thicknesses are influenced by differential motion of Oddeund Fm salt migrating from the depression next to the Fjerritslev Fault Zone and into small salt pillows located up-dip. This is seen at the Lisa structure and at the western part of the Jammerbugt structure and few kilometres to the west of it (Fig. 6.2.1).

The overlying latest Triassic to earliest Jurassic Mors Group is more uniform in thickness than the Oddeund Fm's and is interpreted to have formed following the termination of Triassic rifting (compare Fig. 6.1.2C & D). The relatively uniform thickness of the Mors Group differentiates from the strong thickness variations of the Lower to Middle Jurassic Fjerritslev Fm occurring towards and within the Fjerritslev Trough (Fig. 6.1.2E). Thickness variation was amplified by differential erosion along the mid-Cimmerian unconformity; but most variation resulted from syn-depositional differential subsidence in the Early and Middle Jurassic towards the Fjerritslev Trough resulting in reflector divergence within the trough. This is also seen in the great thickness change of individual Fjerritslev Fm members in the Fjerritslev-1 to the Fjerritslev-2 wells drilled few kilometres apart on either side of the Fjerritslev Fault Zone. Despite the rapid lateral thickness variations, fault offsets are small and restricted primarily to south of the Lisa structure and onshore (Fig. 6.1.2E). This is interpreted to be a result partly of Oddeund Fm salt deforming across the Fjerritslev Fault Zone, restricting fault break-through to areas with the most severe Jurassic extension. Deep-seated, Early and Middle Jurassic extension within the Sorgenfrei-Tornquist Zone is thus considered the forcing mechanism. Fault-controlled thickening of the Fjerritslev Fm also occur in the depression located immediately north of the Jammerbugt structure (Figs. 6.1.1; 6.2.1). In addition to the tectonic driver, the rim-syncline effect from underlying Oddeund Fm salt migrating from the depocenter towards salt pillows increased subsidence even further (Fig. 6.2.1).

Middle Jurassic reflector truncation along the Mid-Cimmerian unconformity signifies a paucity in the rift-controlled subsidence. However, extension continued and may even have intensified during the Late Jurassic and Early Cretaceous, where even larger thickness variations exist from the Hurup Plateau towards the Fjerritslev Trough. This is exemplified by the Lower Cretaceous thickness change from 166 m in Fjerritslev-1 drilled on the edge of the Hurup Plateau to more than 700 m thick in Fjerritslev-2 spotted three kilometres away on the down-faulted side of the Fjerritslev Fault in the trough. Again, fault offset is typically modest resulting from subsurface salt buffering deep-seated faults breaking through to the mid-Mesozoic. Once again, the rim-syncline effect from migrating Oddeund Fm salt added to subsidence in the depocenters (Fig. 6.2.1).

The uppermost Lower Cretaceous is characterized by internally parallel reflections and uniform thicknesses. This indicates that extension was brought to a halt sometimes in the mid-Cretaceous. Long wavelength folding and doming over the crest of the Fjerritslev Trough resulted from subsequent compression and structural inversion. Internal thinning occurs towards the inversions dome near the base of the Chalk Group (Fig. 6.1.8). This represents a complete reversal of the thickness trend over the Fjerritslev Trough compared with the underlying stratigraphy and signifies the onset of mild compression and inversion. This inversion onset occurring sometime during the Turonian

or even Cenomanian is earlier than previously recognized but simultaneous to the onset of inversion in the Kattegat part of the Sorgenfrei-Tornquist Zone (Mogensen & Jensen 1994). Mild inversion presumably continued during the Late Cretaceous causing the seabed relief that guided contour currents along the southern flank of the embryonic inversion dome. Intra chalk thinning also occurs above the Hurup Plateau indicating salt pillow growth. As relief grew and water depth decreased during the Late Cretaceous, seabed currents rerouted south focussing along the southwest flank of the Hurup Plateau as seen in the upward shift in contourite deposits within the Chalk Group (Fig. 6.1.8).

The folding of the entire Chalk Group and the overlying Paleogene siliciclastic succession at the flank of the Fjerritslev Trough show that inversion culminated after the Cretaceous presumably sometime during the Paleogene. Small-offset extensional faulting with up to several tens of milliseconds offsets deform the doming chalk above the Fjerritslev Trough. Most faults are constrained to within the Chalk group, while others offset the base of the chalk and die out in the lower Cretaceous (Fig. 6.1.8). Some faults even reactivate pre-existing faults and have even deeper roots (Fig. 6.2.1.). The faults are speculated to be associated with syn-inversion crestal extension over both the Fjerritslev Trough and the Hurup Plateau, but a younger kinematic history of the deep-seated faults offsetting the chalk cannot be excluded. Earthquake data does not reveal modern tectonic activity (Fig. 6.2.2)

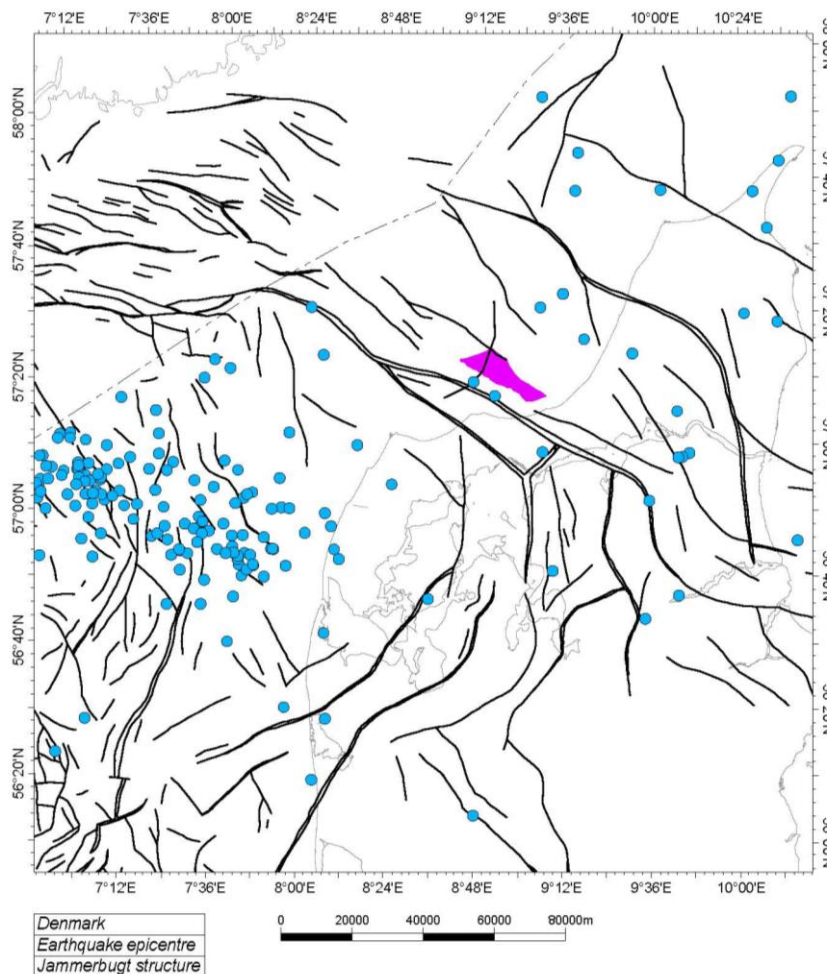


**Figure 6.2.2.** Map showing the calculated epicenter of modern earthquakes recorded after 1929 (blue dots). Pink area indicate the location of the Jammerbugt structure. Deep fault structures

after Vejrbæk (1997) are also shown. Source: <https://www.geus.dk/natur-og-klima/jordskaelv-og-seismologi/registrerede-jordskaelv-i-danmark>

### The Jammerbugt structure

The Jammerbugt structure is a fault-controlled three-way closure on the Top Gassum Fm and Haldager Sand Fm levels (Figs. 6.1.1; 6.2.1; 6.2.3). Two sets of faults and the regional stratigraphic dip confine the structure (Fig. 6.1.3E & F):

- A: An ENE–WSW striking fault delineating the northwestern border of the structure (Fig. 6.2.4),
- B: A NW–SE striking fault zone delineating the northeastern border of the structure and
- C: Regional southwestern dip of stratigraphy delineates the southwestern flank of the structure, but another NW–SE striking fault zone dipping towards the southwest offsets the structure (Fig. 6.1.3).

The seismic cover over the southeastern part of the structure is very limited, and apart from the gentle southeastern plunge of the structure, structural confinement in this direction is unknown (Fig. 6.2.4).

**Fault A** delineating the northwestern border of the structure offsets the top of the pre-Zechstein and is presumably rooted in the basement (Figs. 6.2.1; 6.2.4). The west-southwestern part of the fault detaches in Oddeund Fm salt building up into a salt pillow that floors the westernmost part of the Jammerbugt structure and the area to the west of it. The west-southwestern part of Fault A is therefore less steep above and within the Oddeund Fm compared to the east-northeastern part of the fault.

Stratigraphic thickening on the hangingwall block of Fault A is most significant within the Upper Jurassic to Lower Cretaceous section suggesting the primary timing of faulting. Offset of the Chalk Group indicates moderate reactivation since the mid-Cretaceous and the fault continues to near the seabed. Thickness variations also occur within the Oddeund Fm, but here thickening takes place on the footwall block and is interpreted as a result of differential motion of Oddeund Fm salt mobilized from the depocenter of the Fjerritslev Trough in the south.

**Fault B** is a northeast dipping normal fault conjugate to a NW-SE striking normal fault that is associated with an en echelon fault zone intersecting Jammerbugt from northwest to southeast, down-faulting the top-Pre-Zechstein towards the southwest (Figs. 6.1.1; 6.2.4). The deep-seated faulting triggered instability in the Mesozoic overburden above the Zechstein veneer that blankets the area causing sliding and faulting of the Mesozoic, which added to the overall anticlinal shape of the Jammerbugt structure breached by Fault B (Fig. 6.1.1). The anticline is cored by Oddeund Fm characterized by internally folded and deformed reflectors suggesting internal Oddeund Fm salt mobilization and growth as well as internal sliding that added to the anticlinal relief (Figs. 6.1.1; 6.2.1).

Fault B intersects the stratigraphy to the base of the Chalk Group and seems to die out within the chalk. The most substantial hangingwall thickening occurs within Fjerritslev Fm and within the overlying Upper Jurassic to Lower Cretaceous section indicating the timing of the main fault motion.

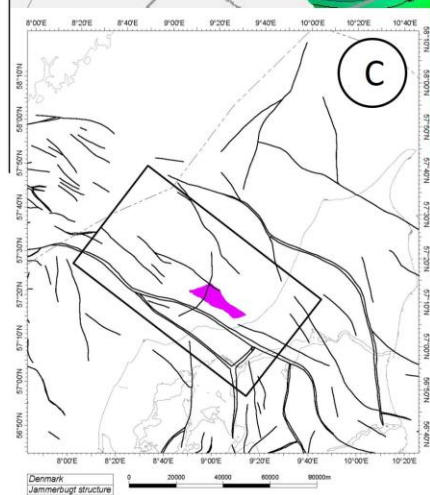
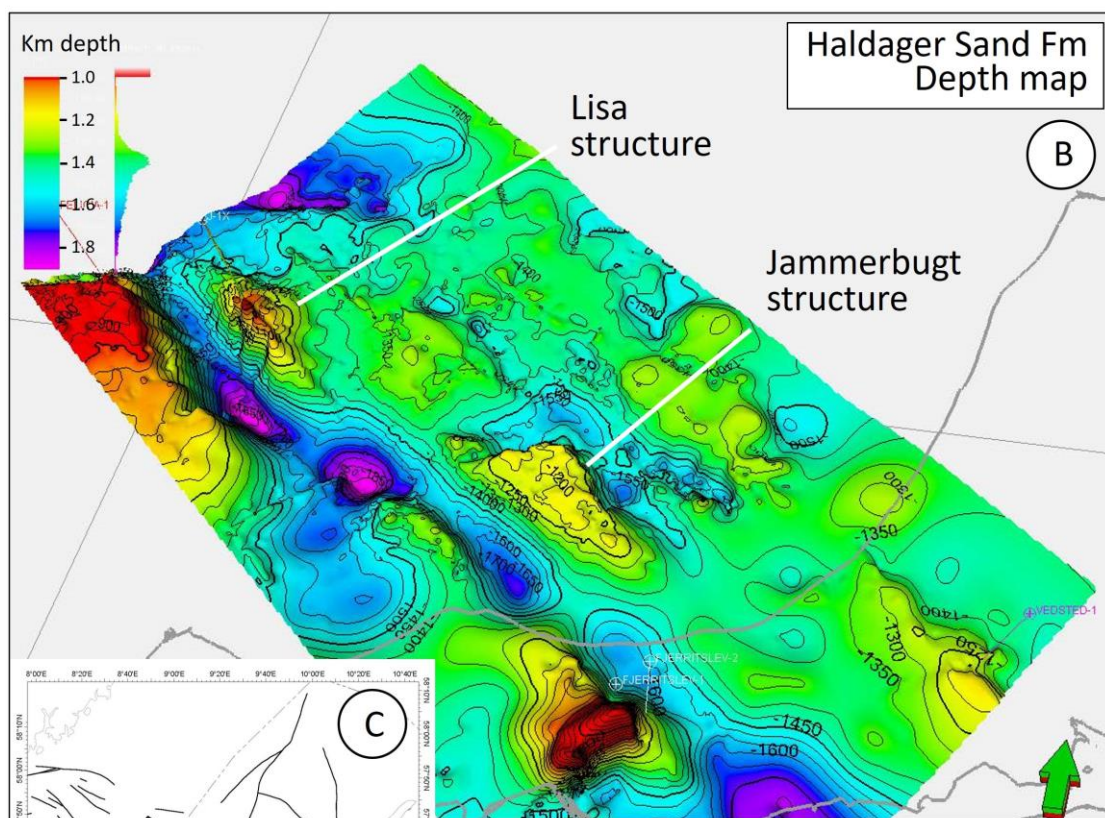
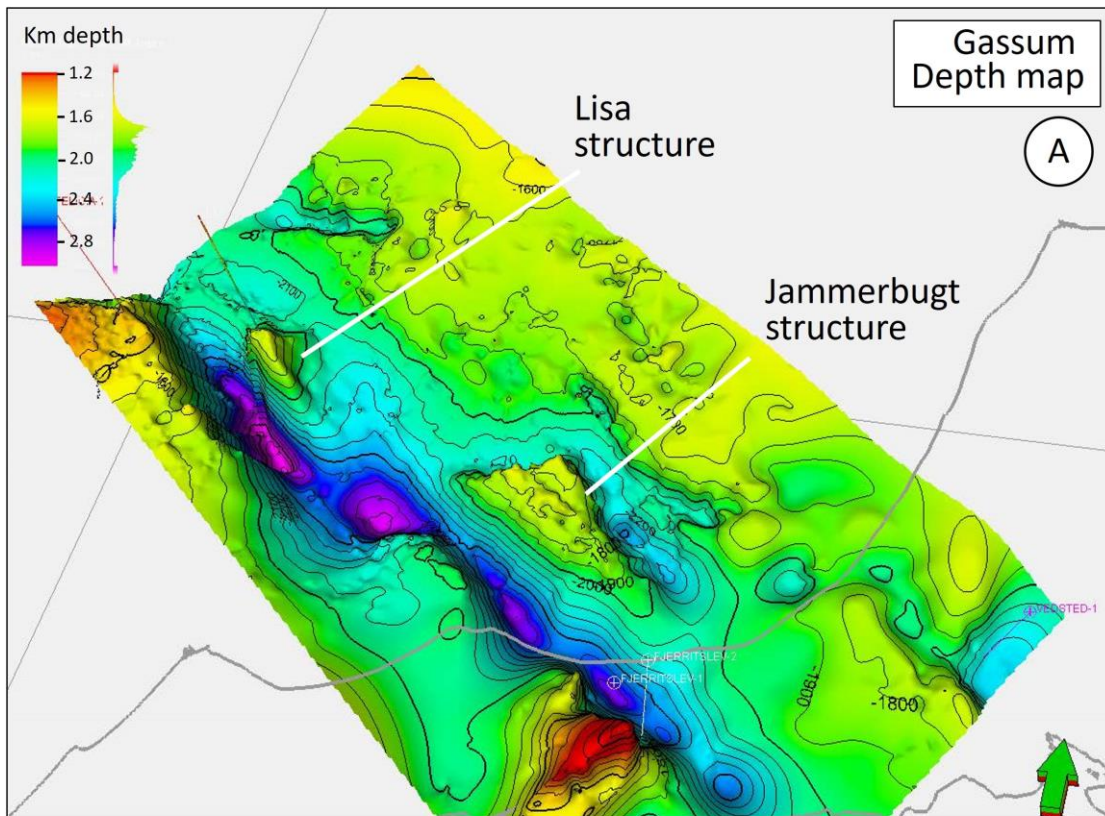


**Figure 6.2.3.** 3-D depth structure maps of the two reservoir intervals over the Jammerbugt structure obliquely viewed from the south. **A** Gassum Fm (near top Triassic) map; **B** near- Haldager Sand Fm (M Jurassic); **C** Basemap.

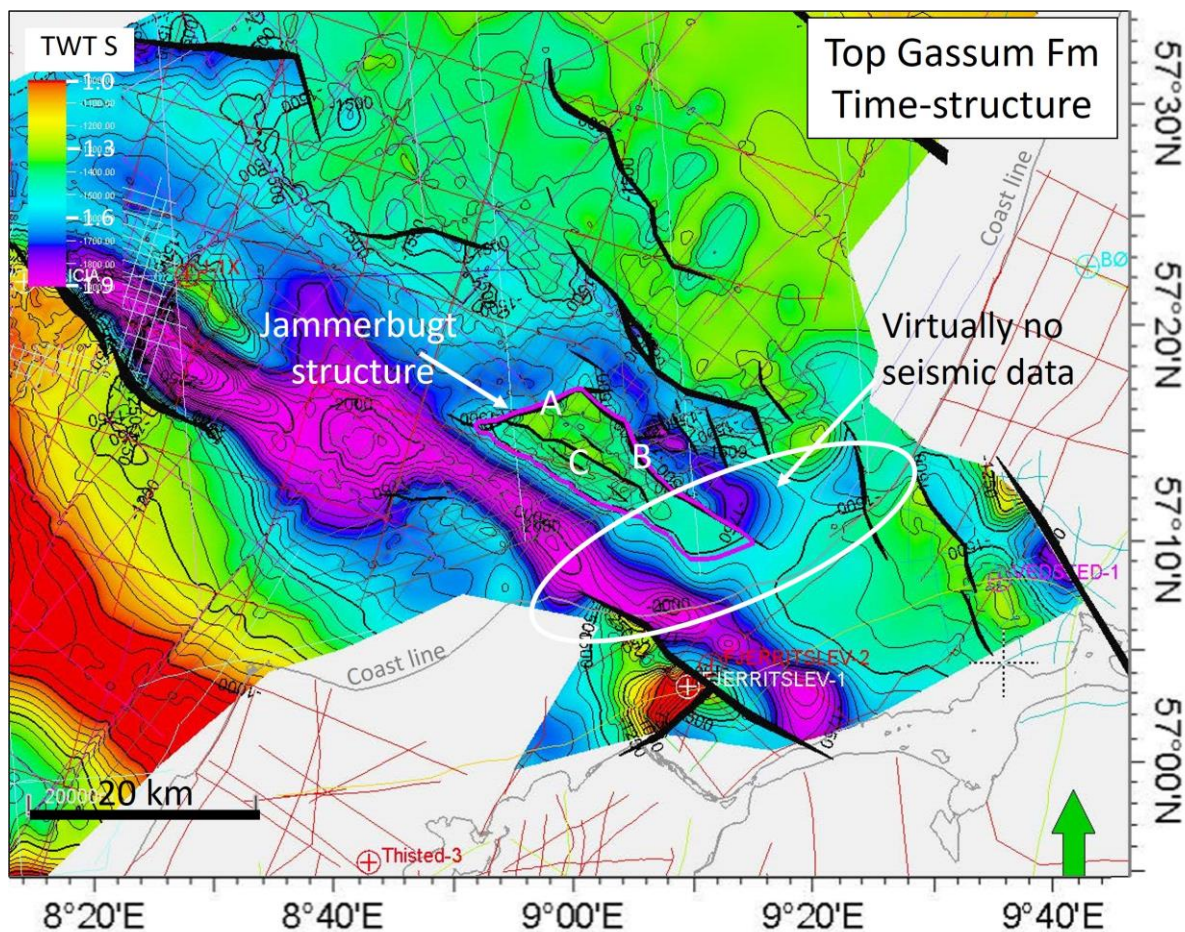


**Figure 6.2.4.** Two-way Time structure map towards the top of the Triassic Gassum Fm locating the Jammerbugt structure and the existing seismic data. A gap in data coverage exist over the shoreward part of the structure. Fault A: A; Fault B: B; Fault zone C: C.

The southwestern flank of the Jammerbugt structure is defined by the regional south-westward stratigraphic inclination dipping towards the Fjerritslev Trough depocenter (Figs. 6.1.1; 6.2.1). Dip-parallel extensional faulting (**Fault zone C**) offset the crest of the Jammerbugt structure with faults detaching within the Oddesund Fm (Figs. 6.1.1; 6.2.4). These faults are interpreted as a result of gravity driven faulting detaching in Oddesund Fm salt. Fault offset amounts to a few tens of milliseconds with offset of the Upper Triassic to Cretaceous section. Faults may locally intersect to near the seabed, although seismic resolution is incapable of resolving this. Growth in hangingwall thicknesses within the Jurassic through Upper Cretaceous suggest protracted and gentle fault activity.

From the seismic covered apex, the axis of the Jammerbugt structure plunges towards the east-southeast (Fig. 6.2.3). The nature of the southeastern-most part of the structure located within the inner, roughly, 10 km from the shore is virtually unknown due to the lack of seismic data (Fig. 6.2.4).

Depth conversion places the apex of the Gassum and Haldager Sand Fm reservoirs in around 1620 and 1160 m depth, respectively. This is in line with the comparable time-depth relationship in the J-1 well. Depth conversion translates the spill point to around 2000 m and 1400 m depth, respectively. While a 240 m closure height at Haldager Sand Fm level seems plausible, a closure relief around 400 m at the Gassum Fm level is higher than expected for a 200 ms seismic relief

at this depth. The depth conversion relies on seismic migration velocities corrected to match borehole stratigraphy. However, the Jammerbugt structure is located at some distance to calibrating wells. Moreover, seismic coverage lacks over the inner part of the structure, the structure is affected by faulting, is characterized by somewhat inclined stratigraphy around the reservoir level, and data was acquired with an only 2.1 km streamer. Therefore, depth conversion of especially the deeper part of the structure may be inaccurate. An overestimation of closure height may result in overestimated reservoir gross rock volumes and hence storage capacity estimates.

## 7. Geology and parameters of the Jammerbugt structure storage complexes

### 7.1 Reservoirs – Summary of geology and parameters

Seismic interpretation correlated with well data suggests the Jammerbugt structure to contain two reservoir intervals under structural closure both known for their excellent reservoir characteristics: The Gassum Fm and the Haldager Sand Fm (Fig. 6.2.3). The Jammerbugt structure is undrilled, and the existing seismic coverage is inadequate to resolve thickness and nature of the Gassum and Haldager Sand fms. Therefore, reservoir parameters such as thickness, net-to-gross, porosity and permeability have been qualified through comparison with nearby wells and regional considerations. Table 7.1.1 and 7.1.2 summarizes the reservoir properties of the two formations in nearby wells assessed through petrophysical analysis. Table 7.1.3 summarizes the reservoir quality of the Flyvbjerg Fm treated as a potential upside to the Haldager Sandstone Fm as elaborated below. The Gassum and Haldager Sand fms have comparable areas under closure (Fig. 6.2.3). The Gassum Fm is considered the primary reservoir due to its typically greater reservoir thickness compared with the Haldager Sand Fm.

**Table 7.1.1.** Gassum Fm reservoir properties obtained from relevant offset wells.

Gassum Fm reservoir properties										
Well name	Formation	Flag Name	Top	Gross	Net	Net to Gross	Av_Vshale	Av_PHIE	Av_PERM	
			m	m	m	m	v/v	v/v	v/v	
Felicia-1/1A	Gassum Fm	RES	1545.8	219.9	90.1	0.41	0.18	0.219	616	
J-1X	Gassum Fm	RES	1733.9	199.1	89.7	0.45	0.12	0.202	228	
Vedsted-1	Gassum Fm	RES	1913.9	162.8	77.3	0.47	0.20	0.167	121	
Thisted-3	Gassum Fm	RES	1126.3	116.6	56.1	0.48	0.21	0.301	2775	
Fjerritslev-1	Gassum Fm	RES	Not intersected							
Fjerritslev-2	Gassum Fm	RES	N/A (no petrophysical logs in interval)							

**Table 7.1.2.** Haldager Sand Fm reservoir properties obtained from relevant offset wells.

Haldager Sand Fm reservoir properties									
Well name	Formation	Flag Name	Top	Gross	Net	Net to Gross	Av_Vshale	Av_PHIE	Av_PERM
			m	m	m	m	v/v	v/v	v/v
Felicia-1/1A	Haldager Sst Fm	RES	945.3	56.0	35.6	0.64	0.19	0.268	1019
J-1X	Haldager Sst Fm	RES	1092.5	18.9	4.6	0.24	0.18	0.245	528
Vedsted-1	Haldager Sst Fm	RES	1149.4	73.9	65.9	0.89	0.17	0.319	1086
Thisted-3	Haldager Sst Fm	RES	977.6	43.5	35.4	0.81	0.20	0.293	1233
Fjerritslev-1	Haldager Sst Fm	RES	564.3	26	14	0.54	0.22	0.241	215
Fjerritslev-2	Haldager Sst Fm	RES	1288.6	33.3	20.6	0.62	0.15	0.133	52

**Table 7.1.3.** Flyvbjerg Fm reservoir properties obtained from relevant offset wells.

Flyvbjerg Fm reservoir properties									
Well name	Formation	Flag Name	Top	Gross	Net	Net to Gross	Av_Vshale	Av_PHIE	Av_PERM
			m	m	m	m	v/v	v/v	v/v
Felicia-1/1A	Flyvbjerg Fm	RES	N/A	0	N/A	N/A	N/A	N/A	N/A
J-1X	Flyvbjerg Fm	RES	N/A	0	N/A	N/A	N/A	N/A	N/A
Vedsted-1	Flyvbjerg Fm	RES	1215.5	24.0	4.7	0.20	0.22	0.304	101
Thisted-3	Flyvbjerg Fm	RES	950.1	27.5	3.6	0.13	0.4	0.184	127
Thisted-4	Flyvbjerg Fm	RES	611.5	29.8	16.9	0.57	0.28	0.294	9423
Fjerritslev-1	Flyvbjerg Fm	RES	546.6	17.7	1.7	0.1	0.29	0.24	313
Fjerritslev-2	Flyvbjerg Fm	RES	1263.3	25.2	2.9	0.12	0.39	0.179	65

### 7.1.1 The primary reservoir: The Gassum Formation

At the Jammerbugt structure, seismic resolution is inadequate to subdivide the Mors Group into the Gassum and Vinding Fm with reasonable certainty. This complicates assessment of the Gassum Fm at the Jammerbugt structure. The Mors Group was penetrated in the Felicia-1a, Thisted-1, -2, -4 and Mors-1 wells. The thickness of the Mors Group varies from 176 m to 370 m in these wells being thickest developed in the Fjerritslev Trough and thinnest over the Hurup Platform. While the thickness varies distinctly, the relative thickness between the Gassum and Vinding fms making up the Mors Group is relative uniform, with the Gassum Fm comprising between 59% and 67% of the Mors Group-thickness in these wells. The thickness of the Mors Group over the Jammerbugt structure, judging by the depth converted seismic interpretation, varies from roughly 300 to 400 meters. Provided a similar thickness relation at the Jammerbugt structure would suggest a Gassum Fm thickness in the order of around 200 m. This thickness is compatible with the Gassum Fm thickness of 220 and 199 m in Felicia-1a and J-1, respectively, drilled nearby and in compatible settings to the Jammerbugt structure. In Vedsted-1 the roughly age-equivalent part of Gassum Fm is 158 m thick, and the base of the unit is not met in the well according to the interpretation in this report (Fig. 6.1.7), whereas the Skagerrak Fm is interpreted to be encountered by Nielsen and Japsen (1991). The latter interpretation is difficult to reconcile with the presence of coal clasts in the lowermost part of the well. In addition, a Lower Jurassic sandstone interlude belonging to a younger 50 m thick part of the Gassum Fm is intersected in the Vedsted-1. The presumably roughly equivalent interval is only 2 m thick in the J-1 well (Fig. 6.1.7). Being located midway between the two wells, a greatness somewhere between these thicknesses is plausible at the Jammerbugt structure. However, the reported possible absence of the sandy interval in the Fjerritslev-2 well (Dapco 1958) introduces uncertainty to its possible existence at the Jammerbugt structure. Later work upgraded the Rhaetian sand content in the well (Sorgenfrei and Buch 1964) [see discussion of this in section 6.1]. Nonetheless, this potential outlier needs explanation warranting further investigation.

**Table 7.1.1.1.** Relation between Mors Group thickness and the thickness of the Vinding and Gassum fms.

Mors Group thicknesses and thickness relations			
Well name	Mors Group thickness	Vinding Fm	Gassum Fm
Felicia-1a	370 m	150 m / 41%	220 m / 59%
Thisted-1	189 m	64 m / 34%	125 m / 66%
Thisted-2	201 m	66 m / 33%	135 m / 67%
Thisted-4	176 m	62 m / 36%	114 m / 64%
Mors-1	255 m	88 m / 35%	167 m / 65%

Gassum Fm sandstones of Herttanganian to Rhaetian age in J-1 is typically porous, fine- to medium grained, argillaceous and well-sorted (Gulf 1970). Olivarius et al. (2019) pointed out that the feldspar content has occasionally been underestimated in original well-site studies in the Danish western part of the Norwegian–Danish Basin and that Gassum Fm sandstones are often arkosic in nature. An arkosic and occasionally micaceous composition of part of the Gassum Fm sandstones, implies a higher concentration of radioactive elements compared to clean quartz sandstones. This increases the uncertainty of the petrophysical lithological interpretations, possibly leading clay bearing interbeds being interpreted as sandstone, thus leading to further uncertainty in the interpretation of the porosity and in particular the permeability.

Gassum Fm net-to-gross ranges between 0.4 and 0.5 in Felicia-1a, J-1X, Vedsted-1, Thisted-1 and -3 (Table 7.1.1) and in Felicia-1a, J-1X and Vedsted-1 average porosities varies between 17% and 21% with the top of the Gassum Fm being situated in roughly the same depth as it is prognosed at the Jammerbugt structure (1620 m based on seismic depth conversion [Fig. 6.2.3A]). The 800 to 1000 m Cenozoic denudation experienced at these three wells (Japsen et al. 2007) is overall compatible with - although slightly larger than - the one having occurred at the Jammerbugt structure judging from the regional inversion-related relief and the level of Chalk Group erosion (Figs. 6.1.2G; 6.1.3G; Table 7.1.1).

### **7.1.2 Secondary reservoir 2: Haldager Sand Formation**

The Haldager Sand Fm varies from 19 m to 74 m in thickness in the wells located closest to the Jammerbugt structure (Table 7.1.2). Net-to-gross varies between 0.24 and 0.89 in the same wells with the lowest net-to-gross occurring at the thinnest developed Haldager Sand Fm in J-1 and vice versa for the thickest developed Haldager Sand Fm in Vedsted. The distinct lateral thickness variation may be rooted in the different tectonic settings tested by the wells (Nielsen 2003). The J-1 well tested the Lisa structure located in the Fjerritslev Trough. The Lisa structure formed above a salt pillow growing in the Jurassic (Fyhn et al. 2023), and coarse-grained deposition may preferably have been guided away from the structure. The Jammerbugt structure were similarly growing during Jurassic time possibly rerouting coarse-grained sediment transport around the structure. A conservative prediction of the Haldager Sand thickness and net-to-gross at the Jammerbugt structure is therefore adopted here.

Based on the seismic depth conversion, the top of the Haldager Sand Fm is located near 1160 m depth at the crest of the structure. This is comparable to its location in the J-1 well where it was encountered in 1092 m depth bmsl. In J-1, the succession consists of 19 m thick mixed sand-, silt and mudstones formed in Bajocian to Callovian time (Middle Jurassic). The sandstones are fine-grained, typically slightly calcareous and composed by angular to sub-angular, colorless to white, quartz grains (Gulf 1970). The succession contains a very impoverished fossil microfauna (Church et al. 1970), which probably owes to a fluvial to near-shore depositional environment typically interpreted for the Haldager Sand Fm (Nielsen 2003).

Information regarding lithology and reservoir quality derives from electrical logs, cuttings samples and a single sidewall core. The sandstones consist primarily of well-sorted, sub-angular, coarse-grained, and loosely consolidated porous sand with an average porosity of around 24%, a derived average permeability of 528 mD. The formation rests on the mid-Cimmerian unconformity and is

interpreted to having formed as a transgressive sand following the culmination of Middle Jurassic uplift in a fluvio-marine environment.

### **7.1.3 Secondary reservoir 2 upside: Flyvbjerg Formation**

In Thisted-3, -4, Fjerritslev-1, -2 and Vedsted-1, the Haldager Sand Fm is overlain by the Upper Jurassic Flyvbjerg Fm ranging from 17 to 30 m in thickness, while the Flyvbjerg Fm lacks in Felicia-1a and J-1. In four of the five wells encountering the Flyvbjerg Fm, the formation has a net-to-gross of only 0.1 to 0.2, while Thisted-4 denotes an outlier with a net-to-gross of 0.57. Porosities range from 0.18 to 0.3. As the tectonic setting of the Jammerbugt structure resembles the Lisa structure exemplified by J-1 the most, it is highly uncertain if the Jammerbugt structure contains Flyvbjerg Fm. The unit is therefore only treated as a potential upside to the Haldager Fm in the evaluation of the Jammerbugt structure.

## **7.2 Seals – Summary of geology and parameters**

Two reservoir/seal pairs are identified over the Jammerbugt structure. These are the Gassum/Fjerritslev fms (primary) and the Haldager Sand/Børglum fms (and overlying Upper Jurassic–Lower Cretaceous fine-grained units) [secondary]. The seals are described in the following sections.

### **7.2.1 The primary seal (for the Gassum Fm): The Fjerritslev Fm**

The Lower Jurassic Fjerritslev Fm works as seal for the Gassum Fm reservoir. The formation consists of a marine, uniform, shaly, slightly calcareous succession with thin silty/sandy interbeds. Fjerritslev Fm is subdivided into four members F-I to F-IV, from base to top, respectively (Michelsen et al. 2003). Over the Jammerbugt structure, the seismic thickness of the Fjerritslev Fm is typically between 0.3 and 0.4 s TWT. While depth conversion (presented in section 5.2) converts this thickness to around 700 m, we consider this estimate to be somewhat high. Comparisons with acoustic velocities from the J-1 well penetrating the Fjerritslev Fm in a comparable depth and with a similar burial history suggests average seismic velocities of approximately 3 km/s, which, if applied on the Jammerbugt structure, would correspond to a thickness between 450–600 m.

The base of the seal is located at 1620 to 2000 m depth but has probably been buried approximately 800 to 1000 meter deeper prior to inversion and Neogene uplift and erosion (Japsen et al. 2007). The mudstones are thus most likely more compacted with better sealing capacity than their present-day depth would indicate.

In the J-1 well, the Fjerritslev Fm consists of claystones and mudstones apart from a few meter-thick sandy to silty beds. The lower 120 m of the Fjerritslev Fm in J-1 consists of shales directly succeeding the Gassum Fm and is likely the most important sealing unit of the Triassic sandstones (Fig. 7.2.1.1). Located stratigraphically higher, the 50 m thick, massive Lower Jurassic, sand-dominated interval met in the Vedsted-1 well is also encased in Fjerritslev Fm mudstones. In the J-1 well, this coarse-grained interlude is overlain by a few hundred meters of claystones

that likely have good sealing characteristics. In J-1, the upper part of the Fjerritslev Fm contains other thin sandy to silty beds separated by roughly 50 m of shales. At the Jammerbugt structure, the entire Fjerritslev Fm forms a structural closure and the sandy to silty interbeds in the formation may form secondary subtle traps themselves reducing the risk for CO<sub>2</sub> escaping from the Gassum reservoir to sea bottom and forming the basis for monitoring for potential CO<sub>2</sub> leakage from the primary reservoir.

Faults propagate upwards through the Gassum Fm, the Fjerritslev Fm and overlying strata (Fig. 6.2.4). These fault breakthroughs formed during the Jurassic and Cretaceous and is presumably inactive. In a worst case, the faults may be critical to CO<sub>2</sub> storage in the underlying Gassum Fm (Bruno et al. 2014). The potential consequences for the sealing efficiency of the Fjerritslev Fm therefore needs to be investigated.

A chemical log panel reflecting the J-1 well is presented in Figure 7.2.1.2 based on selected elements that give a good impression of the key lithologies. The Al and Si are for example the main proxies for clay and coarser material (silt, sand), respectively, in the rock and the Si/Al ratio is the key ratio to examine the relative proportion between coarse- and fine-grained material. Likewise, Ca is the main proxy for carbonate minerals. Fjerritslev Fm mudstones in J-1 can be grouped into two. In the lower part (1734 — c. 1450 m) a clay dominated low carbonate rock type exist. This type grades into an upper type characterized by presumably higher clay content and higher Ca, S and TOC contents (Figs. 7.2.1.2; 7.2.1.3).

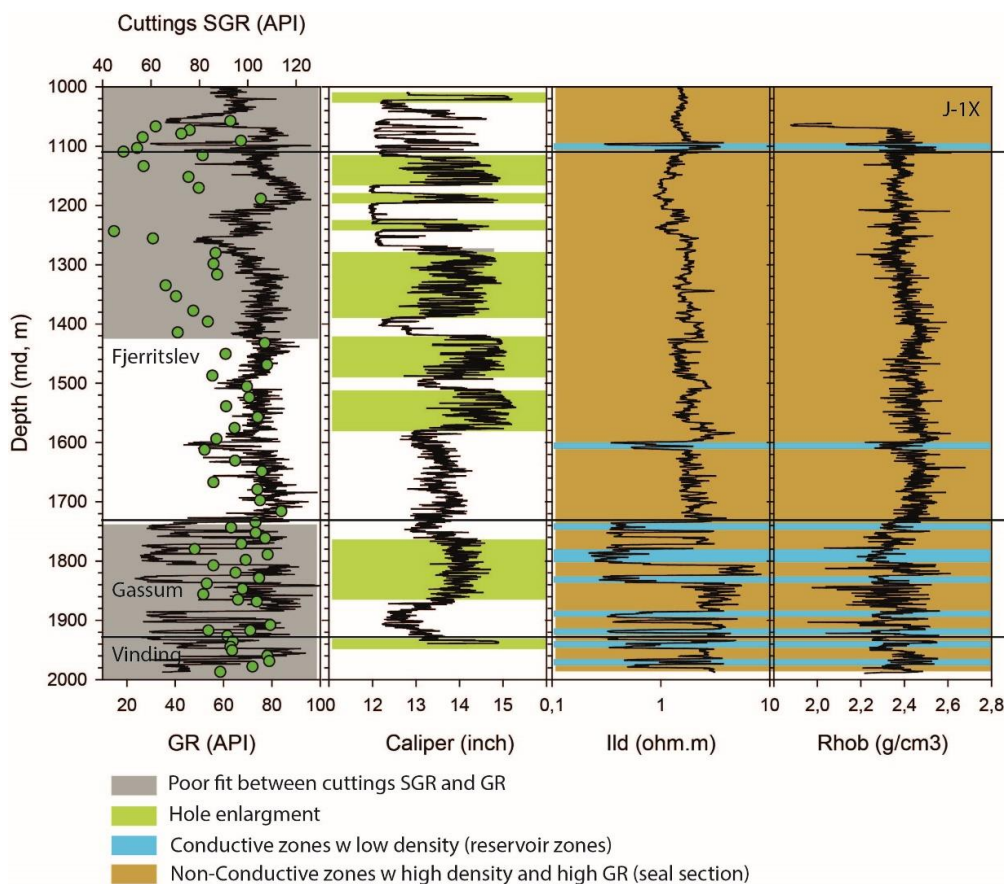


**Figure 7.2.1.1.** J-1 wireline logs over the primary reservoir and seal intervals with seal and reservoir intervals highlighted. The cuttings sum gamma ray (SGR) calculated from handheld-XRF determination of U, Th and K are shown in the left column as green dots and compared with the measured GR wireline log.

The Fjerritslev Fm is commonly rich in organic matter and is typically richest in the upper F-III and F-IV members (mb) (Petersen et al. 2008), but in the J-1 well, the entire formation is fairly organic lean. The TOC varies from only 0.55–2.05 wt.% (Fig. 7.2.1.3). In the Jammerbugt structure, the Fjerritslev Fm is located too shallow to be thermally mature. The sealing properties are thus not expected to be impacted by a high organic matter content or generation of hydrocarbons that could have created fluid migration pathways. In the J-1 well the lower F-I mb has an average TOC content of 0.93 wt.% and an average HI of only 58 mg HC/g TOC. Guiltinan et al. (2017) demonstrated that even thermally mature carbonaceous shales with TOC of up to 8% may have sealing capacity. On a regional average, the F-I mb has a TOC content of 0.97 wt.% with maximum values of around 5 wt.%.

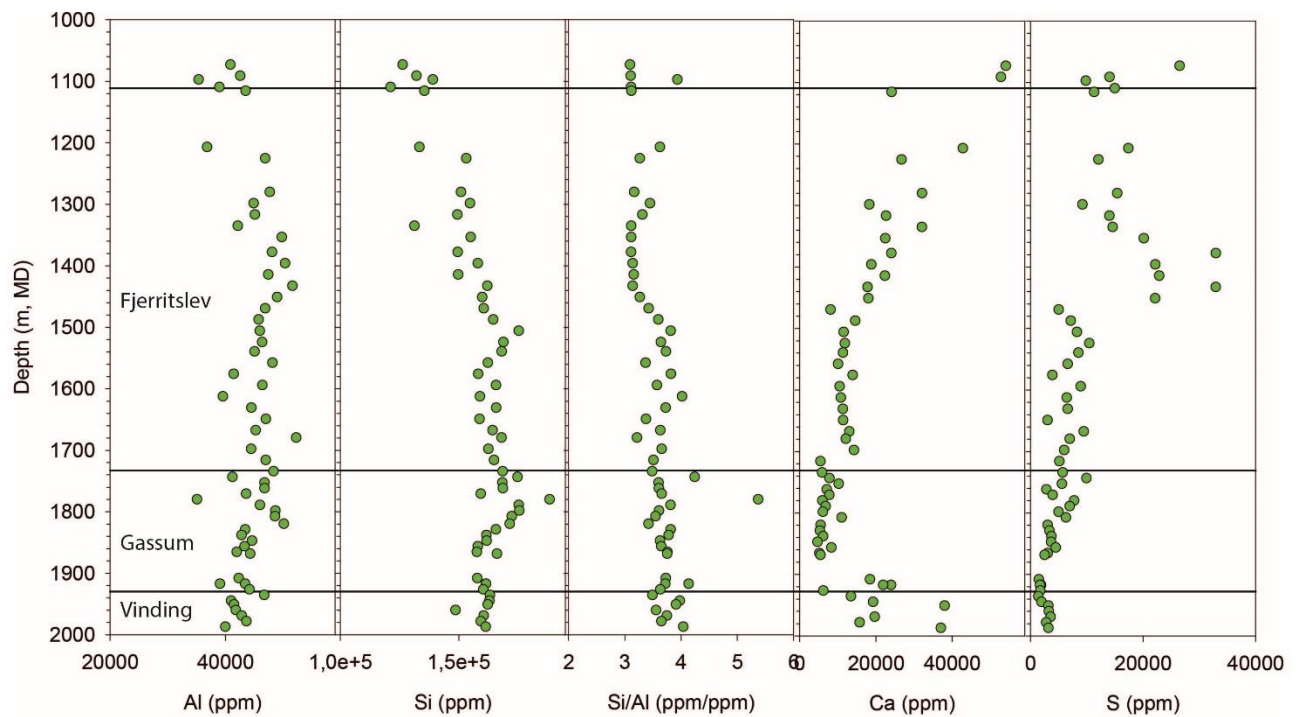


**Figure 7.2.1.2.** Elemental logs of Al, Si, the Si/Al ratio, Ca and S from the J-1.

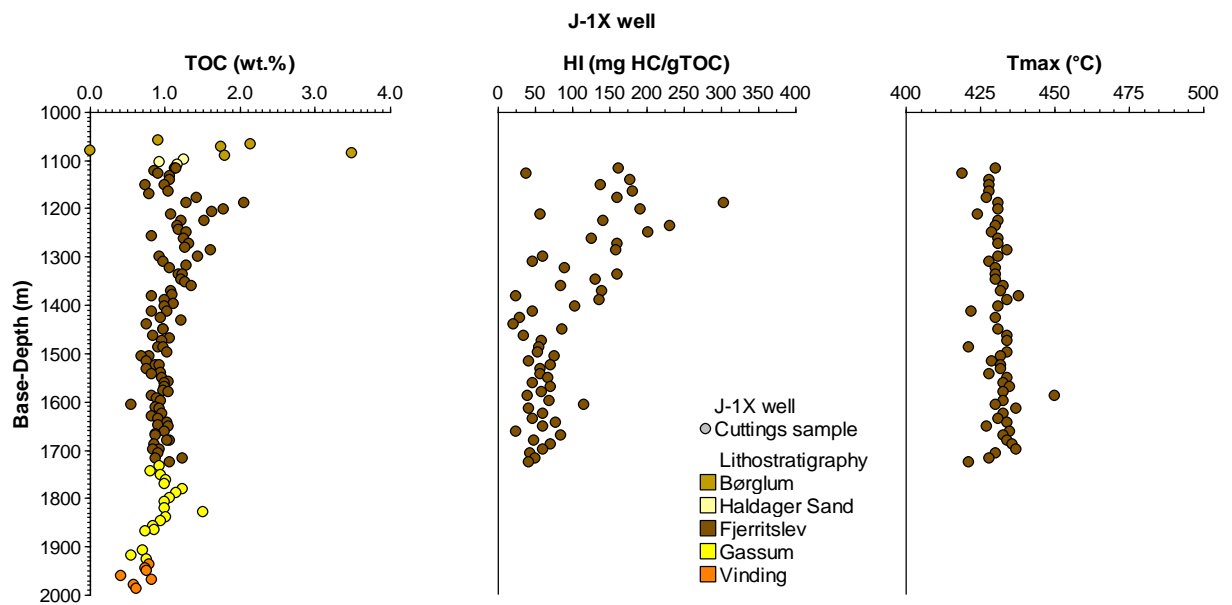


**Figure 7.2.1.3.** The TOC content in the Vinding, Gassum, Fjerritslev, Haldager Sand and Børglum fms and Hydrogen Index (HI) and  $T_{max}$  values of the Fjerritslev Fm in the J-1 well. The TOC content is generally low in the entire section and varies only little around c. 1 wt.% from the middle–upper part of the Gassum Fm and through most of the Fjerritslev Fm.  $T_{max}$  values below approximately 430°C show the Fjerritslev Fm is thermally immature. Very low to low HI values indicate mostly scattered terrigenous organic matter.

Clays in the Fjerritslev Fm mudstones primarily consists of kaolinite and illite but also contains some smectite. Quarts comprise up to half of the bulk mineral composition above the clay-size fraction. A high clay content reduces the size of pore throats, permeability, and thus the capillary entry pressure (Katsube and Williamson 1994). Experiments simulating reservoir conditions on Fjerritslev Fm samples from the onshore Stenlille-2 well demonstrated a fluid permeability of 3 mD making it an excellent cap rock (Springer et al. 2010). Springer et al. (2010) further demonstrated a capillary entry pressure of 70 bar for a massive Fjerritslev Fm mudstone layer during a super-critical (sc) CO<sub>2</sub> seal capacity test. This corresponds to a capability of retaining an at least 1000 m high vertical column of scCO<sub>2</sub> - much thicker than the closure height and reservoir thickness at the Jammerbugt structure.

With the high sealing capacity of the Fjerritslev Fm in general and the few hundred meters thickness in the Jammerbugt structure, the seal risk *sensu* Bruno et al (2014) is low and the unit is likely a good seal. However, the faulting of the Fjerritslev Fm over some of the structure and its potential effect on sealing integrity requires further investigation.

The Fjerritslev Fm is presumably overlain by the Haldager Sand Fm, which in turn is overlain by the fine-grained Upper Jurassic Børglum and Frederikshavn fms which likely form secondary seals of the Gassum Fm. These formations are characterized below.

## 7.2.2 Seals of the secondary reservoir/seal pairs: The Børglum and Frederikshavn fms sealing the Haldager Sand Fm

By comparison to the stratigraphy over the nearby Lisa structure, Upper Jurassic fine-grained deposits are expected to be thickly developed in the Jammerbugt area. In J-1 (drilling the Lisa structure), the Haldager Sand Fm is overlain by close to 300 m Upper Jurassic Børglum (101 m) and Frederikshavn fms (182 m) both fine-grained in nature in J-1. In J-1, Børglum Fm is generally a uniform fine-grained succession dominated by homogenous, often calcareous shales with a highly varying TOC content ranging from completely organic lean to 3.49 wt.% TOC (Fig. 7.2.1.3). The depth of the interval in the Jammerbugt structure suggest that they are thermally immature thus precluding any thermogenic hydrocarbon generation. The formation formed in an open marine environment and in some other wells has a variable content of siltstones and minor sandstones (Michelsen et al. 2003). In the J-1 well, Børglum Fm is overlain by 182 m Frederikshavn Fm consisting of mudstones and subordinate siltstones, although the formation becomes increasingly sandy in wells farther north (Michelsen et al. 2003).

The Børglum and Frederikshavn fms are 113 and 142 m thick, respectively, in the Fjerritslev-2 well, and 48 m and 235 m, respectively in Vedsted-1 and fine-grained. A comparable nature and thickness are anticipated in the Jammerbugt structure. With the high sealing capacity and the substantial thickness of the Børglum Fm and the overlying fine grained succession, the units qualify as a low-risk seal *sensu* Bruno et al. (2014). However, the faulting of the Upper Jurassic in the Jammerbugt structure and its potential effect on sealing integrity requires further investigation.

Apart from forming the primary seal for the Haldager Sand Fm, the Børglum and Frederikshavn fms at the Jammerbugt structure form secondary seals for the Gassum Fm reservoir. The overlying several hundred meter Lower Cretaceous almost entirely consists of mudstones in the J-1, Vedsted-1 and Fjerritslev-1 wells, and in the Jammerbugt structure, a structural closure exists all the way to the top of this unit. The unit has been buried at least 800m deeper than they are today and likely have good sealing properties. However, much of the Lower Cretaceous is located above 800 m depth – the approximate depth below which CO<sub>2</sub> passes from gas to a super critical liquid - and it is not considered a secondary seal *sensu stricto*.

## 8. Discussion of storage and potential risks

### 8.1 Volumetrics and Storage Capacity

Primary input for the CO<sub>2</sub> storage capacity estimation is the presented depth converted seismic interpretation of the Haldager Sand Fm and Gassum Fm reservoirs (see Figure 8.1.1). Secondly, well derived data form the basis for the reservoir characteristics including thickness, net-to-gross and average porosities (Table 7.1.5). The petrophysically-derived information was evaluated in context of the overall geological setting of the undrilled Jammerbugt structure. Thirdly, the expected density of the stored CO<sub>2</sub> is predicted relying on expected temperature and pressure condition in the subsurface reservoir.

The Gross Rock Volume (GRV) is calculated as the total volume between the top and base reservoir surfaces (see Figure 8.1.1.) The so-called Waste Rock Volume (WRV) (*James et. al., 2013*) is subtracted from the total volume to give the resulting GRV. Gross reservoir thickness is corrected with the N/G ratio to obtain the reservoir sand thickness for the GRV.

The Haldager Sand and Gassum fms are defined as the storage units at the Jammerbugt structure. These two potential reservoirs have a mapped closure area of 142 and 119 km<sup>2</sup>, respectively.

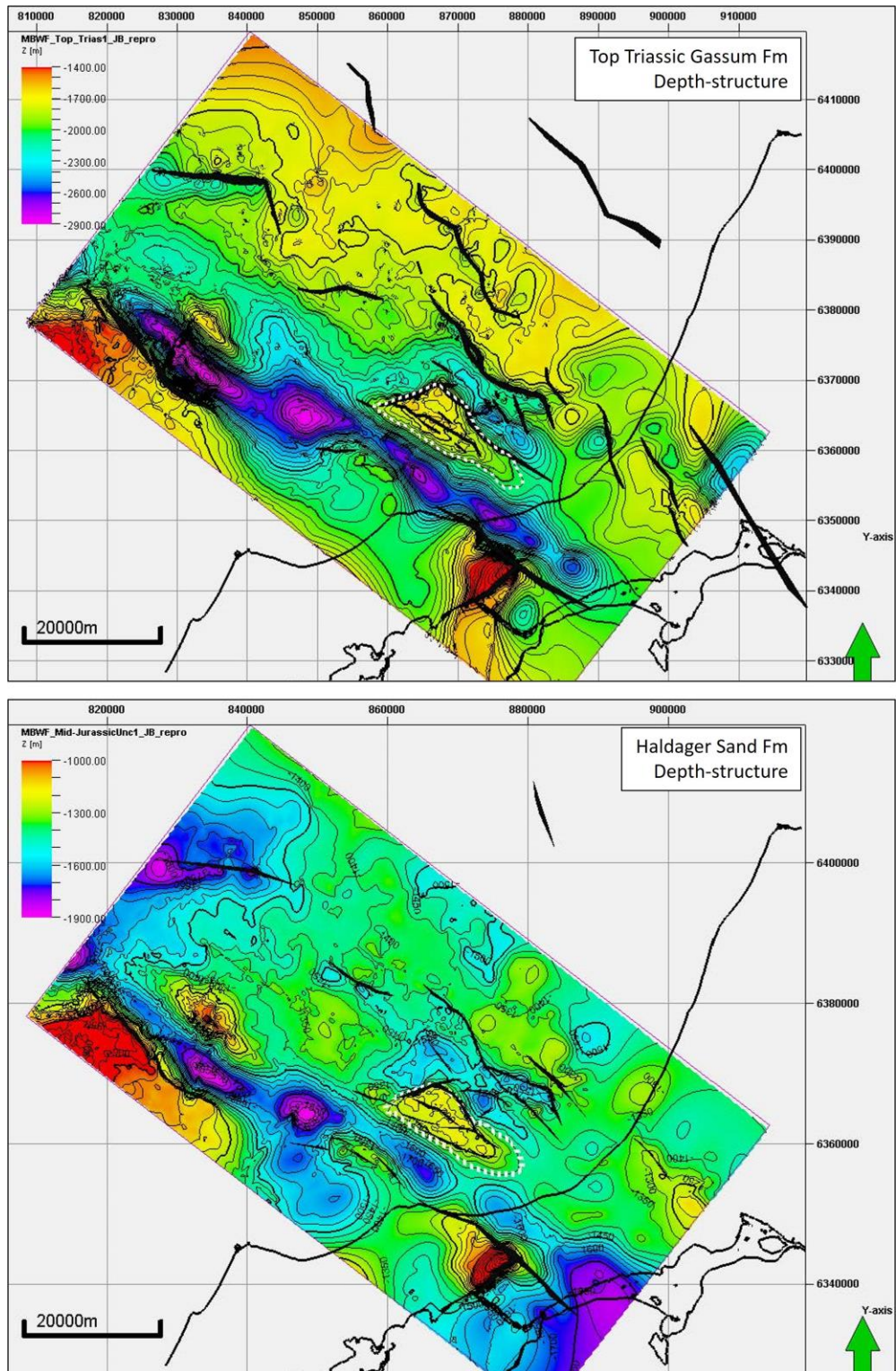


**Figure 8.1.1.** The Top Haldager Sand and Gassum depth structure maps in meters (m) (generated in Petrel®, tied to nearest wells towards the NW and gridded by 250x250 meter) provides the primary input to the capacity assessment. The Jammerbugt structure is confined by faults. The SE structural spill points are located at c. 1400 m and 2000 m TVDSS at the top of Haldager Sand Fm and Gassum Fm level, respectively. The Top Haldager Sand map shows a top point at c. 1160 m, the anticipated most likely gross thickness is c. 20 m. The Top Gassum map shows a top point at c. 1620 m, the anticipated most likely gross thickness is c. 200 m. A conceptual profile (A–A') across the setting is shown in Figure 8.1.2 and 8.1.3.

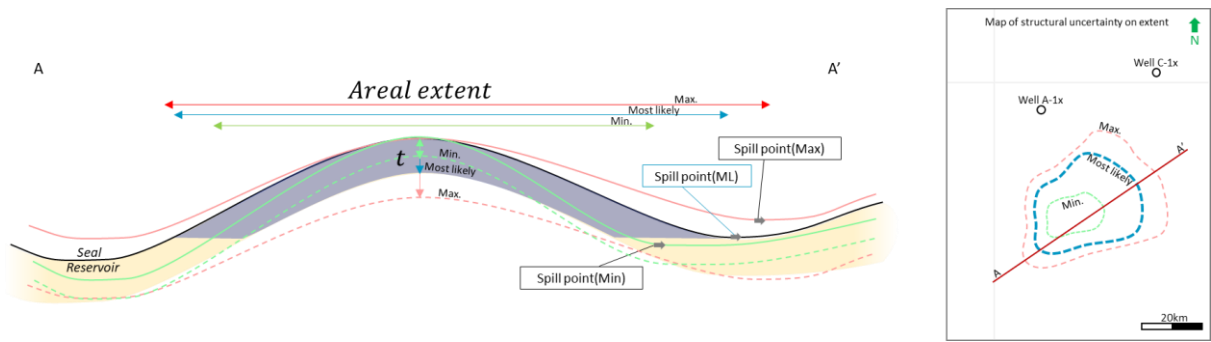


**Figure 8.1.2.** Conceptual profile (A-A') across a closed structure. The uncertainty in mapping the structure results in the hypothetically min. and max. scenarios looking very different from the most likely mapped scenario. Variance in area and in thickness ( $t$ ) will affect the Gross Rock Volume (GRV) of the structure. The uncertainty is addressed by applying uncertainty on the resulting GRV.

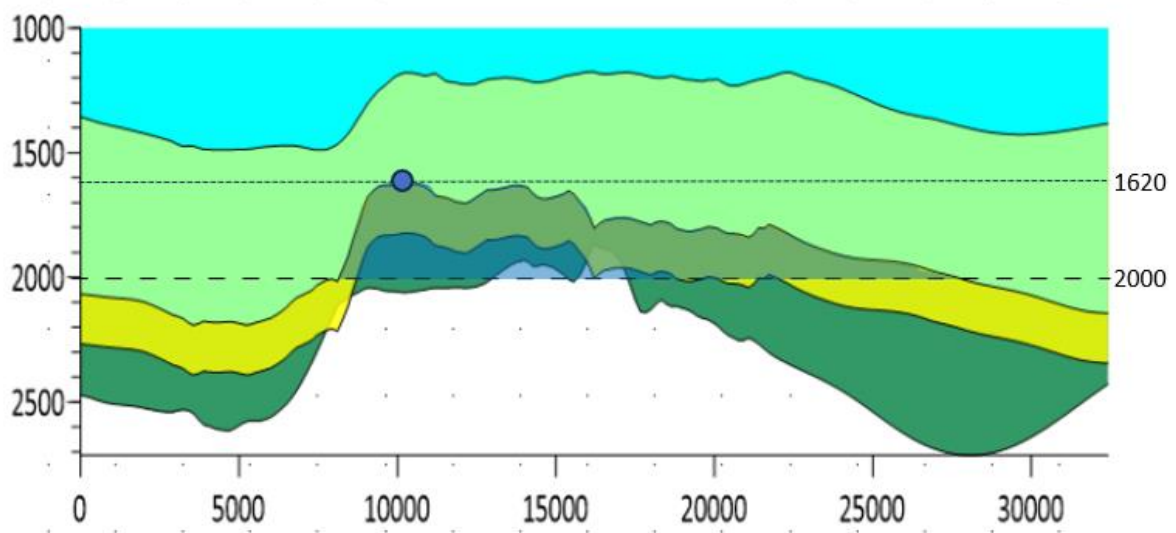


**Figure 8.1.3.** A NW-SE schematic cross section across the Jammerbugt structure showing top and spill points for the Gassum Fm at the 1620 m and 2000 m contour. The cross section includes the base of the reservoir assuming a 200 m gross thickness. This boundary is used as input for a realistic GRV estimation (marked with olive green polygon between 1620 and 2000 m). The Gassum Fm GRV is calculated in Petrel as the volume between the top Gassum and base Gassum surfaces and corrected to fit with the spill point contour as illustrated in the figure. Depth and length scales in meter.

## 8.2 Volumetric input parameters

### 8.2.1 Gross rock volume

The GRV of the Jammerbugt structure have been calculated using the Area and Thickness vs. Depth methodology described by e.g. James et al. (2013). The calculated GRV is estimated from the seismic mapped and depth converted top reservoir surfaces and the assigned reservoir thickness. For the Gassum Fm, the GRV is calculated as the volume between the top Gassum and base reservoir surfaces, the latter defined to seated 200 m deeper than the top and constrained to above the 2000 m spill point depth (Figure 8.1.2. and Figure 8.1.3.).

GRV is obtained by multiplying gross-reservoir volume with the net-to-gross ratio. Calculating GRV using the above steps allows uncertainty ranges on closure area and reservoir sand thickness to be modeled independently. Furthermore, the method allows for a rapid GRV calculation, that can be used in a Monte Carlo simulation, in order to establish an unbiased estimated range of GRV (James et. al., 2013).

To capture the uncertainty on the GRV across the Jammerbugt structure, a minimum and maximum case was also calculated as illustrated in Figure 8.1.2. The estimated GRV was assigned a min., mode and max. uncertainty range, where mode is the data value that occurs most often in the data. This variation in GRV was set up for the areal extent to cover uncertainty in interpretations, seismic well ties, mapping and depth conversion. To reflect this uncertainty, a distribution for the average GRV was constructed by defining the min. and max. of the distribution based on surrounding wells and adding a margin of  $\pm 20\%$  (Table 8.2.1.). It is assumed that the GRV distribution follows a Pert distribution defined by the min., mode and max. values. The Pert distribution is believed to give suitable representation for naturally occurring events following the subjective input estimates (Clark, 1962).

**Table 8.2.1.** Gross Rock Volume assumption input and resultant GRVs for the Haldager Sand and Gassum fms reservoirs in the Jammerbugt structure. Reservoir thicknesses are discussed in chapter 7.

Unit	Apex [m, TVDSS]	Spill point [m, TVDSS]			Area [km <sup>2</sup> ]			Reservoir TCK [m]			GRV [km <sup>3</sup> ]		
		Min.	Mode	Max.	Min.	Mode	Max.	Min.	Mode	Max.	Min.	Mode	Max.
<b>Haldager S</b>	1160	1120	1400	1680	113	142	170	15	20	100	2.26	2.83	4.0
<b>Gassum Fm</b>	1620	1600	2000	2400	96	119	143	100	200	300	19.1	23,9	26.7

### 8.2.2 Net-to-Gross ratio and porosity

Similar to the GRV, net-to-gross and porosity are also defined by min., mode and max. values for, and are assumed to follow Pert distributions. Mode values used for the storage capacity modelling are defined and discussed in chapter 7 based especially on information from J-1 and Felicia-1. Variations in net-to-gross and porosity relative to mode values are defined by min. and max. values varying c.  $\pm 20\%$  from the mode. A Pert distribution has been applied.

### 8.2.3 CO<sub>2</sub> density

The average in-situ density of CO<sub>2</sub> was estimated using the 'Calculation of thermodynamic state variables of carbon dioxide' web-tool essentially based on Span and Wagner (1996) [[http://www.peacesoftware.de/einigewerte/co2\\_e.html](http://www.peacesoftware.de/einigewerte/co2_e.html)]. The average reservoir pressure was calculated on the assumption that the reservoir is under hydrostatic pressure and a single pressure point midway between apex and max spill point was selected representing the entire reservoir.

Temperature for this midway point was calculated assuming a surface temperature of 4°C and a geothermal gradient derived from Fuchs et al. (2020) onshore to be c. 27–28 C°/km, but here adjusted to an offshore 30 C°/km gradient. Assumptions and calculated densities for the individual reservoir units are tabulated in Table 8.2.2. For a quick estimation of the uncertainty on CO<sub>2</sub> density, various P-T scenarios were tested and in general terms a -5% (min.) and +10% (max.)

variation from the calculated mode was applied for building a Pert distribution. All calculations showed that CO<sub>2</sub> would be in supercritical state.

**Table 8.2.2.** CO<sub>2</sub> fluid parameter assumption and estimated values

Unit	Apex depth [TVDSS, m]	'Spill point depth' [TVDSS, m]	Structural relief [m]	Pressure HydroS.[MPa]	GeoThermal grad. [C/km]	Mid Res. Temp. [C]	CO <sub>2</sub> density (Kg / m <sup>3</sup> )
Haldager Sand	1160	1400	240	12.56	30	42.4	684.4
Gassum Fm	1620	2000	380	17.76	30	58.3	685.1

#### 8.2.4 Storage efficiency

Storage efficiency is heavily influenced by local geological subsurface factors such as confinement, reservoir performance, compartmentalisation etc. together with injection design and operation (i.e. financial controlled factors) (e.g. Wang et al. 2013). A sufficient analogue storage efficiency database is not available to this study and accurate storage efficiency factor-ranges lacks at this early stage of maturation. This emphasises the need for further investigations of subsurface and development of scenarios and dynamic reservoir simulation to better understand the potential storage efficiency ranges. In this evaluation, a range from 5% to 20% with a mode of 10% is used as a possible range. The use of a mode of 10% assumes that sandstone reservoir in the Jammerbugt structure have good reservoir characteristics. A Pert distribution for this element has also been applied.

#### 8.2.5 Input summary

In Tables 8.2.3. through 8.2.4, input parameter distributions are listed (all selected to follow Pert distributions defined by min, mode and max). An example of input parameter distributions for the Gassum reservoir is displayed in Figure 8.2.5.

**Table 8.2.3.** Input parameters for the Jammerbugt structure – Haldager Sand Fm

Parameter	Assumption		
	Min	Mode	Max
GRV (km <sup>3</sup> )	2.3	2.83	3.4
Net/Gross	0.10	0.24	0.90
Porosity	0.13	0.27	0.32
Storage eff.	0.05	0.1	0.2
<i>In situ</i> CO <sub>2</sub> density (kg/m <sup>3</sup> )	650	684.4	753

**Table 8.2.4.** *Input parameters for the Jammerbugt structure – Gassum reservoir*

Parameter	Assumption		
	Min	Mode	Max
GRV (km <sup>3</sup> )	19.1	23.9	28.7
Net/Gross	0.33	0.50	0.66
Porosity	0.14	0.20	0.36
Storage eff.	0.05	0.1	0.2
<i>In situ</i> CO <sub>2</sub> density (kg/m <sup>3</sup> )	651	685.1	754

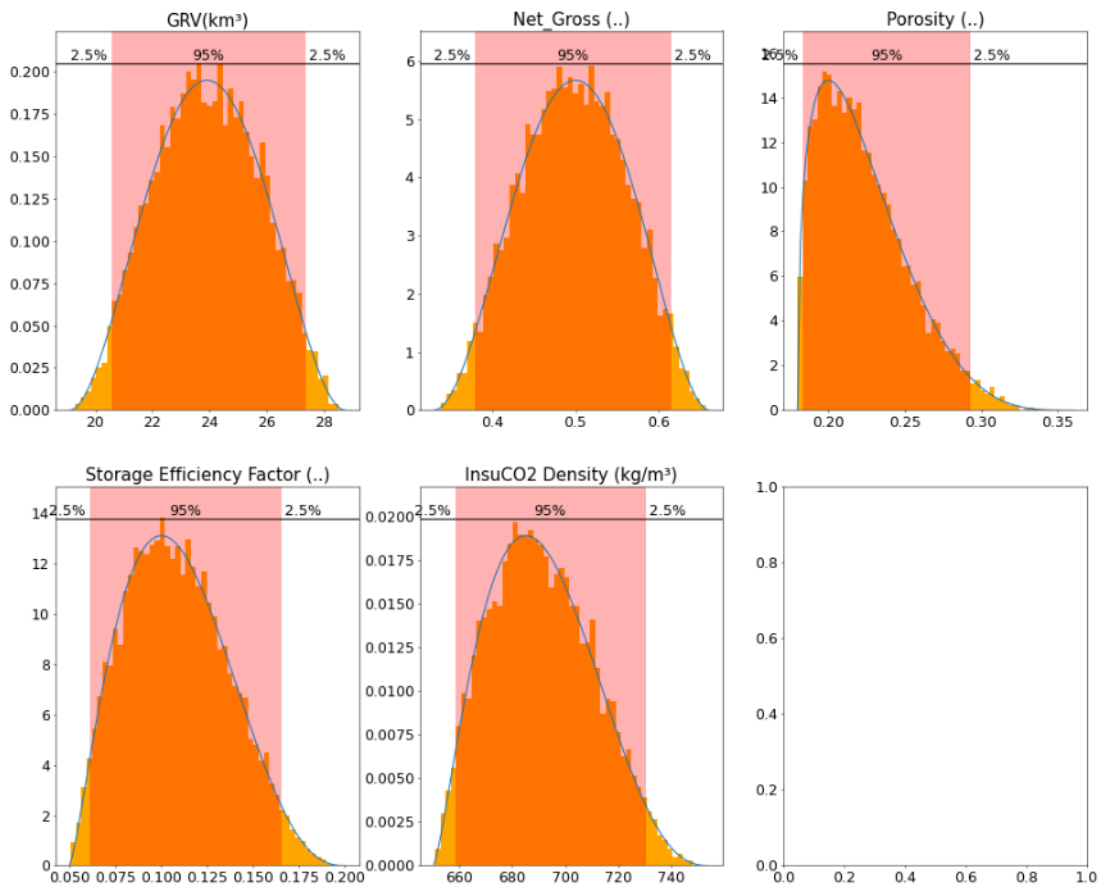


**Figure 8.2.5.** *Example of some of the distribution shapes (Pert distributions) for the 5 input parameters for the Gassum reservoir. The last input distribution plot is empty and not used.*

### 8.3 Storage capacity results

The modelled volumetrics was made on the assumption of the presence of an efficient reservoir/seal pair capable of retaining CO<sub>2</sub> in the reservoir, which needs to be tested by further data acquisition and geological investigation. In Tables 8.3.1 through 8.3.2, the results of the Monte Carlo simulations are tabulated. The tables indicate both the pore volume available within the trap (full potential above structural spill), the effective volume accessible for CO<sub>2</sub> storage (applying the Storage Efficiency factor to pore volume) and mass of CO<sub>2</sub> in megatons (MT) that can be stored. The tables present the 90%, 50% and 10% percentiles (P90, P50 and P10) corresponding to the

chance for a given storage volume scenario to exceed the given storage capacity value. Mean values of the resultant outcome distribution are also tabulated and is considered the “most appropriate” single value representation for the entire distribution.

A mean unrisks storage capacity of c. 17 MT CO<sub>2</sub> is calculated for the Haldager Sand Fm with a range between c. 7 MT CO<sub>2</sub> (P90) and c. 30 MT CO<sub>2</sub> (P10) and a P50 of c. 16 MT CO<sub>2</sub>. An unrisks storage potential of c. 199 MT CO<sub>2</sub> is calculated for Gassum reservoir unit with a range between c. 122 MT CO<sub>2</sub> (P90) and c. 289 MT CO<sub>2</sub> (P10) and a P50 of c. 191 MT CO<sub>2</sub> (Figure 8.3.1). Due to the variability-ranges of the behind-lying factors, the modelled storage capacity has a significant range and is associated with uncertainty. As illustrated in Figure 8.3.2, the storage capacity uncertainty is first of all linked with the uncertainty storage efficiency but also the combined uncertainty in gross rock volume, net-to-gross and porosity. In comparison, CO<sub>2</sub> density at reservoir conditions, is believed to be of minor concern at this stage.

Additional storage capacity may be available in the Jammerbugt structure, if additional reservoir units exist such as at Flyvbjerg Fm level. This speculative additional storage potential has not evaluated in this study but forms an upside to the above figures. Furthermore, potentially critical issues such as seal breach, fault leakage or fault reactivation caused by pressurisation of the reservoir during injection are not evaluated in this study, but for obvious reasons needs to be addressed in the further evaluation of the Jammerbugt structure as potential CO<sub>2</sub> storage site.

**Table 8.3.1.** *Jammerbugt structure – Haldager Sand Fm storage capacity potential*

<b>Results</b>	<b>P90</b>	<b>P50</b>	<b>P10</b>	<b>Mean</b>
Buoyant trapping pore volume (km <sup>3</sup> )	0.1142	0.2184	0.3844	0.2357
Buoyant eff. storage volume (km <sup>3</sup> )	0.0111	0.0227	0.0444	0.0256
Buoyant storage capacity (MT CO <sub>2</sub> )	7.69	15.63	30.42	<b>17.68</b>

**Table 8.3.2.** *Jammerbugt structure – Gassum reservoir storage capacity potential*

<b>Results</b>	<b>P90</b>	<b>P50</b>	<b>P10</b>	<b>Mean</b>
Buoyant trapping pore volume (km <sup>3</sup> )	2.0257	2.6045	3.3833	0.656
Buoyant eff. storage volume (km <sup>3</sup> )	0.1762	0.2768	0.4168	0.071
Buoyant storage capacity (MT CO <sub>2</sub> )	121.72	190.83	288.90	<b>199.36</b>

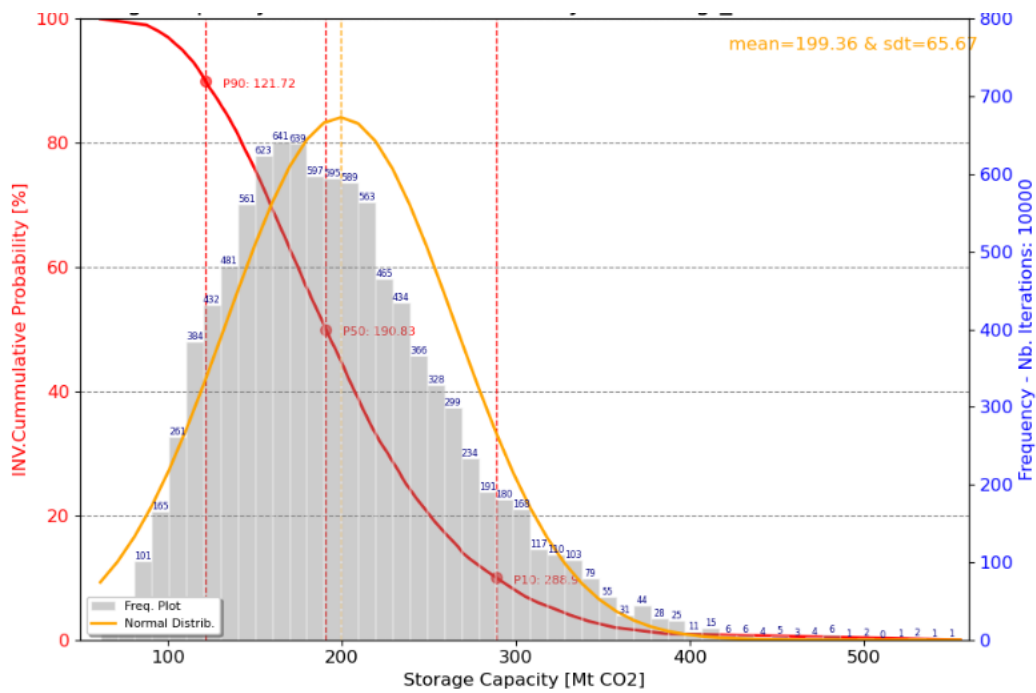


**Figure 8.3.1.** Modelled statistical distribution of the combined storage capacity potential for the Gassum reservoir in the Jammerbugt structure.

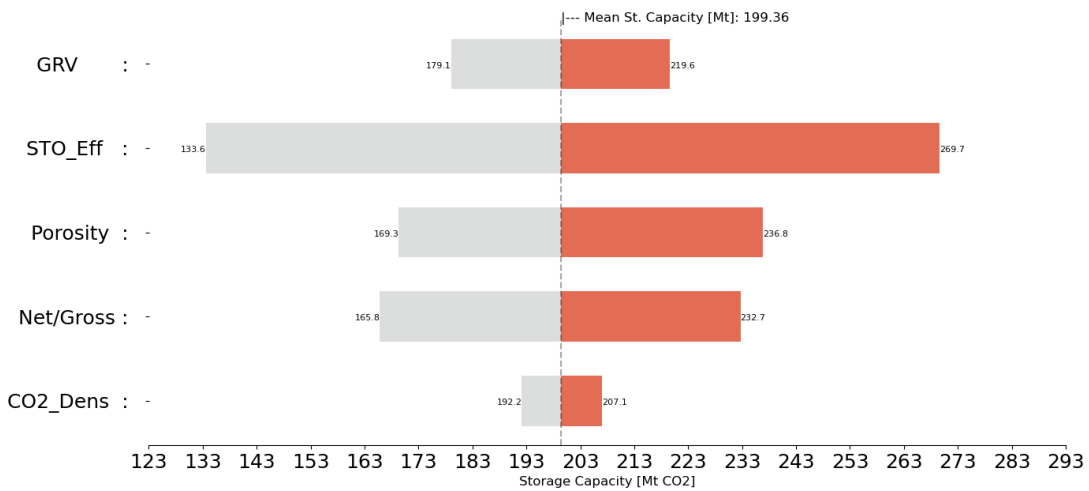


**Figure 8.3.2.** Sensitivity (Tornado) plot to how the various input parameters affect the estimated mean storage capacity (c. 199 MT CO<sub>2</sub>) of the Gassum reservoir unit. The horizontal bars for each parameter indicate change in storage capacity given that only that parameter is changed leaving all other constant (end levels being P90 and P10, respectively, in the parameter input range). The colours show the symmetric representation of the parameters on both sides of the mean storage capacity.

## 8.4 Potential risks

The present report does not comprise a study of risks or risk assessment of the structure for potential storage of CO<sub>2</sub> but provides an initial geological mapping identifying overall elements with reservoir-seal pairs, extent/thickness/closure/volume of the storage complex reservoir formations, and larger faults. Thus, this reporting provides a first geological characterization with these identified elements and geological parameters, that may negatively affect the CO<sub>2</sub> storage potential and it points out some geological related potential risk issues, that is recommended for further evaluation, e.g. in risk assessment studies.

A frontier prospect like the Jammerbugt structure is associated with several such risks. Not all risks can be identified at this early stage, while other risks identified at this early stage will probably turn out to be insignificant once new data have been collected and further investigations have been conducted, which together shed new light on the geology. The four risks listed below is not considered a complete list but rather emphasizes important points that needs further attention in future studies and data collections.

Faulting of the Gassum-Fjerritslev Fm reservoir-seal pair and the Haldager Sand-Børglum Fm reservoir-seal pair is considered the primary risk at the current level of understanding. First of all, despite very thickly developed seals, the faults through the Fjerritslev Fm seal and the Børglum Fm seal introduce a potential risk of vertical leakage from storage in the Gassum and Haldager Sand fms that needs to be addressed when maturing the Jammerbugt structure. This also includes investigating the potential migration pathway of CO<sub>2</sub> leaked from the Gassum and Haldager Sand reservoirs. At the current early stage of understanding, leakage risks are not fully investigated. Future studies should first of all clarify if fault leakage will occur; and if so, if potentially leaked CO<sub>2</sub> form the Gassum Fm will accumulate in the overlying three-way closures in the sandy intervals within the Fjerritslev Fm and the Haldager Sand Fm sealed by the Børglum Fm or if it will leak further upwards through the faults in the Børglum Fm towards the surface.

Secondly, faulting of the reservoirs may be associated with reservoir compartmentalization. The known critical faults in this respect are those roughly aligning with the structure length axis intersecting the reservoir within the closure confinement (fault zone C in Fig. 6.2.4). Their nature, extend and potential barrier effect is thus critical to understanding reservoir communication, pressure build-up and CO<sub>2</sub> migration, and thus to the design of a CO<sub>2</sub> injection scheme. Further fault analyses on existing and new seismic data may mitigate this risk.

The limited amount of reservoir sand presented in vintage interpretations of the Fjerritslev-2 well further introduces some uncertainty concerning the reservoir quality of the Gassum Fm, which needs to be addressed due to the proximity of Fjerritslev-2 and the Jammerbugt structure.

In addition, the inner, eastern part of the Jammerbugt structure virtually lacks seismic coverage. The nature of this part of the structure needs to be investigated by additional data acquisition and future studies. New data covering this inner part of the structure are very likely to influence the mapped closure size of the Jammerbugt structure and the associated volumetrics.

## 9. Conclusions

The Jammerbugt structure is located at the edge of the Fjerritslev Trough. Acquisition of around 1400 km marine 2-D seismic data partly covering the structure has enabled a provisional mapping and geological analyses of the structure and a first assessment of its CO<sub>2</sub> storage potential. The Jammerbugt structure delineates an elongated three-way closure bounded by normal faults at its northeastern and northwestern flank. The southwestern flank is bound by a general stratigraphic plunge towards the deeper part of the Fjerritslev Trough paralleling the structure to the southwest. While confining faulting is rooted in basement tectonism, the northeastern fault zone is also affected by detachment in Zechstein evaporites. The confining fault zone here formed as an antithetic fault to a sub-parallel fault system down-faulting basement towards the southwest and detaching in deep-seated evaporites. The roll-over effect caused by the underlying detachment faulting gave rise to anticlinal bending of strata within the Jammerbugt structure, modifying the simple three-way closure geometry. Additional faulting offset the internal part of the Jammerbugt structure interpreted to detach in Oddesund Fm evaporites. Faulting commenced in the late Middle Triassic to Late Triassic, when rifting laid the foundation of the Fjerritslev Trough. Following a calmer tectonic period in the Latest Triassic, extension resumed in the Jurassic and Early Cretaceous, and faulting of the Upper Cretaceous Chalk Group suggest even younger tectonism. Some of the faults intersect to near the seabed. The Late Cretaceous and Paleogene was characterized by inversion of the Fjerritslev Trough and was followed by Neogene regional uplift and southwester-ward tilting. Chalk therefore subcrop towards a thin veneer of Pleistocene to Holocene strata closely underneath the seabed.

The Jammerbugt is underlain by a several kilometre thick Upper Palaeozoic to Holocene sedimentary succession. The succession includes two important reservoir-seal pairs: (1) the Gassum/Fjerritslev fms and (2) the Haldager Sand/Børglum fms, both under structural closure. The uppermost Triassic to lowermost Jurassic Gassum Fm forms the primary reservoir in the Jammerbugt structure. The formation was deposited in a near-shore environment and is composed by sandstones interbedded with mudstones. The Gassum Fm is overlain by the fine-grained Fjerritslev Fm generally regarded as an excellent seal for CO<sub>2</sub> storage. Seismic mapping indicates it to measure a few hundred meters in thickness. Judging by the depth converted seismic interpretation, the Gassum Fm lies in around 1620 m depth at the crest of the Jammerbugt structure and with a closure of around 110 km<sup>2</sup> having a relief of nearly 400 m. The structure remains to be drilled but based on comparison to adjacent wells supported by seismic mapping a 200 m thickness is very roughly forecasted. By further comparisons with nearby wells, average porosity of around 20% and a net-to-gross in the order of 0.5 is anticipated. A most likely CO<sub>2</sub> storage capacity of 191 MT is modelled within the Gassum Fm based on a Monte Carlo simulation (129 MT CO<sub>2</sub> (P90) and 319 MT CO<sub>2</sub> (P10) with a mean of around 199 MT CO<sub>2</sub>.

While the Gassum Fm is considered to have a high chance of being an excellent reservoir within the Jammerbugt structure, a more conservative forecast is employed for the mid-Jurassic Haldager Sand Fm. Haldager Sand Fm varies from 74 m in thickness with a net-to-gross of 0.89% to only 19 m, and a net-to-gross of 0.24. Jurassic faulting and salt pillow growth at the Jammerbugt structure is likely to have induced a relief at the time of Haldager Sand deposition, reducing coarse-grained deposition across the structure. The Haldager Sand Fm is possibly overlain by Flyvbjerg Fm having a small reservoir potential, and thus treated as an upside to the Haldager Sand Fm. These reservoirs are blanketed by the fine-grained Børglum Fm and higher up by the Frederikshavn Fm generally regarded as cap rocks. With an anticipated combined thickness of a

few hundred meters in the Fjerritslev Trough, these units likely form excellent seals at the Jammerbugt structure.

The study highlights questions of particular importance to the suitability of the Jammerbugt structure as CO<sub>2</sub> storage site, which need to be addressed by future work. First of all, the inner, eastern part of the Jammerbugt structure continuous shoreward outside the existing seismic data coverage and the outline and nature of the inner part of the structure is little known. Over the data covered part of the structure, the potential risk for CO<sub>2</sub> leakage through faults intersecting the Gassum-Fjerritslev- and the Haldager Sand-Børglum Fm reservoir-seal pairs and continuing to near the seabed is currently not fully understood. Furthermore, fault offset of reservoirs within the structure may lead to reservoir compartmentalization lowering the capability for efficient CO<sub>2</sub> injection warranting further investigations. Also, the limited amount of Gassum Fm reservoir sand presented in vintage interpretations of the Fjerritslev-2 well introduces some uncertainty concerning the reservoir quality at the nearby Jammerbugt structure, which requires further attention.

## 10. Recommendations for further work

Acquisition of high-quality 2- and 3-D seismic data over the Jammerbugt structure is an important step towards investigating the shoreward part of the structure, mitigating the fault-related risks and develop scenarios for an eventual well layout. Such data will also enable a more precise definition of trap closures, reservoir- and seal characterization, depositional facies, faults and depth conversion, which again will feed into a refined storage volume calculation. It is recommended, that a further maturation of the structure should include a risk assessment with seal integrity, and in particular leakage risk at faults should be investigated. Before, or in parallel to new seismic acquisition, a careful state-of-the-art reprocessing of the Jammerbugt-23 survey could potentially improve imaging in the Triassic-Jurassic target interval. The current reprocessing brought about an immense improvement of data quality, but experimentation on refining the reprocessing sequence was hampered by the extremely tight deadline of the study. Careful reprocessing can very well add to the data quality enhancing imaging in the target interval and of faults in general.

The vintage interpretation of the Triassic to lowermost Jurassic interval in the Fjerritslev-2 well introduces uncertainty of the Gassum Fm reservoir quality in Jammerbugt. A reinvestigation of Fjerritslev-2 cuttings would be a natural first step towards mitigating this uncertainty, investigating the lithological composition of the interval and doing a detailed biostratigraphic investigation to determine if a gap in stratigraphy exists. Eventually, reservoir and seal quality will need to be tested through drilling a well at or onshore near the Jammerbugt structure.

The modelled static storage capacity is associated with considerable variability-ranges and uncertainty. In order to mitigate the storage capacity uncertainty and narrow the variability range, first of all, the reservoir gross rock volume of the Jammerbugt structure needs to be constrained more accurately e.g. via the collection of seismic data over the shoreward extend of the Jammerbugt structure and through 3-D seismic acquisition that could help improve the structural definition, better constrain trap spill points and interpret tops and bases of reservoirs via an improved seismic quality and density, more sophisticated seismic well ties and a seismic velocity model. In addition, more accurate reservoir parameters could derive from geophysical modelling of 3-D seismic data over the structure.

The modelled storage capacity is a static storage capacity, which gives an impression about the total storage volume of the structure but without dealing with the rates at which CO<sub>2</sub> can be stored. This requires a dynamic storage capacity assessment, which is an indispensable tool for both political and financial planning on the potential utilization of the Jammerbugt structure.

## 11. References

Bashir, Y., Babasafari, A. A., Arshad, A. R. M., Alashloo, S. Y. M., Latiff, A. H. A., Hamidi, R., Rezaei, S., Ratnam, T., Sambo, C., and Ghosh, D. P. (2022). *Seismic Imaging Methods and Applications for Oil and Gas Exploration*. Elsevier.

Bertelsen, F. 1978. The Upper Triassic – Lower Jurassic Vinding and Gassum Formations of the Norwegian–Danish Basin. *Geol. Surv. Denmark Ser. B*, No. 3, 26 pp. <https://doi.org/10.34194/serieb.v3.7058>

Bertelsen, F. 1980. Lithostratigraphy and depositional history of the Danish Triassic. *Danmarks Geologiske Undersøgelse, DGU Serie B*, 4, 59 pp. <https://doi.org/10.34194/serieb.v4.7059>

Bruno, M.S. Lao, K. Diessl, J. Childers, B. Xiang, J. White, N. & van der Veer, E. 2014. Development of improved caprock integrity analysis and risk assessment techniques. *Energy Procedia*, 63, 4708 – 4744, doi: 10.1016/j.egypro.2014.11.503.

Christensen, J.E. & Korstgård, J.A. 1994. The Fjertitslev Fault offshore Denmark-salt and fault interactions. *First Break*, 12, 31-42.

Church, J.W., Fisher, M.J., Haskins, C.W. & Hughes, R.V. 1970. The micropalaeontology and stratigraphy of the Gulf Dansk Nordsø J-1 well. Robertson Research Company Limited.

Clark, C.E. 1962. The PERT model for the distribution of an activity Time. *Operations Research* 10, pp. 405-406. <https://doi.org/10.1287/opre.10.3.405>

Dapco. 1958. Fjerritslev-2, Completion report. GEUS Report file no. 4407. 51 pp.

Dondurur, D. (2018). *Acquisition and processing of marine seismic data*. Elsevier.

Frykman, P. Nielsen, L.H. Vangkilde-Petersen, T. & Anthonsen, K. 2009: The potential for large-scale, subsurface geological CO<sub>2</sub> storage in Denmark. In: Bennike, O. Garde, A.A. & Watt, W.S. (eds): *Review of Survey activities 2008*. Geological Survey of Denmark and Greenland Bulletin 17, 13-16.

Fuchs, S., Balling, N. and Mathiesen, A. 2020. Deep basin temperature and heat-flow field in Denmark – New insights from borehole analysis and 3D geothermal modelling. *Geothermics*, 83. DOI: <http://doi.org/10.1016/j.geothermics.2019.101722>

Funck, T. Ehrhardt, A. Andreasen, N.R. Behrens, T. Christensen, N. Demir, Ü. Ebert, T. Nielsen, T.B. Nørmark, E. Pedersen, H. Schramm, B. Smith, L. Steinborn, P. and Trinhammer, P. 2023. Acquisition of marine seismic data in Jammerbugt in 2023. CCS2022-2024 WP1: Seismic data acquisition across the Jammerbugt structure on research vessel Jákup Sverri, *Danmarks og Grønlands Geologiske Undersøgelse Rapport 2023/39*, 120 pages, Geological Survey of Denmark and Greenland, Copenhagen, Denmark, doi:10.22008/gpub/34706

Fyhn, M.B.W. Gregersen, U. Hjelm, L. Jensen, T.D. Laghari, S. Lauridsen, B.W. Mathiesen, A. Mørk, F. Petersen, H.I. & Rasmussen, L.M. 2022. CCS2022-2024 WP1: The Lisa structure. Seismic data and interpretation to mature potential geological storage of CO<sub>2</sub>. *GEUS Rapport 2022/30*.

Glennie, K.W., Higham, J. & Stemmerik, L. 2003. Permian, In: Evans, D., Graham, D., Armour, C., Bathurst, P. (Eds): *The Millennium Atlas: Petroleum geology of the central and northern North Sea*. Geol. Soc. London. 91–103 pp.

Goodman, A., Hakala, A., Bromhal, G., Deel, D., Rodosta, T., Frailey, S., Samll, M., Allen, D., Romanov, V., Fazio, J., Huerta, N., McIntyre, D., Kutcho, B. and Guthrie, G. 2011. U.S. DOE methodology for the development of geologic storage potential for carbon dioxide at the national and regional scale. *International Journal of Greenhouse Gas Control*, 5 (4), 952–965. <https://doi.org/10.1016/j.ijggc.2011.03.010>.

Gorecki, C.D., Holubnyak, Y.I., Ayash, S.C., Bremer, J.M., Sorensen, J.A., Steadman, E.N. and Harju, J.A. 2009. A New Classification System For Evaluating CO<sub>2</sub> Storage Resource/Capacity Estimates. Paper presented at the SPE International Conference on CO<sub>2</sub> Capture, Storage, and Utilization, San Diego, California, USA, November 2009. ISBN: 978-1-55563-267-0. <https://doi.org/10.2118/126421-MS>.

Gregersen, U., Hjelm, L., Vosgerau, H., Smit, F.W.H., Nielsen, C.M., Rasmussen, R., Bredesen, K., Lorentzen, M., Mørk, F., Lauridsen, B.W., Pedersen, G.K., Nielsen, L.H., Mathiesen, A., Laghari, S., Kristensen, L., Sheldon, E., Dahl-Jensen, T., Dybkjær, K., Hidalgo, C.A. and Rasmussen, L.M. 2023. CCS2022-2024 WP1: The Stenlille structure - Seismic data and interpretation to mature potential geological storage of CO<sub>2</sub>. *Danmarks og Grønlands Geologiske Undersøgelse Rapport 2022/26*. GEUS. 164 pp. DOI: <https://doi.org/10.22008/gpub/34661>

Guiltinan, E.J., Cardenas, M.B., Bennett, P.C., Zhang, T. & Espinoza, D.N. 2017. The effect of organic matter and thermal maturity on the wettability of supercritical CO<sub>2</sub> on organic shales, *International Journal of Greenhouse Gas Control* 65, 15-22, <https://doi.org/10.1016/j.ijggc.2017.08.006>.

Gulf, 1970. Completion report, Dansk Nordsø J-1X, 59 pp.

Hjelm, L. Anthonsen K. L. Dideriksen, K. Nielsen, C.M. Nielsen, L.H. & Mathiesen A. 2022. Capture, Storage and Use of CO<sub>2</sub> (CCUS). *Danmarks og Grønlands Geologiske Undersøgelse Rapport 2020/46*, 141 pp. <https://doi.org/10.22008/gpub/34543>

IPCC (Intergovernmental Panel on Climate Change) 2022. *Climate Change 2022: Mitigation of Climate Change*. Working Group III contribution to the Sixth Assessment Report of the Intergovernmental Panel on Climate Change. UN, New York. 2913 pp.

James, B. Grundy, A.T. & Sykes, M.A. 2013. The Depth-Area-Thickness (DAT) Method for Calculating Gross Rock Volume: A Better Way to Model Hydrocarbon Contact Uncertainty, AAPG International Conference & Exhibition. AAPG Search and Discovery Article #90166©2013, Cartagena, Colombia, 8-11 September.

Japsen, P. Green, P.F. Nielsen, L.H. Rasmussen, E.S. & Bidstrup, T. 2007. Mesozoic–Cenozoic exhumation events in the eastern North Sea Basin: a multi-disciplinary study based on palaeothermal, palaeoburial, stratigraphic and seismic data. *Basin Research*, 19, 451–490, doi: 10.1111/j.1365-2117.2007.00329.x

Katsube, T.J. & Williamson, M. A. 1994. Effects of diagenesis on shale nano-pore structure and implications for sealing capacity. *Clay Minerals*, 29, 451-461.

- Liboriussen, J., Ashton, P. & Thygesen, T. 1987. The tectonic evolution of the Fennoscandian Border Zone in Denmark. *Tectonophysics* 137, 21–29.
- Mathiesen, A. Dam, G. Fyhn, M.B.W. Kristensen, L. Mørk, F. Petersen, H.I. & Schovsbo, N.H. 2022. Foreløbig evaluering af CO<sub>2</sub> lagringspotentiale af de saline akviferer i Nordsøen. Grønlands Geologiske Undersøgelse Rapport. 2022/15, 151 pp. + App.
- McKie, T. 2014. Climatic and tectonic controls on Triassic dryland terminal fluvial system architecture, central North Sea. *In: A. W. Martinius, R. Ravnås, J. A. Howell, R. J. Steel, and J. P. Wonham (Eds.), Depositional Systems to Sedimentary Successions on the Norwegian Continental Margin. Int. Assoc. Sedimentol. Spec. Publ., 46, 19–58.*
- McKie, T. & Williams, B. 2009. Triassic palaeogeography and fluvial dispersal across the north-west European Basins. *Geological Journal*, 44, 711–741, DOI: 10.1002/gj.1201.
- Michelsen, O & Clausen, O.R. 2002. Detailed stratigraphic subdivision and regional correlation of the southern Danish Triassic succession. *Marine and Petroleum Geology* 19, 563–587.
- Michelsen, O. Nielsen, L.H. Johannessen, P.H. Andsbjerg, J. & Surlyk, F. 2003. Jurassic lithostratigraphy and stratigraphic development onshore and offshore Denmark. *In: Ineson, J.R. and Surlyk, F. (Eds.), The Jurassic of Denmark and Greenland. Geological Survey of Denmark and Greenland Bulletin 1, 145–216. https://doi.org/10.34194/geusb.v1.4651.*
- Mogensen, T.E. & Jensen, L.N. 1994. Cretaceous subsidence and inversion along the Tornquist Zone from Kattegat to the Egersund Basin. *First Break*, 12, 211–222.
- Mogensen, TE. & Korstgård, J.A. 2003. Triassic and Jurassic transtension along part of the Sorgenfrei-Tornquist Zone in the Danish Kattegat. *In: Surlyk, F. Ineson, J.R. (Eds) he Jurassic of Denmark and Greenland, Geol. Surv. Den. Green. Bull. 1, Copenhagen, 439–458.*
- Nielsen, L.H. 2003. Late Triassic–Jurassic development of the Danish Basin and the Fennoscandian Border Zone, southern Scandinavia. *In: Surlyk, F. Ineson, J.R. (Eds) he Jurassic of Denmark and Greenland, Geol. Surv. Den. Green. Bull. 1, Copenhagen, 459–526.*
- Nielsen, L.H. & Japsen, P. 1991. Deep wells in Denmark 1935-1990. Lithostratigraphic subdivision. *Danmarks Geologiske Undersøgelse, DGU Serie A, 31, 177 pp.*
- Olivarius, M. Sundal, A. Weibel, R. Gregersen, U. Baig, I. Thomsen, T.B. Kristensen, L. Hellevang, H. & Nielsen, L.H. 2019. Provenance and Sediment Maturity as Controls on CO<sub>2</sub> Mineral Sequestration Potential of the Gassum Formation in the Skagerrak. *Frontiers in Earth Science*, 7. doi:10.3389/feart.2019.00312
- Olivarius, M. Vosgerau, H. Nielsen, L.H. Weibel, R. Malkki, S.N. Heredia, B.D. & Thomsen, T.B. 2022. Maturity Matters in Provenance Analysis: Mineralogical Differences Explained by Sediment Transport from Fennoscandian and Variscan Sources. *Geosciences*, 12, 308. <https://doi.org/10.3390/geosciences12080308>
- Petersen, H.I. Nielsen, L.H. Bojesen-Koefoed, J.A. Mathiesen, A. Kristensen, L. & Dalhoff, F. 2008. Evaluation of the quality, thermal maturity and distribution of potential source rocks in the Danish part of the Norwegian–Danish Basin. *Geol. Surv. Denm. Greenl. Bull. 16, 66.*

Phillips, T.B. Jackson, C.A.-L. Bell, R.E. & Duffy, O.B. 2018. Oblique reactivation of lithosphere-scale lineaments controls rift physiography – the upper-crustal expression of the Sorgenfrei–Tornquist Zone, offshore southern Norway. *Solid Earth*, 9, 403–429, <https://doi.org/10.5194/se-9-403-2018>

Realtime Seismic, 2023. GEUS2022-JAMMERBUGT-RE2023. Reprocessing of the GEUS2022-JAMMERBUGT 2D Seismic Survey for the Geological Survey of Denmark and Greenland. Realtime Seismic Pty. Ltd. France. 57 pp. Link to info: GEUS2022-JAMMERBUGT-RE2023 report, [GEUS2023-JAMMERBUGT-RE2023 report](#).

Sorgenfrei, T. & Buch, A. 1964. Deep tests in Denmark 1935–1959, DGU III, 36, 180 pp.

Span, R. & Wagner, W. 1996. A new equation of state for carbon dioxide covering the fluid region from the triple-point temperature to 1100K at pressures up to 800 MPa, *J. Phys. Chem. Ref. Data*. 25, 1509-1596 PP.

Springer, N. Lotentzen, H. Fries, K. & Lindgreen, H. 2010. Caprock seal capacity evaluation of the Fjerritslev and Børglum Formations. Contribution to the EFP-project AQUA-DK. Danmarks og Grønlands Geologiske Undersøgelse Rapport nr. 112.

Statoil, 1988. Completion report Well 5408/18 – 1.1A Licence 8/86 Felicia. 134 pp & App. I-III.

Stemmerik, L., Ineson, J.R. & Mitchell, J.G. 2000. Stratigraphy of the Rotliegend Group in the Danish part of the Northern Permian Basin, North Sea. *Journal of the Geological Society, London*, 157, 1127-136.

Surlyk, Finn & Lykke-Andersen, H. 2007, Contourite drifts, moats and channels in the Upper Cretaceous chalk of the Danish basin. *Sedimentology*, 54, 405–422.

Vejbæk, O.V. 1997. Dybe strukturer i danske sedimentære bassiner. *Geologisk Tidsskrift*, 4, pp. 1-31. <https://2dggf.dk/xpdf/gt1997-4-1-31.pdf>.

Vejbæk, O. & Andersen, C. 2002. Post mid-cretaceous inversion tectonics in the Danish Central Graben - regionally synchronous tectonic events? *Bull. Geol. Soc. Denmark* 49, 139–144.

Verschuur, D. J., Berkhout, A., and Wapenaar, C. (1992). Adaptive surface-related multiple elimination. *Geophysics*, 57(9):1166–1177.

Vosgerau, H. Gregersen, U. Hjuler, M.L. Holmslykke, H.D. Kristensen, L. Lindström, S. Mathiesen, A. Nielsen, C.M. Olivarius, M. Pedersen, G.K. & Nielsen, L.H. 2016. Reservoir prognosis of the Gassum Formation and the Karlebo Member within two areas of interest in northern Copenhagen. The EUDP project “Geothermal pilot well, phase 1b”. GEUS Rapport 2016/56. 138 pp + app 1–5. <https://doi.org/10.22008/gpub/32477>

Wang, Y. Zhangb, K. & Wua, N. 2013. Numerical Investigation of the Storage Efficiency Factor for CO<sub>2</sub> Geological Sequestration in Saline Formations, *Energy Procedia*, Volume 37, 2013, 5267-5274 PP.

Yilmaz, Ö. (2001). *Seismic data analysis: processing, inversion, and interpretation of seismic data*. Society of Exploration Geophysicists.